

University of Southern Queensland
Faculty of Engineering and Surveying

A study into the behaviour of FRP bolted connections

An Engineering Research Project submitted by

Adam Robinson

In fulfilment of the requirements of

ENG4111 and ENG4112

towards the degree of

Bachelor of Civil Engineering

Submitted: October 2015

Abstract

It has only been in the recent decade that fibre reinforced polymers (FRP) are being utilized in civil structures through use of pultruded sections. The joining and connection of these members are critical for the integrity of the structures. Due to the orthotropic nature of FRP and the vast number of pultrusion manufacturers in the industry the development of standards for connections has been restricted to only guidelines such as the EUROCOMP handbook. In the last decade construction using FRP pultrusion has become more widely used and there has been more research to investigate the failure of connections by mostly experimental testing. Previous research and the current guidelines both from EUROCOMP and manufacturers show variations in recommended and minimum geometry associated with joint design with FRP pultruded sections.

This research will study the stress behaviour of simplified lap-joints with a single and multi-bolt configuration with particular attention to the critical failure planes associated with net-tension, bearing and shear-out failure modes. A finite element analysis and theoretical study into geometric parameter changes will also be investigated to establish differences between previous research conducted and the current guidelines set out in the pultrusion industry. There has been little research conducted in multi-bolt (single row) connections so this will be incorporated into the study in an attempt to show any irregularities and differences when compared to single-bolt connections. Based on results of the FEA conclusions will be made and findings presented with a focus on suggested geometry for FRP tension joints.

University of Southern Queensland

Faculty of Health, Engineering and Sciences

ENG4111/ENG4112 Research Project

Limitations of Use

The Council of the University of Southern Queensland, its Faculty of Health, Engineering & Sciences, and the staff of the University of Southern Queensland, do not accept any responsibility for the truth, accuracy or completeness of material contained within or associated with this dissertation.

Persons using all or any part of this material do so at their own risk, and not at the risk of the Council of the University of Southern Queensland, its Faculty of Health, Engineering & Sciences or the staff of the University of Southern Queensland.

This dissertation reports an educational exercise and has no purpose or validity beyond this exercise. The sole purpose of the course pair entitled “Research Project” is to contribute to the overall education within the student’s chosen degree program. This document, the associated hardware, software, drawings, and other material set out in the associated appendices should not be used for any other purpose: if they are so used, it is entirely at the risk of the user.

University of Southern Queensland

Faculty of Health, Engineering and Sciences

ENG4111/ENG4112 Research Project

Certification of Dissertation

I certify that the ideas, designs and experimental work, results, analyses and conclusions set out in this dissertation are entirely my own effort, except where otherwise indicated and acknowledged.

I further certify that the work is original and has not been previously submitted for assessment in any other course or institution, except where specifically stated.

Adam Robinson

21/10/2015

Acknowledgment

This research was carried out under the supervision of Dr Sourish Banerjee and I would like to thank him for his assistance and guidance during the course of the research. His input and recommendations are much appreciated.

Table of Contents

Abstract	i
Limitations of Use.....	ii
Certification of Dissertation.....	iii
Acknowledgment	iv
List of Figures.....	viii
List of Tables	xi
List of Appendices	xii
Nomenclature.....	xiii
Chapter 1	
Introduction	1
1.1 Background.....	1
1.2 Objectives of research	5
1.3 Structure and Outline.....	6
1.4 Scope of research	7
Chapter 2	
Literature Review.....	8
2.1 Introduction.....	8
2.2 Bolted Connections.....	11
2.3 Single and Multi-bolt Finite Element Analysis (FEA) research.....	13
2.4 Experimental Analysis	17
2.5 Conclusion	19
Chapter 3	
Methodology.....	20
3.1 Introduction.....	20

3.2 Material Properties	21
3.2.1 Pultruded plate properties.....	21
3.2.2 Bolt properties	22
3.3 Theoretical Study	23
3.3.1 Overview	23
3.3.2 Bearing Failure	23
3.3.3 Net-Tension Failure	24
3.3.4 Shear-out failure	29
3.3.5 Cleavage Failure	30
3.4 Finite Element Analysis.....	31
3.4.1 Introduction	31
3.4.2 Model development	31
3.4.3 FEA Model Validation.....	37
3.5 Analysis Schedule	42
3.5.1 Overview	42
3.5.2 Single Bolt Connection Analysis Schedule.....	43
3.5.2 Multi-Bolt (single row) Analysis Schedule.....	44
Chapter 4	
Results	45
4.1 Introduction.....	45
4.2 Single Bolt Connection.....	46
4.2.1 Net-Tension Stress.....	46
4.2.2 Shear Stress	52
4.2.3 Bearing Stress	56

4.3 Multi-Bolt Single Row Connection.....	58
4.3.1 Net-tension Stress	58
4.3.2 Shear Stress	65
4.3.3 Bearing Stress	66
4.4 Change in thickness	67
4.5 Single Bolt Failure mode prediction.....	69
4.6 Multi-Bolt Failure Mode Prediction	72
4.7 Summary of Results.....	74
Chapter 5	
Conclusion.....	76
5.1 Summary.....	76
5.2 Conclusions.....	76
5.3 Achievement of Objectives	79
5.4 Recommended Future Research	81
List of References	82

List of Figures

Figure 1 FRP reinforcing bar (PlastiComp, 2013)	1
Figure 2 Wrapping of column in FRP (Sika, 2012)	2
Figure 3 Pultruded FRP industrial staircase (dura composites, 2008).....	3
Figure 4 Bolted connections on FRP staircase (Creative Pultrusions, Inc, 2008).....	4
Figure 5 Composite lamina (FAO, 2010).....	9
Figure 6 Uni-directional fabric forming a laminate (FAO, 2010).....	10
Figure 7 The pultrusion process (Creative Pultrusions Inc, 2008).....	10
Figure 8 Tension joints failure modes a) bearing b) net tension c) shear out d) cleavage (Mottram, Zafari, 2010)	11
Figure 9 EUROCOMP (1996) evaluation method of connections. a) net-tension b) bearing c) shear-out planes.....	13
Figure 10 Methods of modelling bolt interaction a) Cosine distribution b) radial restraints and c) contact (Okutan, 2001)	14
Figure 11 Normalised bearing stress (Turvey and Wang, 2007)	15
Figure 12 Typical terminology used for connections.....	20
Figure 13 Bearing failure (Marra, 2011)	24
Figure 14 Net-tension failure (Marra, 2011)	25
Figure 15 Concept of a) infinitely wide connection b) single hole connection (Hassan, 1997)	26
Figure 16 Shear-out failure (Marra, 2011)	30
Figure 17 Cleavage failure (Mottram, 2012)	30
Figure 18 Strand7 FEA single bolt connection.....	32
Figure 19 Quad8 and Quad4 elements (Strand7, 2012)	32
Figure 20 Template of symmetrical bolt hole for model development	33
Figure 21 Element aspect ratio (University of Colorado, 2013).....	34
Figure 22 FRP mechanical properties used for analysis in Strand7	35

Figure 23 Mesh refinement with Quad4 and Quad8 elements.....	35
Figure 24 Multi-bolt connection with restraints and loading applied	36
Figure 25 Single bolt connection with restraints and loading applied	36
Figure 26 Validation results of unloaded open hole.....	37
Figure 27 Tserpes (2001) validation of open hole	38
Figure 28 Strand7 Validation of Tserpes (2001) model.....	38
Figure 29 a) Turvey (2009) bearing stress results b) net-tension stress results	39
Figure 30 Validation against Turvey (2009) with a) bearing stress and b) net-tension stress	40
Figure 31 Net-tension, bearing and shear-out failure planes of a typical joint (Turvey, 2009)	45
Figure 32 Single bolt stress concentration values	46
Figure 33 Comparison of theory and FEA results for net-tension stress.....	47
Figure 34 Net-tension stress and e/d ratio	48
Figure 35 Net-tension stress and w/d ratio	48
Figure 36 a) Net-tension stress profile $w/d=3$ b) Net-tension stress profile $w/d=7$	49
Figure 37 Net-tension stress profile comparison	50
Figure 38 Free edge stress relationship	51
Figure 39 Stress around the bolt hole edge.....	52
Figure 40 Shear stress profiles for e/d ratios on shear-out plane	53
Figure 41 Shear stress along shear-out plane for $e/d = 1$	54
Figure 42 Shear stress along shear-out plane when $e/d = 5$	54
Figure 43 Shear-stress around hole edge.....	55
Figure 44 Point of maximum shear stress in relationship to the shear-out plane.....	56
Figure 45 Bearing stress along the bearing plane	57
Figure 46 Bearing stress on the bearing plane a) $e/d = 1$ b) $e/d = 5$	58
Figure 47 Kte values for multi-bolt connections.....	59
Figure 48 Comparison of FEA and theory results for multi-bolt connections.....	59
Figure 49 Net-tension stresses in multi-bolt connections (Hassan, 1997).....	60
Figure 50 Multi-bolt net-tension stress.....	60

Figure 51 a) Net-tension stress when $w/d=4$ b) Net-tension stress when $w/d=6$	61
Figure 52 Net-tension stress when $w/d=8$	63
Figure 53 Shear and longitudinal stress around bolt hole edge	63
Figure 54 Distribution of net-tension stress on interior and exterior sides of the hole.....	64
Figure 55 Net-tension stress concentration at hole edge for connection geometry	64
Figure 56 Shear stress on shear-out plane as e/d changes	65
Figure 57 Shear stress on x-y plane for multi-bolt connection	66
Figure 58 Longitudinal stress around bolt hole edge with a change in thickness	68
Figure 59 Stress profile for net-tension plane when thickness is changed	69
Figure 60 Von Mises stress distribution showing shear-out failure to net-tension failure	70
Figure 61 Progression from net-tension to bearing failure modes	71
Figure 62 Progression from tear-out failure to net-tension failure mode	72
Figure 63 Tear-out failure a result of shear and tension stress (PADA, 2011)	73
Figure 64 Progression from net-tension failure to bearing failure mode.....	74

List of Tables

Table 1 Suggested geometric ratio's for FRP connections (Mottram, 2002).....	19
Table 2 Exel Composites (2012) Mechanical properties of FRP.....	21
Table 3 Comparison of net-tension stresses between theory, contact and radial modelling.....	41
Table 4 Comparison of bearing stress against Turvey (2009)	41
Table 5 Comparison of recommended geometry for single and multi bolt tension joints.....	42
Table 6 Analysis schedule for single hole tension joints.....	43
Table 7 Multi-bolt joint analysis schedule.....	44
Table 8 Percentage of peak stress as w/d changes	50
Table 9 Percentage of peak stress along shear-out plane	53
Table 10 Percentage of stress to peak stress along the bearing plane	57
Table 11 Percentage of stress along net-tension plane with a change in w/d	62
Table 12 Percentage of peak shear stress halfway along shear-out plane	65
Table 13 Percentage of stress on bearing plane as e/d changes	67
Table 14 Suggested connection geometry from research	78
Table 15 Steel and FRP minimum geometry	79

List of Appendices

Appendix A	Project Specification	85
Appendix B	Theoretical Calculations.....	86
Appendix C	Net-tension plots.....	87
Appendix D	Shear stress plots.....	91
Appendix E	Bearing stress plots	96
Appendix F	Theoretical data for thickness effects	101
Appendix G	FEA plots - minimum and recommended joint ratio's.....	102

Nomenclature

e	edge distance
w	width
d	diameter of bolt hole
s	side distance from hole centre to free edge
g	gauge distance between hole centres on multi-bolt connection
k_{tc}	composite material stress concentration factor
k_{te}	elastic stress concentration factor
C	correlation coefficient
E_1	longitudinal Young's modulus (y axis) (GPa)
E_2	transverse Young's modulus (x axis) (GPa)
E_3	Young's modulus z axis (GPa)
ν_{21}	major in-plane Poisson's ratio
G_{12}	in-plane shear modulus (GPa)
σ_b	bearing stress (MPa)
σ_{nt}	net-tension stress (MPa)
τ_s	shear stress (MPa)
σ_y	stress along the longitudinal axis (MPa)
τ_{xy}	shear stress on the x-y plane (MPa)
δ	fastener diameter to pitch ratio
p	pitch spacing of bolt holes along row
P	load imposed at bolt hole location (kN)
t	thickness of plate
n	number of bolt holes
FRP	Fibre Reinforced Polymer
PFRP	Pultruded Fibre Reinforced Polymer

Chapter 1

Introduction

1.1 Background

Fibre reinforced polymers (FRP) have been used in civil construction for over 50 years but it has only been in the last 10 years that there has been considerable growth in FRP use particularly in construction and rehabilitation of existing structures. Historically the first use of FRP for civil applications was for reinforcing bars and mesh for concrete slabs mostly due to the corrosive resistance of FRP over traditional steel reinforcement.

During the 1980's research and development was taking place in the use of FRP for bridge decks and for uses in other corrosive environments such as coastal and industrial uses. This led to a handful of manufacturers to start producing FRP bars and mesh on a larger scale and has now become common practise for use in highly corrosive environments such as underground tunnels, bridges and manufacturing.



Figure 1 FRP reinforcing bar (PlastiComp, 2013)

In the 1980's FRP was first used to strengthen concrete structures typically by wrapping columns or beams by using hand lay-up with sheets of either carbon or glass FRP. To date this is still widely used and is effective to strengthen structural members to comply with updated building codes or for adding strength to degrading structural members.



Figure 2 Wrapping of column in FRP (Sika, 2012)

The civil construction industry makes use of mostly pultruded FRP sections (PFRP) which describes the manufacturing process to produce profiles of a constant cross section suitable for load bearing purposes. The use of FRP in bridge construction and industrial applications are areas that have seen considerable growth over the years mostly due to the light weight and non-corrosive properties. This particularly holds true for the applications to retro fit degrading bridge decks where the ability to replace the heavy and corroded concrete or timber deck with a light weight FRP deck would not only protect against corrosion but also allow a reduction in dead weight of the structure (Heslehurst, 2013).

FRP use in single and multi-level construction has been limited to mostly industrial uses such as cooling towers or structures that are susceptible to corrosion such as in manufacturing as seen in figure 3 below which shows a pultruded FRP industrial staircase ready for installation. The lack of codes and guidelines particularly with regards to connecting

members has limited growth in the residential and commercial areas (Bank, 2008) and although research has taken place in this area there is still no effective connection method for pultruded FRP.



Figure 3 Pultruded FRP industrial staircase (dura composites, 2008)

The connections are typically either bonded or mechanical connections when used with pultruded members. Mechanical connections for civil applications typically consist of either steel or FRP bolts which are used to connect structural members with the aid of a gusset plate. Bolted connections have become the preferred method of joining members mostly due to the constructability aspect and the advantage of being able to replace structural members with ease if necessary or to carry out maintenance inspections. This would not be possible with bonded connections. In Figure 4 below a typical bolted connection is shown on an industrial staircase and platform. Usually, bolted connections would consist of either high strength stainless steel bolts or FRP bolts with a smooth shaft.



Figure 4 Bolted connections on FRP staircase (Creative Pultrusions, Inc, 2008)

The problems associated with construction with FRP and particularly FRP connections is that there is a vast number of PFRP manufacturers designing and selling products of various structural properties and different manufacturing processes which make predicting the failure of the connection difficult. This combined with the brittle and orthotropic nature of the material makes designing connections a challenge. Guidelines have been set up by EUROCOMP in 1996 as well as the American Society of Civil Engineers (ASCE) in 2011 to offer assistance to engineers in designing structures and connections in FRP giving the most up to date and accurate data available for design purposes as we know. Since these guidelines have been published there has been continued growth in the use of PFRP in structures and is becoming more widely accepted as a construction material.

1.2 Objectives of research

The main objectives of this research are to:

1. Conduct a literature review into bolted FRP connections and determine areas that are lacking research or credible data that would be useful for advances in the FRP industry.
2. Use Finite Element Analysis (FEA) to model and show behaviour and effects of geometry changes on various bolted connections. Material properties from pultruded manufacturers will be used to determine stresses and behaviour of a tension joint when edge distance, width, gauge and side distance dimensions are varied.
3. Use theoretical calculations to calculate stress concentrations and investigate the failure mode of the connection under various geometric parameter changes.
4. Investigate FEA results and theoretical results and suggest recommended geometry for bolted connections based on these results.
5. Compare results to EUROCOMP and other research data to verify or critique current guidelines.

1.3 Structure and Outline

This research includes chapter 1 where a brief background and history of its FRP use will be discussed as well as the different applications of FRP and pultruded members in the civil construction industry.

A detailed literature review indicating past and present research in bolted connections is given in chapter 2. The main focus of the literature review is the progress and research done in the area of tension lap joints in pultruded FRP. Ultimate stresses and failure modes of the tension joints will be reviewed with particular attention focused on analysis methods and joint geometry from the research papers. The different recommendations from researchers for joint geometry compared to the current guidelines such as EUROCOMP 1996 will be examined.

Chapter 3 includes the methodology of the research from the theoretical investigations to Finite Element Analysis (FEA) of the tension joints being studied. The theoretical investigation will use known equations to predict stress and the study of failure modes. The FEA will analyse the same joints as the theoretical study and behaviour will be examined through varying the geometry of the connections and validation of the model will occur through comparison of theoretical and FEA results.

The results of the validation will be discussed in chapter 4 and suggestions made into minimum and recommended joint design geometry for the tension lap joints being studied. The suggestions will be based on the parametric study conducted in chapter 3.

Chapter 5 will include a conclusion of the results and recommendations for potential future work.

1.4 Scope of research

In an effort to simplify the analysis procedure some assumptions have been made with some data and conclusions made by previous research assumed correct without further validation. The following points will outline important aspects of the research and limitations imposed.

- FEA will be orthotropic homogeneous in 2 dimensions
- Material is assumed to be perfectly elastic in theory and FEA
- Bolt hole clearance is zero
- Bolted lap-joints simplified to "pin loaded" with only a single lap analysed
- Only stress analysis will be performed on the x-y plane
- Failure will not be investigated due to homogeneous limitations and lack of composite ply data
- Analysis will be linear only

Chapter 2

Literature Review

2.1 Introduction

Fibre reinforced polymers (FRP) consist of two major constituents, the reinforcing fibres and the matrix as shown in figure 5 below. The fibres typically consist of thousands of individual continuous fibres bundled together and may be in the form of the following;

- Glass fibres are the most common used in civil structural applications due to the relative lower cost compared to carbon and Aramid products. The E-glass (electrical glass) is used predominantly due to its electrical resistivity in structural engineering (Bank, 2006).
- Carbon fibres are much lighter than Glass and typically have a higher tensile modulus giving a stiffer material. Carbon is more suited to FRP strengthening strips or prestressed tendons in the civil industry. The aerospace industry has used the light weight and high stiffness characteristics to their advantage by manufacturing airframes and aerospace products out of carbon (Bank, 2006).
- Aramid fibres were used widely in civil application in the 1980's mostly to produce prestressing tendons (Bank, 2006). Due to the high costs and high moisture absorption and lack of fire resistance they are rarely used in the civil industry today.

The matrix or resin is needed to bond the fibres together to form a structural element that can withstand loads (Jones, 1999). Not only is the matrix used in bonding but it also protects

the fibres and can transfer stresses between broken fibres. For civil application the thermosetting resins are most widely used and can be broken down into three main types;

- Polyester resins are mostly used in the pultrusion industry to make FRP profiles for structural engineering.
- Epoxy resins are typically used with carbon products in the aerospace industry and in civil applications used to bond reinforcing strips to concrete.
- Vinyl ester resins are also widely used for structural uses such as pultrusion due to their corrosion resistance and ease of manufacturing (Vipel, 2012).

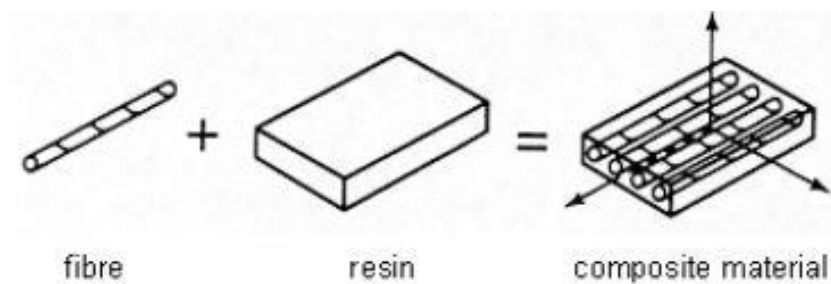


Figure 5 Composite lamina (FAO, 2010)

One benefit of FRP is that through using multiple laminas (single layer) and varying the orientation of the fibres a material can be designed specifically according to the loading environment of the structure (Jones, 1999). Typically a laminate will consist of uni-directional plies oriented and arranged according to the principle axis and then bonded together with resin and can be seen in figure 6 below. These laminates are used in pultruded profiles, sheets and mouldings and allows for specifically designed strength and failure characteristics.

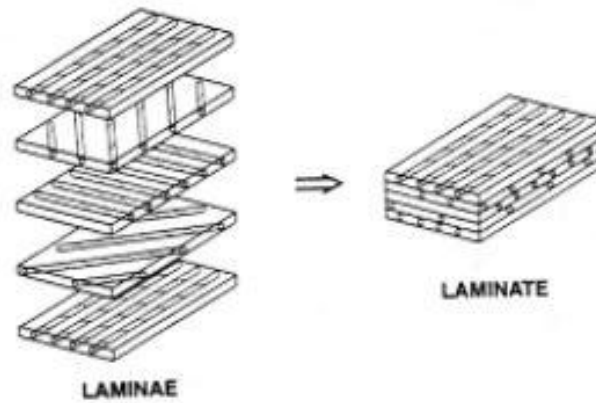


Figure 6 Uni-directional fabric forming a laminate (FAO, 2010)

For the civil construction industry the manufacture of FRP profiles is accomplished through the pultrusion process. This process uses uni-directional rovings and mats which are covered in resin and pulled through a heated die. Inside the die the resin cures and exits in a solid state in the shape of the desired profile (Creative Pultrusions, 2008).

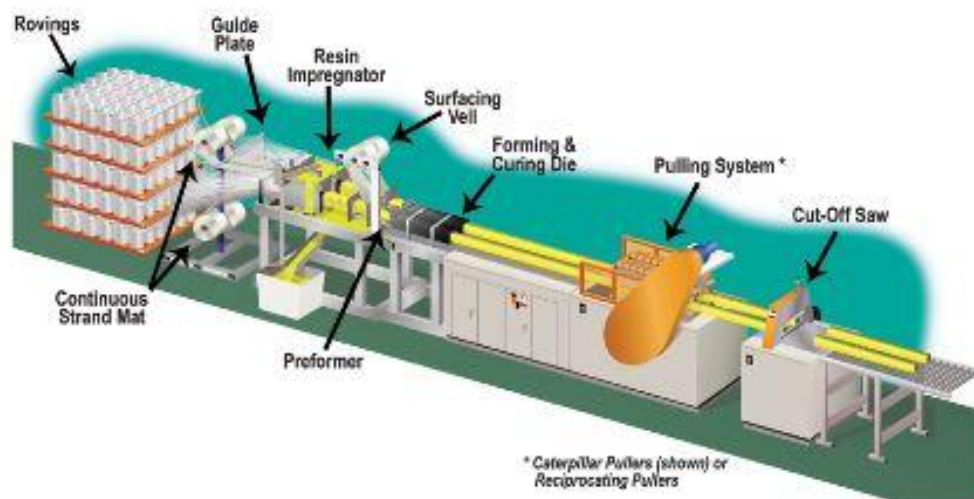


Figure 7 The pultrusion process (Creative Pultrusions Inc, 2008)

This pultrusion process as illustrated above in figure 7 enables any length of profile or cross section to be manufactured in large quantities.

2.2 Bolted Connections

Bolted or mechanical connections may come in the form of bolts, screws or rivets. They are the preferred method of joining members due to the relative ease of construction and they enable inspections and maintenance to take place in the future in a less restrictive manner. Bolts are more commonly used in civil applications due to their higher strength and control over the clamping force (Rosner, 1992) unlike screws and rivets which generally have a lower load carrying capacity.

The main disadvantage with bolted connections is the high stress concentrations created from the bolt holes (Park, 2009) particularly in pultruded and composite materials. The orthotropic nature of composites makes the design of connections and joints much more complex compared to an isotropic material such as steel. The reason for this is the number of failure modes, changes in material properties with orientation of fibre, linear elastic nature and lack of ductility of composites (Mottram, 2009).

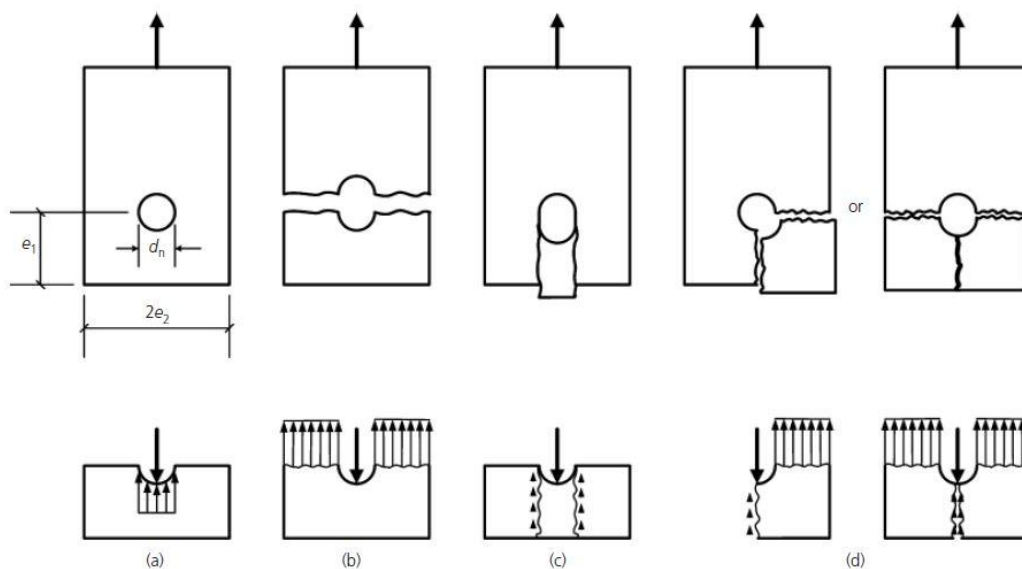


Figure 8 Tension joints failure modes a) bearing b) net tension c) shear out d) cleavage

(Mottram, Zafari, 2010)

Failure modes in tension joints can be described as bearing, net tension, shear-out, cleavage or a combination as can be seen in Figure 8 above. In addition to these, bolt failure or pull-through may occur. The factors that directly influence failure mode is the joint geometry (Mosallam, 2011) with emphasis on edge distance and width.

Failures in bearing are considered less catastrophic and occur at the contact point between the bolt and the composite which generates a buckling compressive force in the lamina when excessive stress occurs (Mosallam, 2011). Typically a shear-out failure will occur when the end distance is short with high shear stresses along the bolt hole edge and on the shear-out plane. The net tension failure would typically occur when the bolt hole to width ratio (d/w) is high creating a compressive stress on the bearing area and tension stress along the net section (Broughton, 2002).

In recent years researchers have investigated and performed both experimental and analytical testing on Pultruded FRP (PFRP) materials to get a better understanding of the failure modes and behaviour in order to establish guides and standards for FRP connections. Data gathered lead to the creation of the EUROCOMP design code and guidelines for pultruded member which was published in 1996. There has been some doubt over the accuracy and assumptions made with the simplified method of the EUROCOMP code (Turvey & Wang, 2007) particularly in regards to friction and lack of clearance holes in the analysis.

The EUROCOMP design guide (1996) specifies methods for determining failure of lap-joints with compliance check's to be made along critical failure planes namely the net-tension, shear-out and bearing planes. The net section should be examined from the hole edge to the free edge and if the characteristic strength of the of the material is reached then failure is expected to occur. Bearing failure is expected to occur when the radial stress in any area of

the bearing contact area exceeds the characteristic compressive strength seen in figure 9, while the shear-out stress should be defined by analysis of the shear-out planes if the maximum shear stress exceeds that of the characteristic shear strength of the laminate.

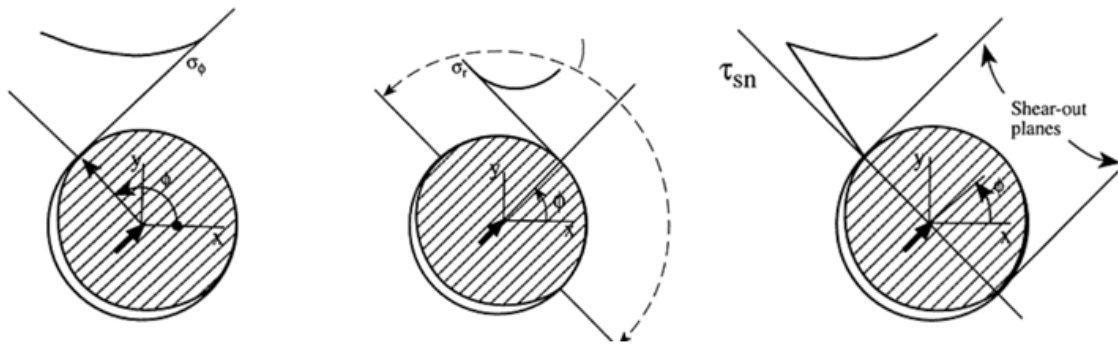


Figure 9 EUROCOMP (1996) evaluation method of connections. a) net-tension b) bearing c) shear-out planes

Manufacturers of pultruded FRP have developed guides based on their own in-house tests and research however the approach is similar to that of isotropic ductile materials rather than elastic brittle materials such as FRP (Turvey, Wang, 2007). Manufacturers such as Strongwell, Creative Pultrusions Inc and Fiberline have all produced design manuals to cater for their customers using only their products.

2.3 Single and Multi-bolt Finite Element Analysis (FEA) research

Okutan (2001) investigated stress and failure in composite tension joints for his PhD thesis using both FEA and experimental results. The importance of modelling FEA correctly to get representative results was shown in the methodology for the model development. Representation of the bolt and connection interaction was investigated through use of the cosine distribution, contact elements and radial displacement restraints as seen in figure 10 below. It was found that the radial displacement restraint of the hole edge nodes provided fast

and accurate data for stress distributions when compared with the non-linear contact method and cosine distribution of pressure.

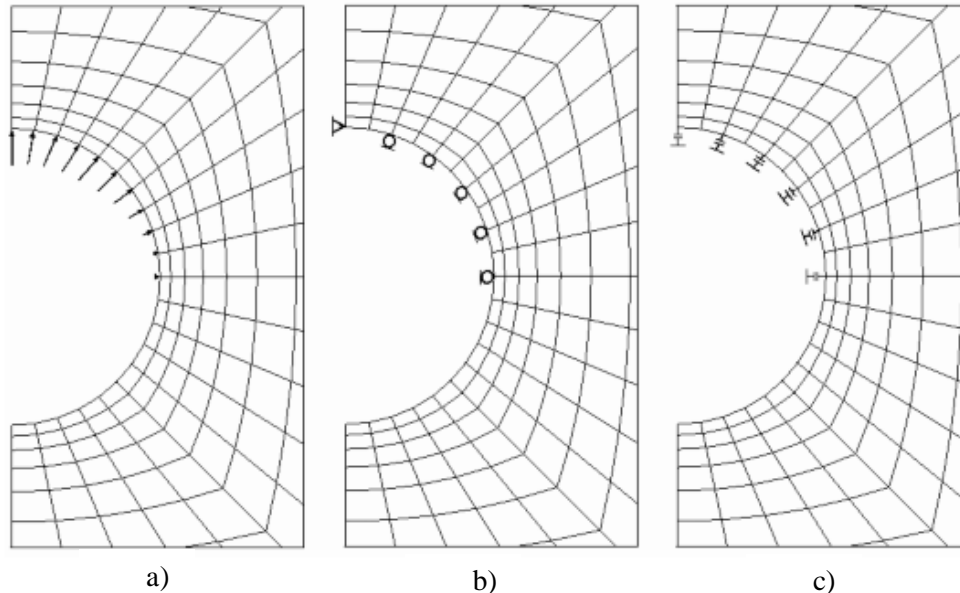


Figure 10 Methods of modelling bolt interaction a) Cosine distribution b) radial restraints and c) contact (Okutan, 2001)

Turvey and Wang (2007) used finite modelling to investigate the failure and stresses under various loads in a single bolt configuration with a nominal hole clearance of zero. The results presented were for only one geometric parameter giving a bearing failure mode and showed that single curve normalized stress distributions do not apply to civil construction as clearance holes and friction should be accounted for as they are always present. This research shows the EUROCOMP simplified method which is based on the assumption that all stresses when normalized should fall to a single curvature is not entirely accurate. In figure 11 below the normalised values do not fall to the single curve as required by the EUROCOMP guidelines.

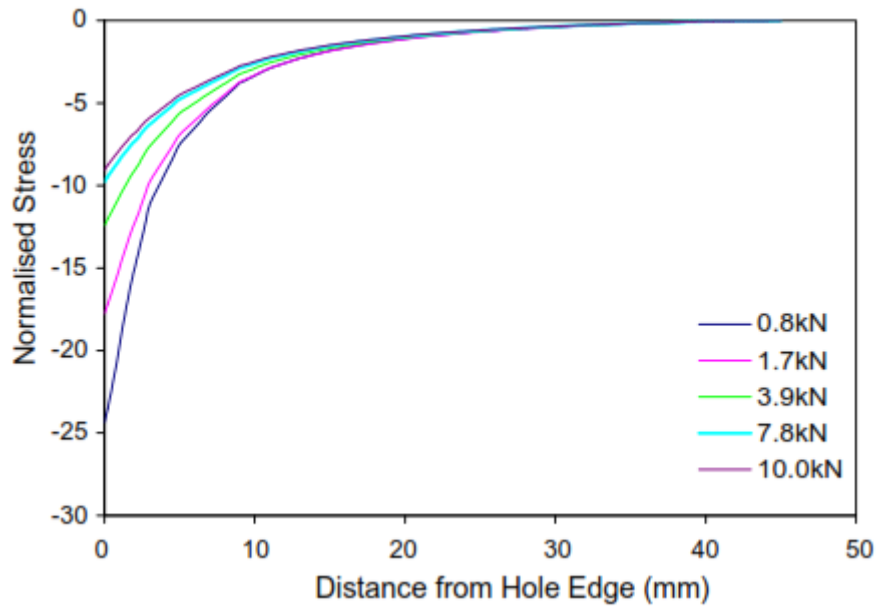


Figure 11 Normalised bearing stress (Turvey and Wang, 2007)

Park, Lee, Joo and Yoon (2009) also investigated the effects of geometry and failure modes on one, two and four bolt connections under single lap shear configuration. The finite element analysis was done in parallel to experimental tests and showed that there were differences in results between the two test methods. Although the data indicates minimum e/d ratios the results vary significantly which only stresses the need for further research. The conclusion on the variation in results can be attributed to most likely errors in the finite element modelling and the limited number of test specimens used in experimental testing.

Results obtained from McClendon (2011) from FEA research into bearing stress behaviour on FRP material revealed that quasi-isotropic material could achieve the highest bearing stresses in comparison to uni-directional and angled ply. This study used ANSYS to model three different materials properties using glass-epoxy under a pin-loaded scenario without the consideration for frictional effects or clearance holes for bolts in the analysis. Uni-directional results for net-tension were under estimated by ANSYS with accurate representation of the bearing and shear-out planes. Discrepancies in this case could be due to

the homogeneous lay-up performed for the analysis which may have lead to errors in the stress normalization procedure as well.

A recent study done by Feo, Marra and Mossallam (2012) used finite element modelling to find the shear stress distributions around bolt holes on one, two, four, nine and sixteen hole configurations, with and without washers. The finite element model results were compared to experimental testing using strain along the longitudinal axis as a comparison. The conclusions made are that the load is not distributed equally due to the varying bolt position, bolt hole clearance and washer size. It was concluded that the optimal washer size was $2d_b$. The shear stress distribution were representative of Ascione (2010) who investigated the shear stress distributions on a 3x3 double lap shear connection which showed less than 5% variation between the two studies.

2.4 Experimental Analysis

Researchers such as J. Turvey and C. Rossner have done extensive experimental testing into the failure of bolted FRP joints. The testing regime is typically done under a double lap shear configuration on pultruded flat plates manufactured by the popular pultrusion manufacturers such as Creative Pultrusions Inc. Investigation into the failure modes and strain values around the joints has been researched extensively with mixed results.

Cooper and Turvey (1995) performed experimental tension testing on single bolt connections under double lap shear configuration to determine the effects of geometry changes notably e/d and w/d changes as well as bolt clamping force on the pultruded flat test specimen. The thickness of the test specimen was 6.35mm and results showed that the minimum e/d and w/d were 3 and 4 respectively. It was also noted that the clamping force of the bolt had a significant effect on the failure load of the specimen increasing from 45% to 80% for snug fit bolt and 30Nm torque bolt compared with a single pin joint.

Hassan (1997) used experimental data to investigate a rational model for multi-bolt connections. The net-tension failure mode was studied to determine if an elastic stress concentration factor could be used combined with a cleavage reduction factor to predict failure as compared to experimental results. The results show that provided sufficient experimental results are obtained on strength properties with different orientations of fibre an accurate prediction can be made.

Turvey (2011) performed further experimental testing on single bolt connections this time under single lap shear configuration. The test used 6.35mm thick EXTREN© 500 flat plate from Creative Pultrusions Inc and investigated the effects of geometry change on the ultimate failure load of the specimen. The test used a snug fit 10mm bolt with a 0.2mm clearance hole

with a smooth shank. The experimental results showed that as the e/d ratio approached 2.5 there is a rapid increase in ultimate load and above 3 the effects are fairly constant. Changes made to the w/d ratio have little effect on ultimate load. From the results it was concluded that a threshold value e/d should be at least 3.

Experimental testing on EXTREN© Inc. flat pultruded sheet was also undertaken by Rossner (1992) for his Master's thesis on single bolt connections on pultruded materials. This investigated the effects of geometry changes on various thicknesses of pultruded sheet as well as the effects of fibre orientation. The test results showed that the main failure modes were bearing, net-tension and cleavage failure with no shear-out failure seen most likely due to the effects of transverse fibre orientation. The effects of geometry change indicated that recommended w/d and e/d values are both 5 based on uni-directional test specimens. The effects of increasing the thickness of the material had little effect on failure mode however the ultimate load was increased. The conclusions made show conflict with Turvey's research performed on EXTREN© sheets of a lesser thickness and is reason for further investigation.

Lee, Choi and Yoon (2014) performed tension testing on pultruded plates cut from I-sections and angled FRP. Each of the three plates consisted of different properties and thicknesses to study the behaviour of geometry changes on the failure modes of bolted connections. The experimental tests consisted of only single bolt connections performed under a double lap configuration. The results of the investigation showed that an e/d ratio of below 3 had a strong influence on not just the failure load but also the failure mode. The study recommended an e/d ratio of at least 4 which is in line with the ASCE guidelines. The research also suggests a w/d ratio of at least 3 to allow for bearing failure rather than a more catastrophic failure such as net tension.

2.5 Conclusion

The various recommendations for joint geometry has been tabulated below in table 1 (Mottram, 2002) and shows the vast number of different geometric ratio's being suggested by researchers and manufacturers as well as EUROCOMP (1996).

Table 1 Suggested geometric ratio's for FRP connections (Mottram, 2002)

Source	Plate thickness t (mm)	Bolt diameter / Plate thickness D/t	Edge distance / Bolt diameter E/D	Side distance / Bolt diameter S/D	Width distance / Bolt diameter W/D	Clearance hole size (mm)	Washer diameter / Bolt diameter
Strongwell (1989)	6.35 to 19.05	1.0 to 3.0	2.0 to 4.5 (3) ¹	1.5 to 3.5 (2) ¹	4 to 5 (5) ¹	1.6	-
Fiberline (1995)	3 to 20	0.5 to 16.0	2.5 & 3.5	2.0	4	1.0	2
EUROCOMP ² (1996)	Unspecified	1.0 to 1.5	≥ 3	≥ 0.5W/D	≥ 3	≤ 0.05D	>2
Creative Pultrusions (1999)	6.35 to 12.7	Unspecified	2.0 to 4.5 (3.0) ¹	1.5 to 3.5 (2.0) ¹	4 to 5 (5.0) ¹	1.6	2.5
Rosner & Rizkalla (1995)	9.53 to 19.05	0.5 to 1.0	5 ³	Single-bolt	5 ³	1.6	-
Cooper and Turvey ⁴ (1995)	6.35	1.6	3	Single-bolt	4	Close fit (0.1 to .3)	-

Notes: 1. Recommended minimum design value. 2. General glass fibre reinforced plastics (including PFRPs). 3. D is hole diameter (bolt diameter and hole clearance). 4. From joint tests with tensile load in direction of pultrusion.

Due to the large array of recommendations and lack of standards available for pultruded connections more data is needed into the behaviour of FRP joints and the reason for variations should be outlined so as to provide better assistance for guidelines to be developed in the future.

Chapter 3

Methodology

3.1 Introduction

The investigation into the behaviour of FRP bolted tension joints will consist of a theoretical study as well as Finite Element Analysis of single bolt and multi-bolt tension joints in pultruded material. A parametric study will take place with regards to joint geometry to analyse the behaviour of the joints at ultimate failure loads. Parameters investigated will be e/d , w/d , g/d and s/d ratio's shown on figure 12 below on two different plate thicknesses with similar material properties. The investigation will determine failure modes such as bearing, net-tension, shear out and cleavage under different joint geometry and the stress behaviour analysed.

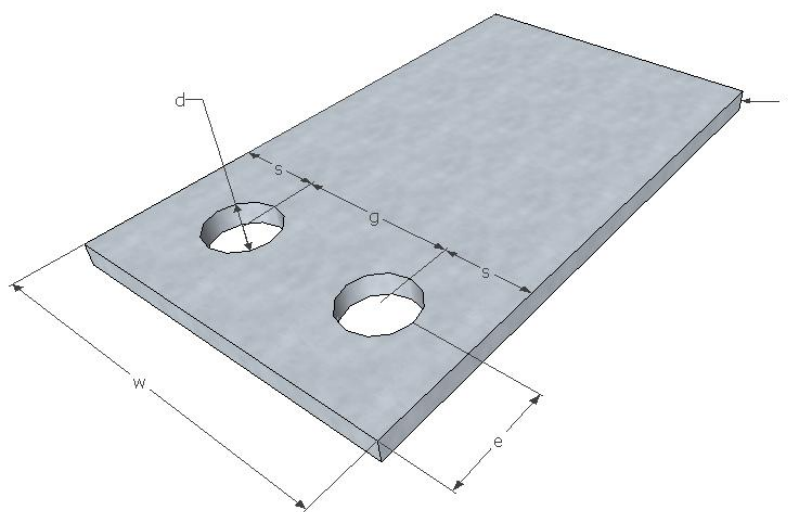


Figure 12 Typical terminology used for connections

3.2 Material Properties

3.2.1 Pultruded plate properties

In an effort to apply this research to the real world the material properties from an Australian pultrusion manufacturer will be used. The properties from two different PFRP plates will be used from Exel Composites© consisting a polyester-resin Series 500 6.4mm plate and a Vinyl-ester resin Series 650 9.5mm plate. Material properties are shown in figure below courtesy of Exel Composites© (2012).

Table 2 Exel Composites (2012) Mechanical properties of FRP

MECHANICAL PROPERTY	ASTM TEST	UNITS	SERIES 500 / 525	SERIES 625
Tensile Stress (L)	D638	MPa	207	207
Tensile Stress (C)	D638	MPa	48.3	48.3
Tensile Modulus (L)	D638	GPa	17.2	17.9
Tensile Modulus (C)	D638	GPa	5.52	5.52
Compressive Stress (L)	D695	MPa	207	207
Compressive Stress (C)	D695	MPa	103	110
Compressive Modulus (L)	D695	GPa	17.2	17.9
Compressive Modulus (C)	D695	GPa	6.89	6.89
Flexural Stress (L)	D790	MPa	207	207
Flexural Stress (C)	D790	MPa	68.9	68.9
Flexural Modulus (L)	D790	GPa	11.0	11.0
Flexural Modulus (C)	D790	GPa	5.52	5.52
Modulus of Elasticity, E	Full Section	GPa	17.9	19.3
Modulus of Elasticity, E* *W & I Shapes > 100mm	Full Section	GPa	17.2	17.2
Parallel Compressive Shear Stress (L)	D3846	MPa	20.7	20.7
Shear Modulus (L)	-	GPa	2.93	2.93
Short Beam Shear (L)	D2344	MPa	31.0	31.0
Bearing Stress (L)	D953	MPa	207	207
Poisson's Ratio (L)	D3039	-	0.330	0.330
Notched Izod Impact (L)	D256	J/mm	1.33	1.33
Notched Izod Impact (C)	D256	J/mm	0.214	0.214

In table 2 above the (L) being lengthwise or long axis and (C) being crosswise or short axis. In the case of this research (L) is the Y axis and (C) is the X axis.

3.2.2 Bolt properties

As the research is focused on the behavioural aspects of the joint and not failure of the bolt in any way the scope will not consider bolt failure. Therefore the bolts strength and modulus will be considered as infinity.

3.3 Theoretical Study

3.3.1 Overview

Determining the stresses of in-plane lap joints can be estimated through equations presented by Bank (2006) which are based on one dimensional mechanics and assume linear elastic material behaviour. Because of the orthotropic nature of the FRP material Heslehurst (2013) has published refined stress prediction equations based on research completed by Hart-Smith (1979). The biggest difference between the analysis of isotropic and orthotropic material using these equations are the stresses at the bolt hole are a combination of hoop and bearing stresses (Heslehurst, 2013).

Failure modes of FRP tension joints can be one or a combination of the following:

- Bearing failure
- Net-tension failure
- Shear out failure
- Cleavage failure (combination of net-tension and shear out)

3.3.2 Bearing Failure

Bearing failure is considered less catastrophic than other failures modes and more of a ductile or gradual failure of the bearing area. The bearing area is considered the contact area between the bolt and the FRP material with failure occurring due to compressive stresses buckling or kinking the fibres leading to delamination (Mosallan, 2011). Bearing failure in composites is usually a combination of buckling, fibre kinking and matrix crushing and will

induce a stress concentration factor (Heslehurst, 2013) similar to elastic isotropic material but with reduced stress. A typical bearing failure can be seen in figure 13 below showing the bearing contact area undergoing compressive failure.

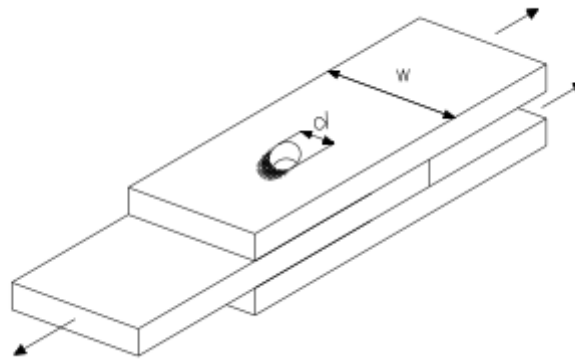


Figure 13 Bearing failure (Marra, 2011)

Calculation of the average bearing stress in the base material at the bolt hole can be represented by:

$$\sigma_{br} = \frac{P}{dt} \quad (3.1)$$

Where P is the load transferred at the bolt, d is the bolt diameter and t is the plate thickness.

3.3.3 Net-Tension Failure

Net-tension failure will occur along the net section due to unfavourable joint geometry such as low w/d ratio's. When the strength properties of the material are exceeded failure will occur initially at the stress concentration located at midpoint on the hole edge and will propagate towards the free edge along the net section as seen in Figure 14 below:

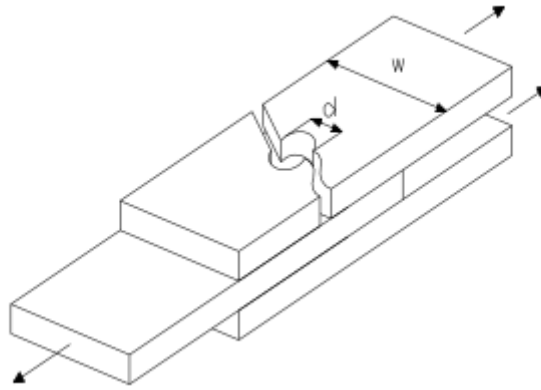


Figure 14 Net-tension failure (Marra, 2011)

The maximum stress along the net section adjacent to the bolt hole can be found through the equation:

$$\sigma_{net} = \frac{P}{A_{net}} \quad (3.2)$$

where P is the load transferred at the joint and A_{net} is the cross sectional surface area of the net section through the bolt hole with A_{net} being:

$$A_{net} = t(w - nd) \quad (3.3)$$

where w is the width of the plate, n is the number of bolts in a row and d is the bolt hole diameter.

For single bolt connections a correction factor must be used to calculate the stress concentration at the hole edge to allow for the various joint geometry. An elastic concentration factor (K_{te}) will be used published by Heslehurst (2013) and is as follows:

$$K_{te} = 2 + (a + 1) - \left[\frac{3(a+1)}{2(a+1)} \right] \theta \quad (3.4)$$

where,

$$\alpha = \frac{w}{d}, \beta = \frac{e}{w}$$

and,

$$\theta = \frac{3}{2} - \frac{1}{2\beta} \quad \text{for} \quad \beta \leq 1$$

$$\theta = 1 \quad \text{for} \quad \beta > 1$$

For multi-bolt connections assuming an infinitely wide panel the Kte value is calculated differently to allow for the slightly higher stress concentration on the interior side of the bolt hole. In figure 15a below an explanation of an infinitely wide panel is shown with p being the distance between bolts. Figure 15b shows a single bolt connection with w being the width of the plate.

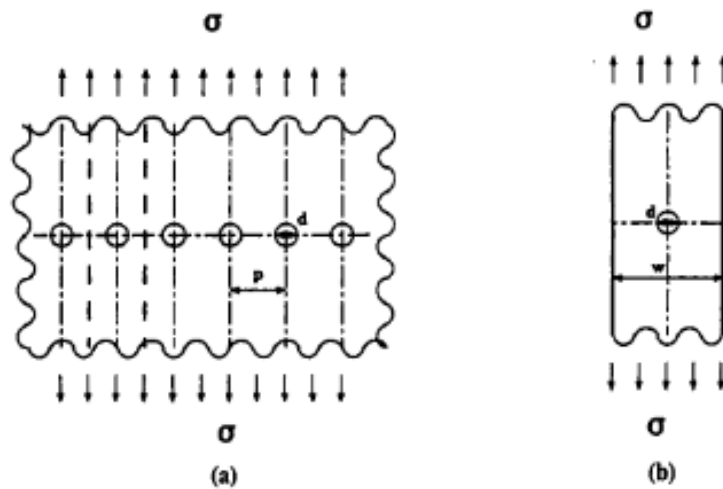


Figure 15 Concept of a) infinitely wide connection b) single hole connection (Hassan, 1997)

The appropriate concentration factor for brittle elastic materials with multiple bolts in a single row has been published by Heslehurst (2013) and is as follows:

$$K_{te} = 1 + (1 - \delta^2)^{2.41} + \frac{1-\delta}{\delta} - \frac{3}{2} \left[\frac{1-\delta}{1+\delta} \right] \theta \quad (3.5)$$

where,

$$\delta = \frac{d}{p}$$

and,

$$\theta = \frac{3}{2} - \frac{1}{2\beta} \quad \text{for} \quad \beta \leq 1$$

$$\theta = 1 \quad \text{for} \quad \beta > 1$$

With the Kte factor introduced the net-tension stress for loaded bolt hole under tension for a perfectly elastic material can be estimated by the equation from Hart-Smith (1979):

$$\sigma_{net} = \frac{K_{te}P}{(w-nd)t} \quad (3.6)$$

Where,

P = load applied to the bolt

t = thickness of plate

w = width of plate

n = number of bolt holes

d = diameter of bolt hole

It is also assumed that the material is a perfectly elastic brittle composite and therefore $K_{te}=K_{tc}$. The assumption that all only a uni-direction ply exists and runs in the 0° orientation allows for $C=1$. With C being the constant of proportionality. Since,

$$C \approx \frac{P_0}{100} \quad (3.7)$$

where P_0 is the percentage of 0° ply's in the material.

Hart-Smith (1979) has published the general relationship between elastic and composite material as:

$$K_{tc} = C(K_{te} - 1) + 1 \quad (3.8)$$

For perfectly elastic material when the applied stress reaches the tensile strength of the material initial failure will occur through crack propagation and failure will become catastrophic (Rosner, 1992) through the net section.

For calculation of single hole net-tension stresses in single loaded bolt hole joint the equation 3.4 should be substituted into equation 3.6 and for multi-bolt single row joints the net-tension stress concentration can be found through substituting equation 3.5 into equation 3.6.

For *open hole* conditions when there is no bolt load and only tension is applied at the plate edges the stress values in the longitudinal axis (σ_y) can be calculated using a closed form equation (Callus, 2007) along the net-tension plane and is as follows:

$$\sigma_y(x,0) = \frac{\sigma^\infty}{2} \left\{ 2 + \left(\frac{r}{x}\right)^2 + 3\left(\frac{r}{x}\right)^4 - (K_T^\infty - 3) \left[5\left(\frac{r}{x}\right)^6 - 7\left(\frac{r}{x}\right)^8 \right] \right\} \quad (3.9)$$

where σ^∞ is the nominal stress applied, r is the radius of the hole, x is the distance along the net-tension plane from the hole centre and K_T is the orthotropic correction factor (equation 3.10).

Since there is no yielding in composite materials and high inter-laminar stresses are developed around the bolt hole Heslehurst (2013) has published a correction factor that

should be applied to single open hole, with no bolt, brittle, and orthotropic materials. The *single open hole* composite stress concentration factor or k_{tc} can be expressed as:

$$k_{tc} = 1 + \sqrt{2 \sqrt{\left[\frac{E_1}{E_2} - \nu_{21} \right]} + \frac{E_1}{G_{12}}} \quad (3.10)$$

where,

E_1 = longitudinal modulus

E_2 = transverse modulus

G_{12} = in-plane shear modulus

ν_{21} = major in-plane Poisson's ratio

3.3.4 Shear-out failure

Shear-out failure occurs when the end edge distance or the e/d ratio is low giving a high shear stress gradient along the shear-out plane. Failure will occur when the area below the bolt hole is torn out and is shown in figure 16 below. As the e/d ratio is increased typically maximum shear stress will decrease and the gradients will decrease indicating failure is less likely.

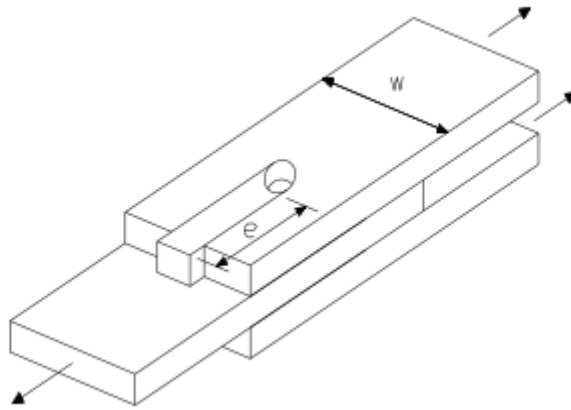


Figure 16 Shear-out failure (Marra, 2011)

3.3.5 Cleavage Failure

The cleavage failure is a combination of both the shear-out and net-tension failure and can be seen in figure 17 below where the quarter section is torn out due to both shear and tensile failure occurring simultaneously as indicated by the blue arrow. This is usually attributed to low e/d and w/d ratio's with fibre orientation also playing a role in failure.

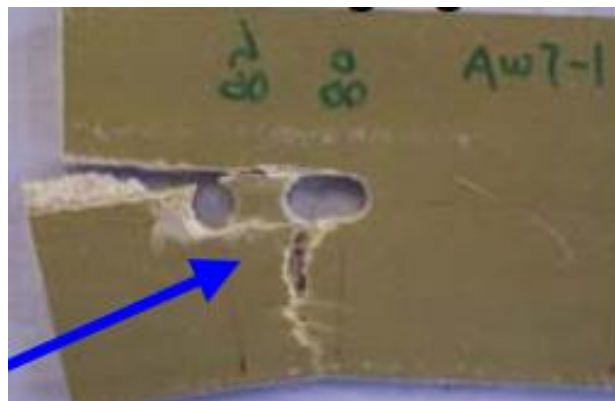


Figure 17 Cleavage failure (Mottram, 2012)

3.4 Finite Element Analysis

3.4.1 Introduction

Strand7 Finite Element Analysis (FEA) software will be used to analyse both the single and multi-hole tension joints. The pultruded material will be analysed as an orthotropic homogeneous material as the manufacturer has supplied all necessary data for this analysis without the need to make unnecessary assumptions with regard to laminate material properties. As the FRP material being analysed is considered a plate with the length and width greater than the thickness the analysis will only take place on the x and y axis (2D).

3.4.2 Model development

This research program will use a similar approach as Turvey and Wang (2008) to develop a simple but representative model that will accurately show stress distributions necessary for the research. Symmetry will be used to model the plate models as the geometry and loading will be identical on either side of the longitudinal axis (Strand7, 2010) giving the same stress distributions. Not only does this reduce analysis time but the model will also be simplified to omit unnecessary duplicated data. This is of particular importance when fine meshes are used such as in this research or if the model is large and complex. In figure 18 below an example of the single hole connection can be seen with loading taking place in the longitudinal axis with the line of symmetry acting through the middle of the hole.

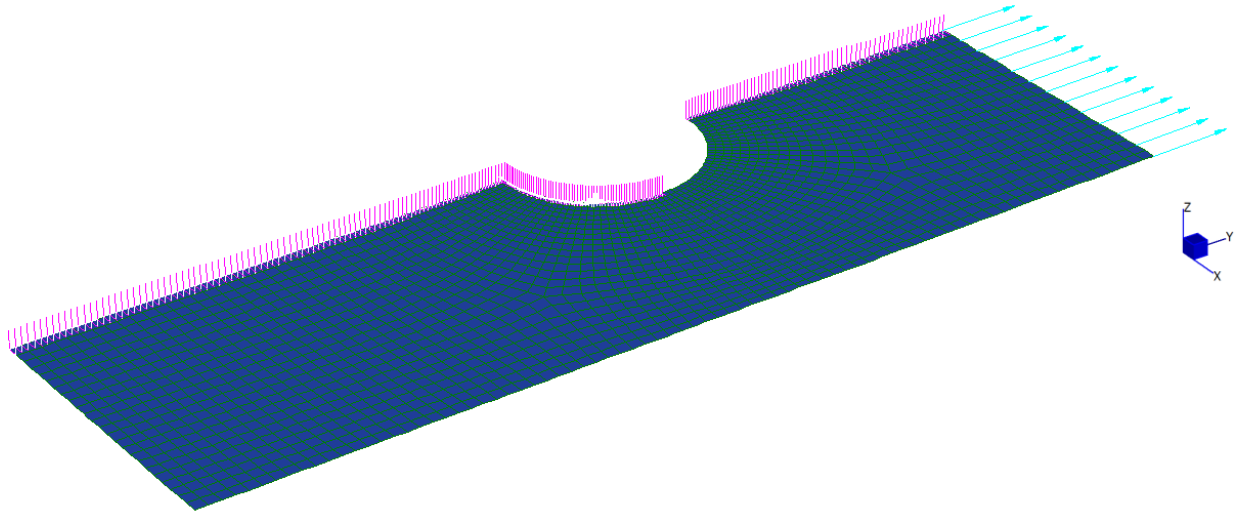


Figure 18 Strand7 FEA single bolt connection

The plate elements selected for use are the Quad8 type elements. These elements allow for quadratic interpolation which is recommended for curved surfaces such as holes (Strand7, 2010) with each element having four corner nodes and four side nodes. The Quad8 elements provide for 2 degrees of freedom for each of the 8 nodes giving better representation than the Quad4 element with only 4 nodes seen in the figure below. Turvey and Wang (2008) both used the equivalent to Quad8 type elements in close proximity to the bolt hole to allow for curvature of the hole and Quad4 equivalent elements being used further away from the hole to reduce analysis time. Based on analysis time this research will use Quad8 elements throughout the entire model.

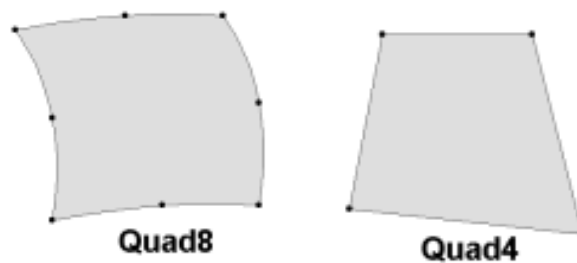


Figure 19 Quad8 and Quad4 elements (Strand7, 2012)

The global freedom conditions will be set to 2D plane which will prevent rotation about the x,y and z axis and translation will be prevented on the z axis. This will assure the plate does not deform out of plane giving unwanted data and give only data in the x and y directions. To model the single hole connection around the bolt a template was created with dimensions $x=10\text{mm}$ and $y=20\text{mm}$ using a line of symmetry along the y-axis. This was then graded to form half a circle with dimensions of 10mm to represent the bolt hole as can be seen in the figure below.

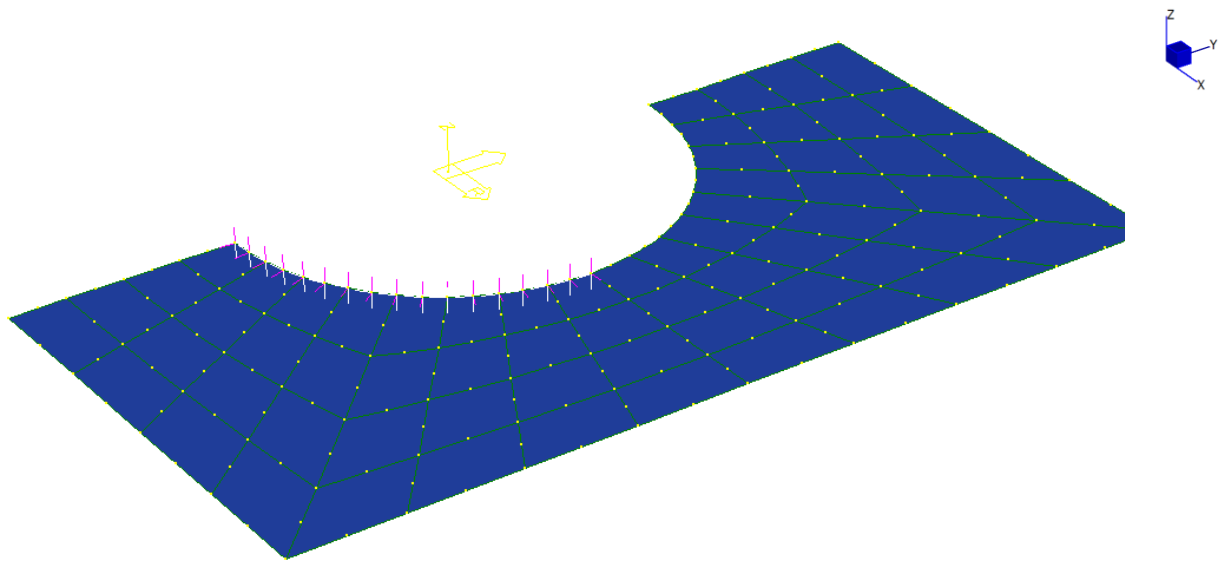


Figure 20 Template of symmetrical bolt hole for model development

To simulate the pressure on the bearing area created from the bolt when a tension load was applied, the nodes along the bearing area in the lower half had full rotation restraints as well as radial and z-axis translational restraint. Based on a PhD thesis by Okutan (2001) who investigated three different methods to analyse lap joints the method of allowing the bearing nodes to move tangentially as I have adopted proved most reliable compared to other methods such as modelling contact areas or applying a cosine load distribution around the bolt hole.

The length to width ratio for each element has been inspected to reduce the number of disproportional elements particularly around the bolt hole. High aspect ratios such as long and thin elements as seen in the figure below may introduce problems depending on loading and boundary constraint (University of Colorado, 2013) and should be avoided if possible.

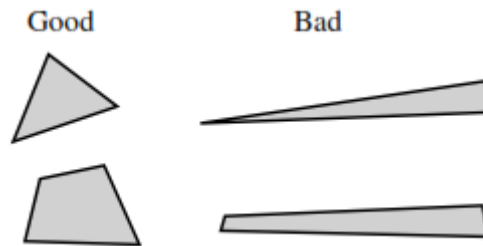


Figure 21 Element aspect ratio (University of Colorado, 2013)

The bolt hole template was then added to the connection being modelled and the mesh cleaned and smoothed before analysis. Further mesh refinement around the bolt hole was sometimes needed if subdivision showed irregular patterns or disproportional elements.

The edge restraints need to be considered and due to symmetry on the y-axis full rotational restraints were applied as well as translation restraint on the z and x-axis. This would assure appropriate stress distribution around the symmetry line.

The model would be analysed as orthotropic 2D plane stress so only the mechanical properties for the x and y directions need to be considered. The manufacturers data sheet for each pultruded material will be entered as shown in figure 22 below and the thickness of each plate entered under the geometry tab.

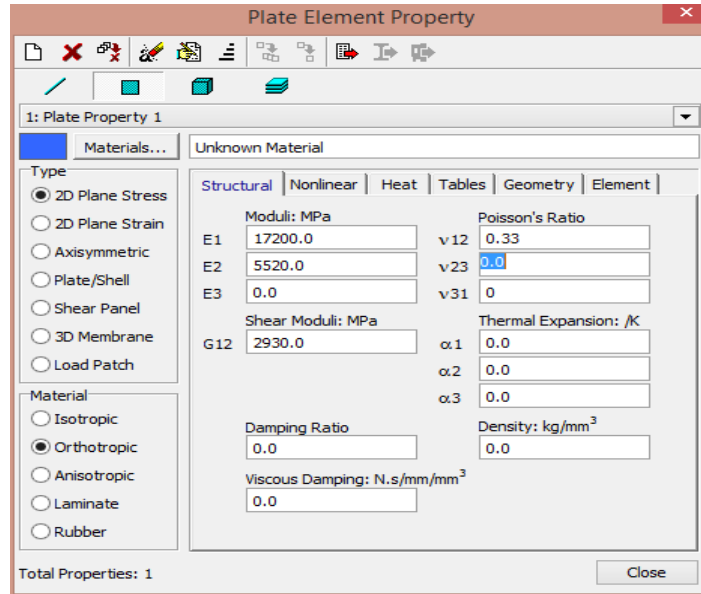


Figure 22 FRP mechanical properties used for analysis in Strand7

The final stage was to check convergence of the results to the theoretical results and it was trialled using both Quad4 and Quad8 elements. It was found that in order to get the required accuracy at least 1500 elements per model would be needed which can be seen in the figure below.

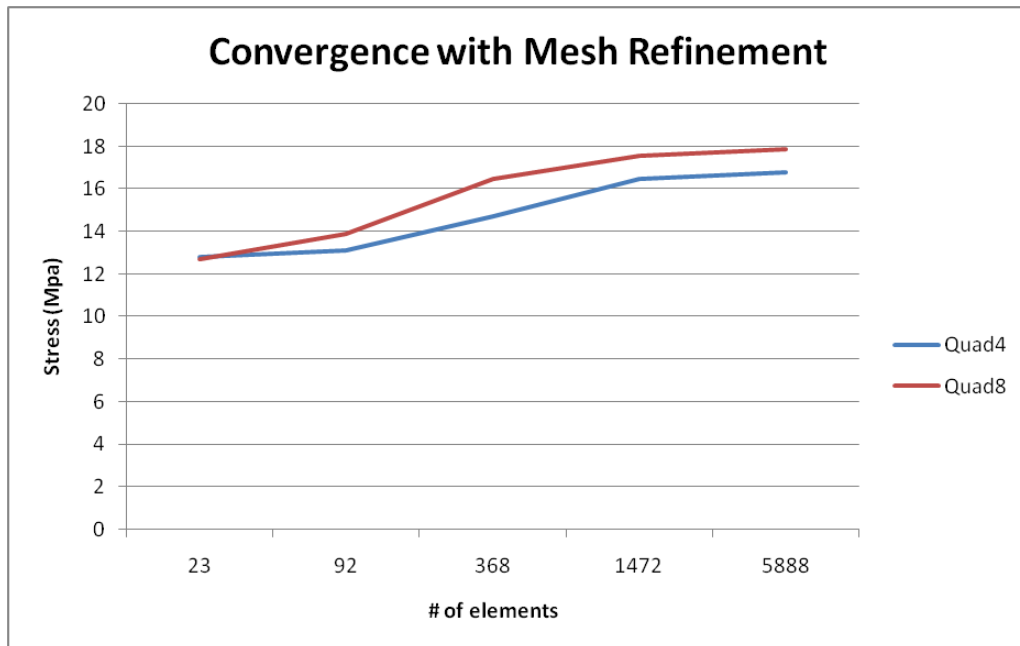


Figure 23 Mesh refinement with Quad4 and Quad8 elements

The process to develop the multi-bolt connection was the same with a template produced for the bolt hole and the model built around the bolt hole with geometric parameters outlined in the analysis schedule. An example is shown below in figure 24 and 25 for the multi-bolt connection and single bolt connection respectively.

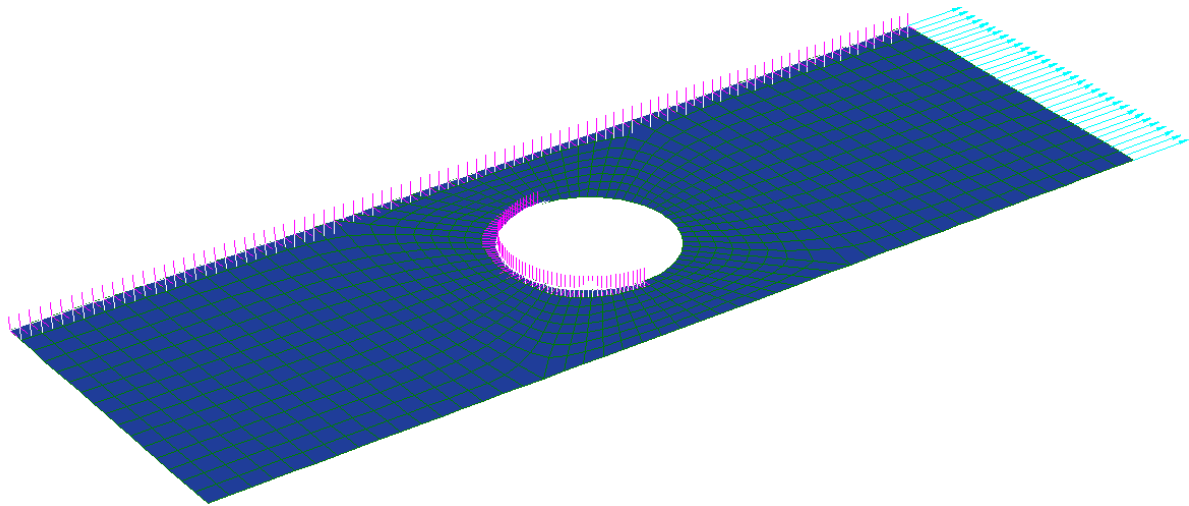


Figure 24 Multi-bolt connection with restraints and loading applied

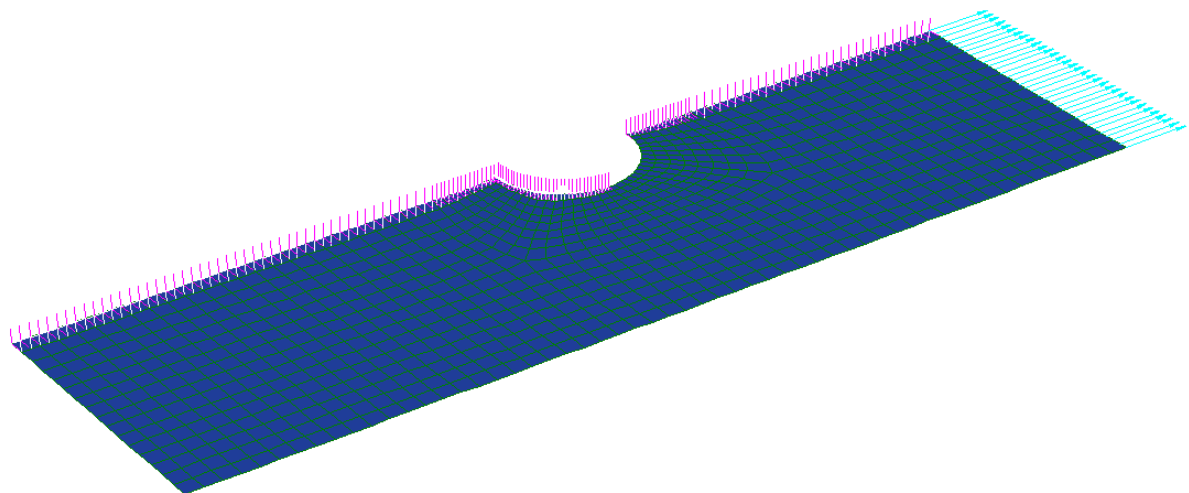


Figure 25 Single bolt connection with restraints and loading applied

3.4.3 FEA Model Validation

To confirm the validity of the Strand7 FEA data a thorough validation process will be used. Firstly, an unloaded open hole model was validated by applying a 1kN uniform tension load at one end while fully restraint at the opposite end. Equation 3.10 was used and allows for the orthotropic properties of the material which was substituted into equation 3.9 to calculate stress data for the net-tension plane. In figure 26 below the overall results between theory and FEA are comparable with the exception of the initial stress concentration at the hole edge which has 14% variation. For this reason a further validation process will be required.

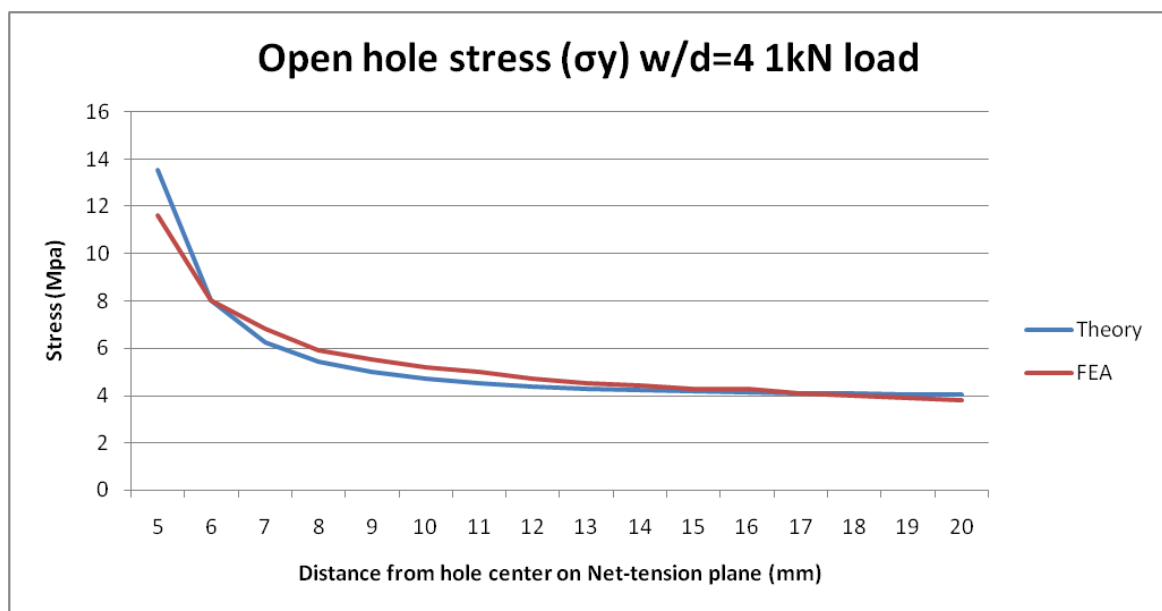


Figure 26 Validation results of unloaded open hole

A further model was developed based on Tserpes (2001) who researched open hole stress damage in 3D FEA models with all orthotropic data and connection geometry duplicated to assure consistency in the validation model. The longitudinal stress has been plotted against distance along the net-tension plane with Tserpes plotting against the hole centre rather than the hole edge. The stress data from Tserpes (2001) in figure 27 and the Strand7 validation in

figure 28 of the same connection geometry and material confirms accuracy of the models developed.

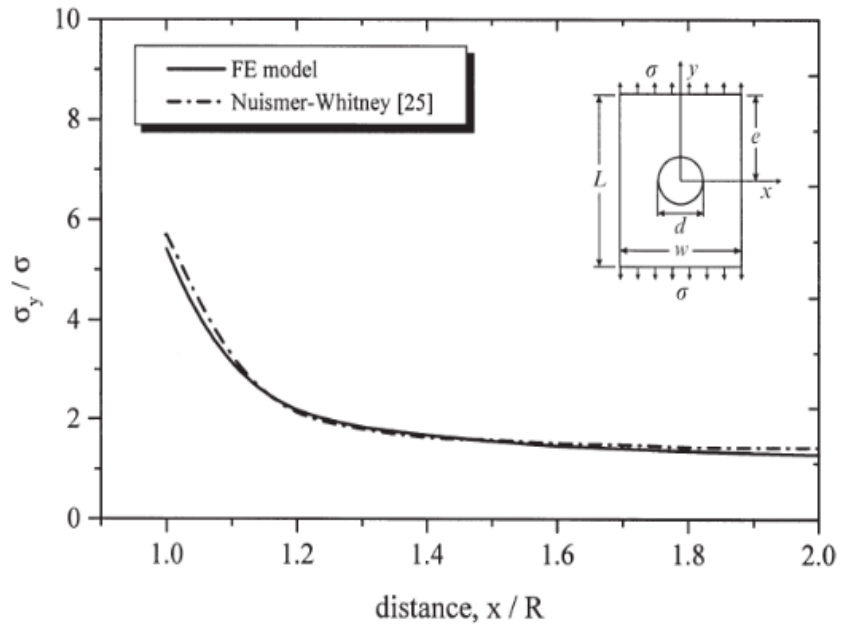


Figure 27 Tserpes (2001) validation of open hole

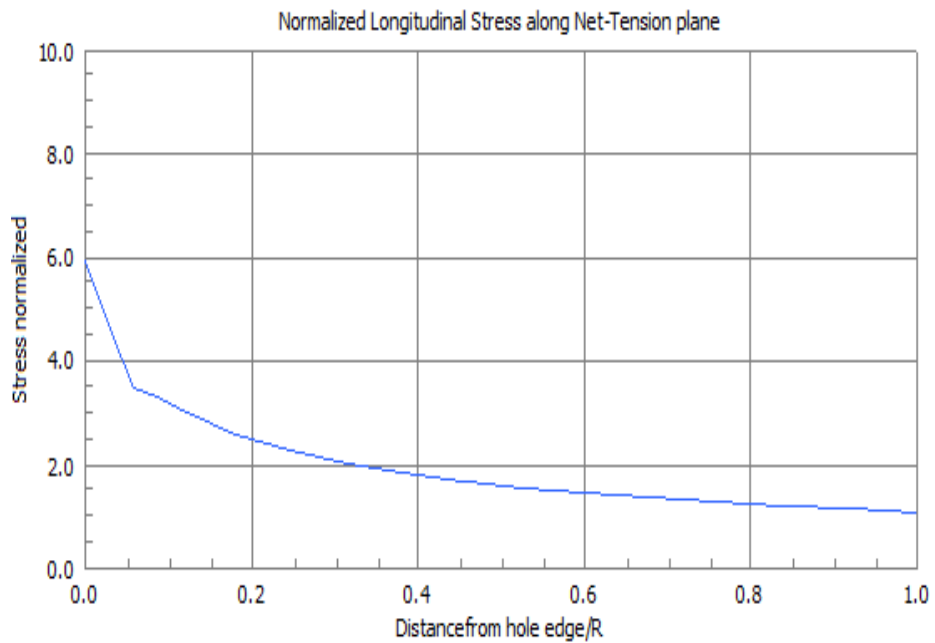


Figure 28 Strand7 Validation of Tserpes (2001) model

Because the FEA models require a bolt to replicate a lap joint connection the validation process will also require the model to incorporate the radial translation restraints for the bolt interaction to confirm the accuracy of stress data around the bolt hole. The interaction between the bolt and connection material is vital for accurate data and validating the FEA without experimental test data is difficult. As a result the validation of the loaded bolt hole will be based on Turvey and Wang (2009) FEA model who used contact elements between the bolt shaft and material.

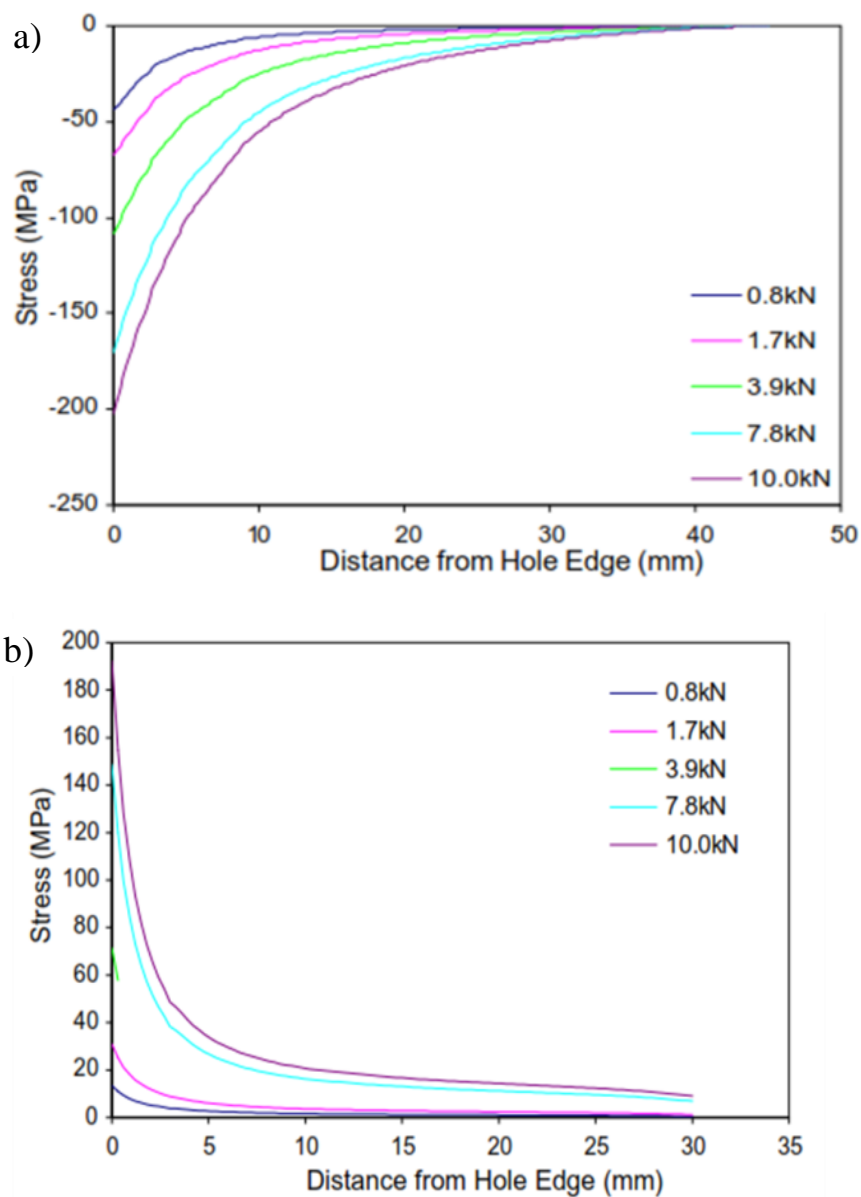


Figure 29 a) Turvey (2009) bearing stress results b) net-tension stress results

The above Figures 29a) bearing stress b) net-tension stresses (Turvey & Wang, 2009) from the bearing plane and net-tension plane respectively. Turvey used a 2D homogeneous orthotropic analysis with non-linear contact to model the bolt compared to this research which is using radial displacement restraints to represent the bolt interaction.

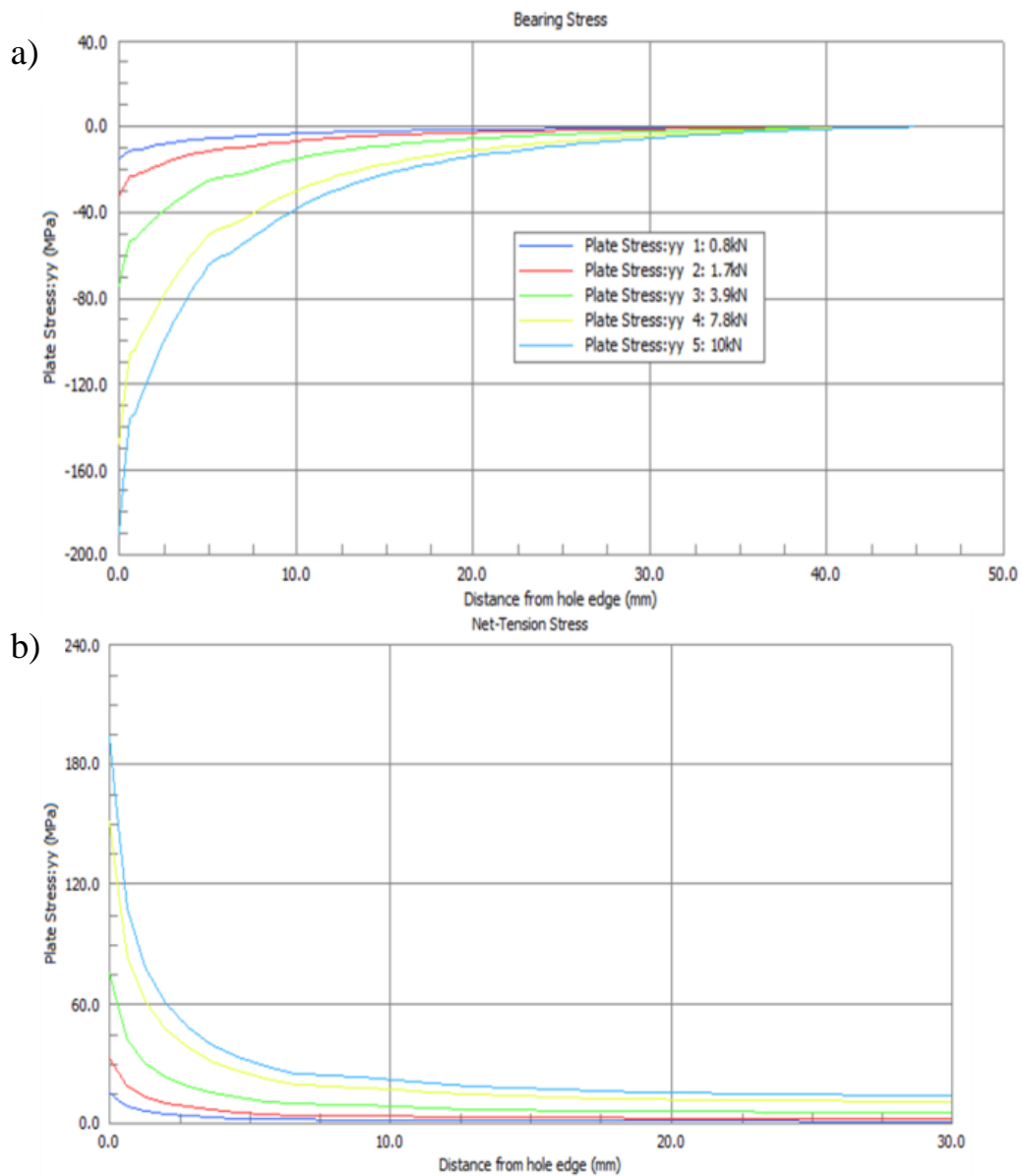


Figure 30 Validation against Turvey (2009) with a) bearing stress and b) net-tension stress

The results of the Strand7 FEA is shown above in figure 30a) bearing stress b) net-tension stress and can be compared to Turvey and Wang (2009) in figure 29a) and b). The variation between the two models for the net-tension stress is accurate regardless of the bolt modelling

method being either the contact method (Turvey & Wang, 2009) or radial restraint method (current research validation) with the radial displacement method varying only 5% from theory and tight correlation between the two methods seen in table 3.

Table 3 Comparison of net-tension stresses between theory, contact and radial modelling

Net-Tension Stress comparison						
parameter	Load (kN)	Maximum tension Stress (Mpa)			Variation from theory (%)	
		Theory	FEA (contact)	FEA (radial)	FEA (contact)	FEA (radial)
w/d=7 e/d=5	0.8	14.8	16	15.5	8.1	4.7
	1.7	31.35	30	32.9	-4.3	4.9
	3.9	71.9	70	75.6	-2.6	5.1
	7.8	143.8	145	151.2	0.8	5.1
	10	184.4	195	193.8	5.7	5.1

The bearing stress distribution on the bearing plane showed inconsistent results when comparing the two stress profiles. The results between the two models are shown in table 4 below with data only reproducible with the higher tension loads. It can be seen that particularly during light loads that there is a large variation between the contact and radial methods due to the connection plate and bolt interaction. A non-linear analysis will allow for the yielding and relaxation of the bolt into the bearing area of the material while a linear analysis will not. To reduce the scope of this difficult validation process loads of greater than 8kN will be adopted in an attempt to reduce the variation between the two methods.

Table 4 Comparison of bearing stress against Turvey (2009)

Bearing Stress comparison			
parameter	Load (kN)	Stress (Mpa)	
		FEA (contact)	FEA (radial)
w/d=7 e/d=5	0.8	45	15.2
	1.7	70	32.3
	3.9	110	74.2
	7.8	175	148.3
	10	205	190

3.5 Analysis Schedule

3.5.1 Overview

Recommended geometry data has been compiled for single and multi-bolt lap joints from EUROCOMP (1996) and research conducted by Mottram (2001) and a combined effort with Turvey (2003). Manufacturers data has also been supplied from Bank (2006) and recompiled into table 5 below.

Table 5 Comparison of recommended geometry for single and multi bolt tension joints

Recommended geometry for single and multi-bolt lap joints					
	Researched*		Manufacturer		EUROCOMP (1996)
	Recommended	Minimum	Recommended	Minimum	Recommended
edge distance/bolt diameter e/d	≥ 3	2	≥ 3	2	≥ 3
width/bolt diameter w/d	≥ 5	3	≥ 4	3	≥ 6
side distance/bolt diameter s/d	≥ 2	1.5	≥ 2	1.5	$\geq 0.5g/d$
pitch/bolt diameter p/d	≥ 4	3	≥ 5	4	4
guage/bolt diameter g/d	≥ 4	3	≥ 5	4	4
bolt diameter/plate thickness d/t	≥ 1	0.5	2	1	1.5
hole size clearance	0.05d	1.56mm	1.56mm	NA	0.05d

*Research conducted by Mottram (2001), Mottram & Turvey (2003)

The analysis schedule will be based on previous research conducted and also recommendations from the manufacturers and EUROCOMP in an attempt to highlight areas of disagreement particularly with the w/d and e/d ratio's. A comprehensive analysis program will investigate the behaviour under various geometry changes with the selected pultruded plates.

3.5.2 Single Bolt Connection Analysis Schedule

Table 6 below shows the planned analysis schedule for this single bolt connections.

Table 6 Analysis schedule for single hole tension joints

Single hole tension joint analysis Schedule				
Geometric ratio		Dimensions (mm)		
w/d	e/d	w	e	d
3	1	30	10	10
	2		20	
	3		30	
	4		40	
	5		50	
4	1	40	10	10
	2		20	
	3		30	
	4		40	
	5		50	
5	1	50	10	10
	2		20	
	3		30	
	4		40	
	5		50	
6	1	60	10	10
	2		20	
	3		30	
	4		40	
	5		50	
7	1	70	10	10
	2		20	
	3		30	
	4		40	
	5		50	

The analysis will consider w/d ratios in the range of 3 to 7 and e/d ratios ranging from 1 to 5. This will ensure full coverage of values from table 1 as well as give data for extreme values beyond that recommended from previous research. As can be seen from table 6 above the matrix of models will be extensive with 5 separate models for each w/d ratio with analysis on two different pultruded plates giving data on d/t ratio in addition.

3.5.2 Multi-Bolt (single row) Analysis Schedule

The table below shows the analysis schedule to be performed on the multi-bolt connection. This connection will consist of 2 bolt holes in a single row and will investigate a range of parameters from Table 1 to show how multi-bolt joints can differ from a single bolt connection.

Table 7 Multi-bolt joint analysis schedule

Multi-Bolt (single row) Joint Analysis Schedule								
Geometric ratio				Dimension (mm)				
w/d	e/d	s/d	g/d	w	e	s	g	d
4	1	1	2	40	10	10	20	10
	2				20			
	3				30			
	5				50			
6	1	1.5	3	60	10	15	30	10
	2				20			
	3				30			
	5				50			
8	1	2	4	80	10	20	40	10
	2				20			
	3				30			
	5				50			

The multi-bolt analysis schedule will investigate width changes as well as edge distance changes and these will be compared to data from the single hole connections to show any similarities or trends. The side distance and gauge distance will also change as the width varies. The test schedule will provide sufficient data on stress distributions over a range of parameters needed to make a conclusion.

Chapter 4

Results

4.1 Introduction

This chapter will discuss the results found through the theoretical calculations and FEA using Strand7 software package. The stress on the net-tension, bearing and shear-out planes will be analysed on both single and multi-bolt connections as well as the bolt hole edge stresses. The investigation will also consider a change in thickness of the pultruded plate and the effect of this on the stress levels.

The stress along the critical failure planes will be studied in particular the bearing, net-tension and shear-out planes seen in figure 31 below as well as stresses around the hole edge.

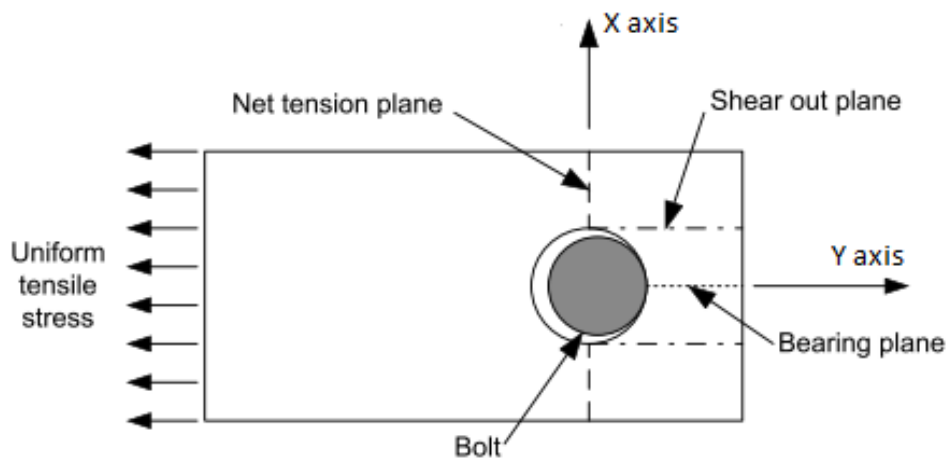


Figure 31 Net-tension, bearing and shear-out failure planes of a typical joint (Turvey, 2009)

4.2 Single Bolt Connection

4.2.1 Net-Tension Stress

To calculate the stress concentration at the hole edge on the net-tension plane the elastic concentration (Kte) equation 3.4 was used to get the required correction factors needed for the stress calculations. Figure 32 below shows Kte data for the full range of analysis parameters. For values of $e/d = 1$ the values are significantly higher due to the higher stress gradients encountered with a short edge distance with the values decreasing significantly as the e/d ratio increases. The opposite effect is noticed as the width of the connection plate is increased the stress concentration factor reduces significantly.

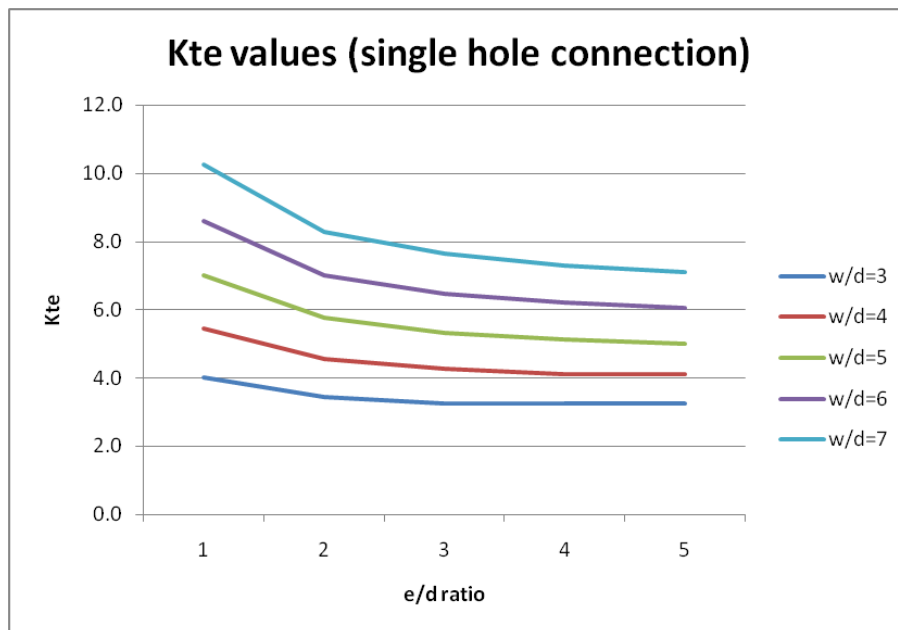


Figure 32 Single bolt stress concentration values

By utilising the net-tension stress equation 3.6 the maximum stress (σ) can be calculated at the bolt hole edge (on the net-tension plane) for the full range of parameters. The results are in table B1 of Appendix B and also show the theoretical stress values as well as FEA

results. Overall the theory correlated to the FEA results accurately with the average error being 2.1%. The trend indicated that FEA showed 2.1% less than that reported by theoretical calculations. The same data has been presented in figure 33 below to show better representation over the range of stress values.

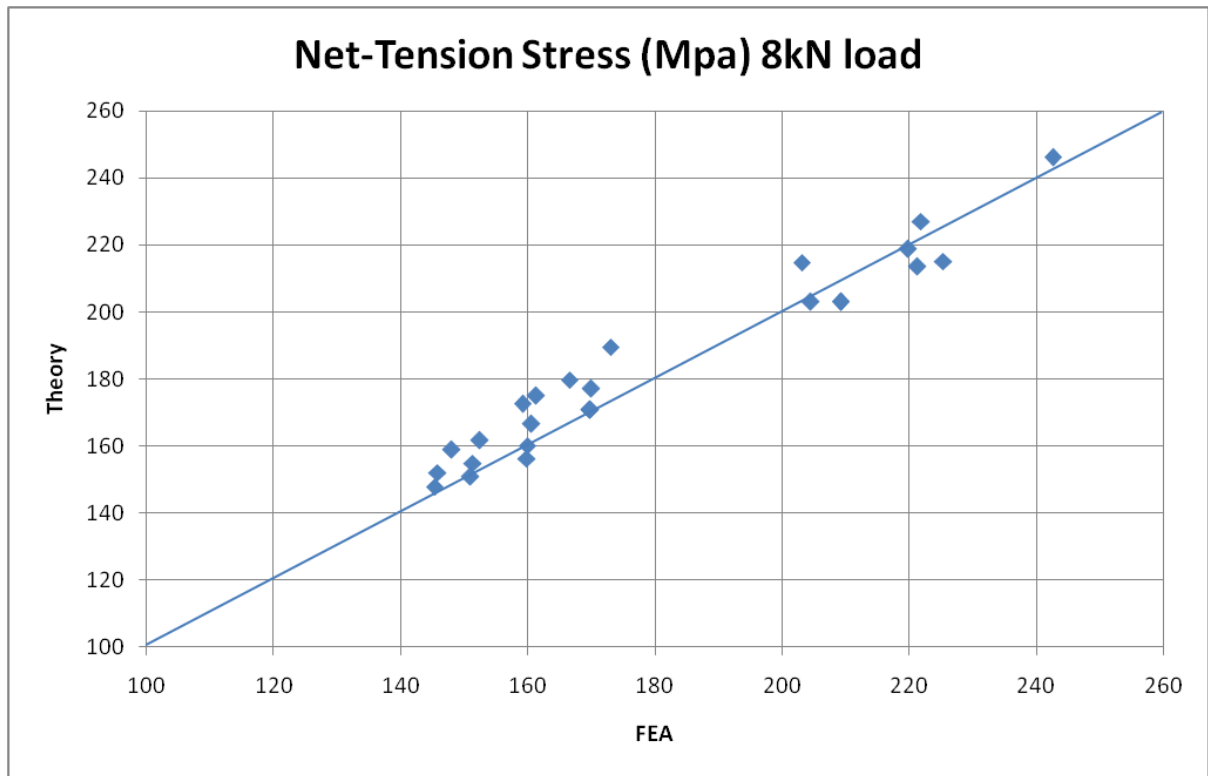


Figure 33 Comparison of theory and FEA results for net-tension stress

By evaluating the stress concentration area adjacent to the bolt hole on the net-tension plane the longitudinal stress (σ_y) is highest when $e/d = 1$ and $w/d = 3$ when examined through the range or parameters. In figure 34 and 35 below the stress behaviour can be seen with direct comparison between the edge distance and width of the connection.

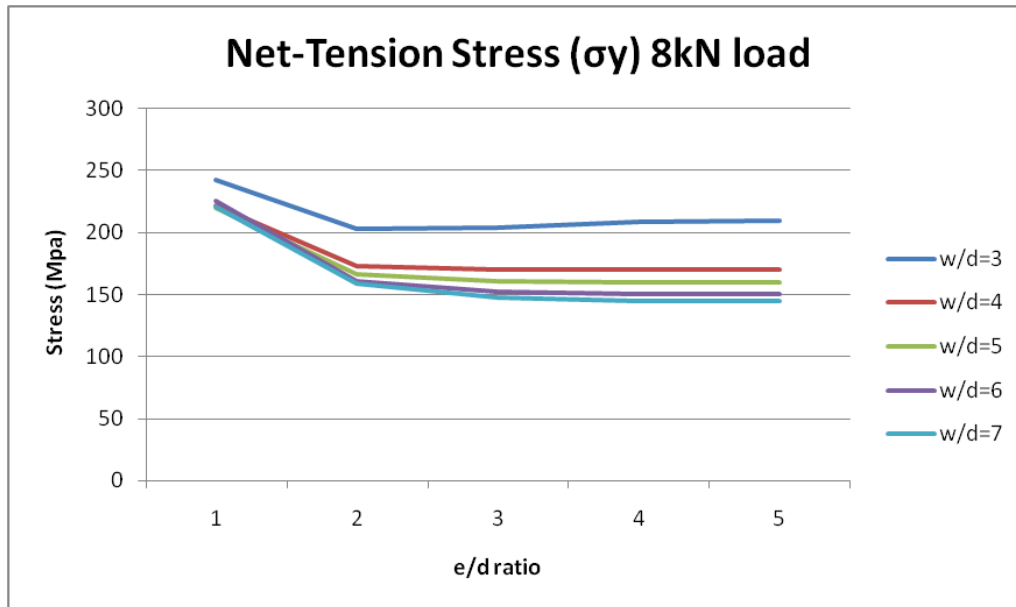


Figure 34 Net-tension stress and e/d ratio

Clearly it can be seen that when $w/d = 3$ ($w=30\text{mm}$) the connection yields a significantly higher stress concentration at the hole edge since the net-section is reduced to only 20mm due to the bolt diameter. Combined with the short end edge a high gradient stress area is created.

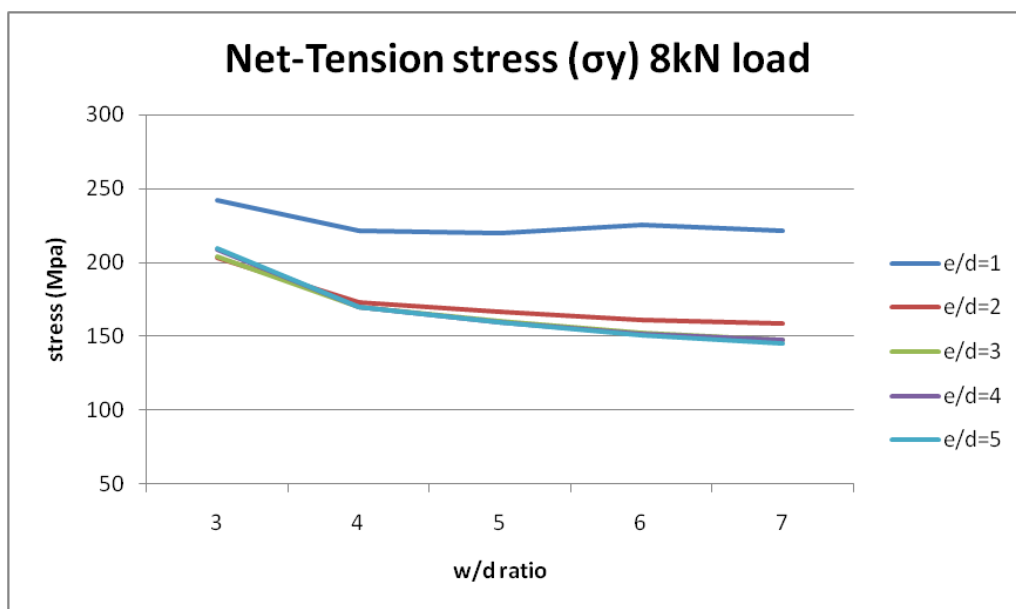


Figure 35 Net-tension stress and w/d ratio

By examining the higher stress values at the hole edge in the figure 34 and 35 above certainly any joint with $e/d < 2$ should be avoided regardless of width and any joint with w/d

< 4 should also be avoided to reduce the high stress concentrations on the hole edge making net-tension failure less likely.

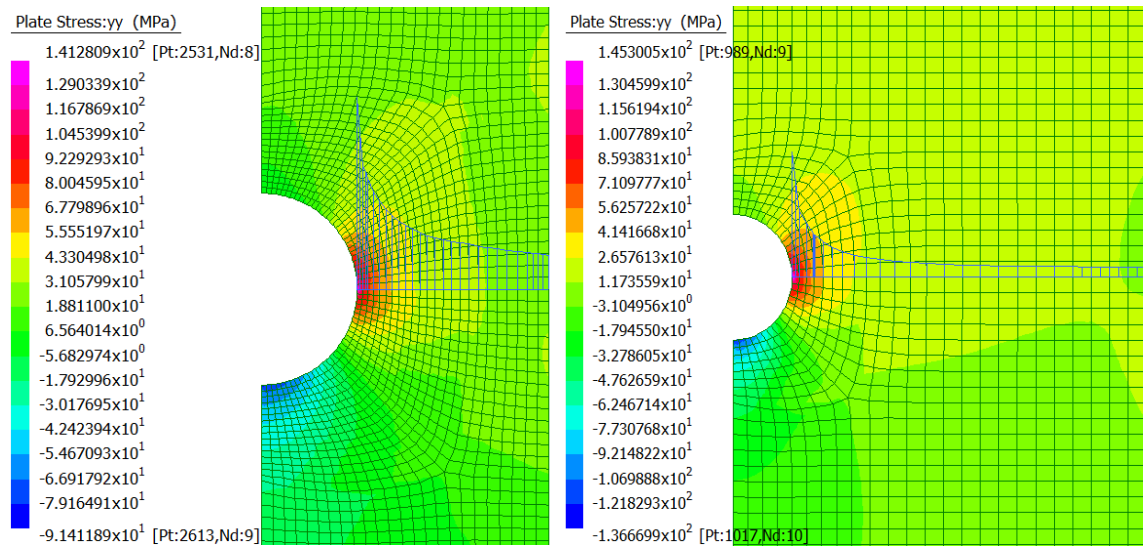


Figure 36 a) Net-tension stress profile $w/d=3$ b) Net-tension stress profile $w/d=7$

When the net-tension plane is examined from the hole edge to the free edge the stress can be identified at each location along the plane. The most critical state being a narrow connection plate (30mm) which is shown in figure 36a) above. The Strand7 analysis can be viewed in figure 36a) and b) above which shows the decay of the stress as the width is increased. In figure 36a) $w/d = 3$ with average stress still significantly higher over the entire width of the net-section when compared to b) which is $w/d = 7$ where average stress in the net-section is much lower with both initial concentration levels approximately equal.

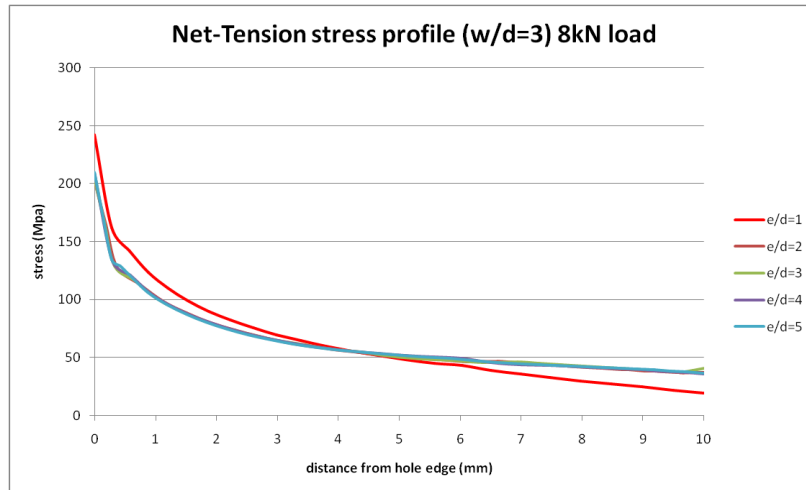


Figure 37 Net-tension stress profile comparison

It should also be noted that at distance of $0.5d$ ($d=10\text{mm}$) from the hole edge on the net-tension plane the stress is approximately 25% of the initial concentration level and at $0.25d$ the stress is approximately 30% of the initial concentration regardless of the e/d or w/d ratio. This gives an indication of the critical nature of the initial stresses encountered at the hole edge up to a distance of $0.25d$ which is most susceptible to net-tension failure. Table 8 below gives an indication to the decay rates of the stress showing the longitudinal stress as a percentage of initial stress concentration at mid-point along the net-tension plane as the width changes. With the $e/d > 1$ the edge distance ratio does not play a significant factor in stress variation for the net-tension plane so the table below is representative of all widths with data taken from $e/d = 3$.

Table 8 Percentage of peak stress as w/d changes

% of peak σ_y at distance $0.5 \times$ (net-tension plane length) measured from hole edge					
w/d	3	4	5	6	7
% of peak σ_y	25%	24%	21%	11%	8%

As can be seen the lower w/d ratio of 3 and 4 still show approximately 25% of maximum stress at midpoint along the net-tension plane and this then drops as the width is increased

further giving indicators that failure in net-tension is less likely for larger widths. Although this is a percentage of peak stress, the peak concentrations at the hole edge should be considered from figures 34 and 35.

For all joint geometries there exists free edge stress due to the uniform tension load applied at the connection end. By examining figure 37 above for the $w/d = 3$ connection it can be seen that there is variation between free edge stress as the e/d ratio changes. The values of $e/d \geq 2$ all show the same trend in that they all increase in stress ratio (peak stress : free edge stress) when the w/d decreases. With narrow connections such as $w/d = 3$ the percentage stress on the free edge is 18% of the initial concentration compared to only 2% for a wide connection such as $w/d = 7$. When $e/d = 1$ the overall ratio between the hole edge stress and free edge stress is lower as seen in figure 38 below.

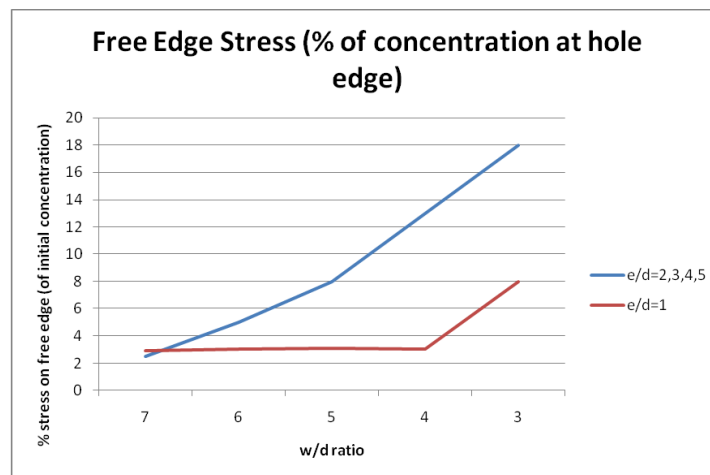


Figure 38 Free edge stress relationship

The stresses around the bolt hole also show significantly important features giving indicators of likely failure modes in lap-joints. The σ_y stress around the bolt hole on the net-tension plane (0°) has a higher gradient on the bearing area of the hole until the point of maximum compression is reached on the bearing plane (-90°) as seen in figure 39 below. This higher gradient area would mean the likely net-tension failure may actually be directed

slightly angled (towards the bearing area of the hole) rather than perpendicular to the y-axis. In all ratios of width the σ_y stress converges on zero at the 70° mark near the top of the bolt hole.

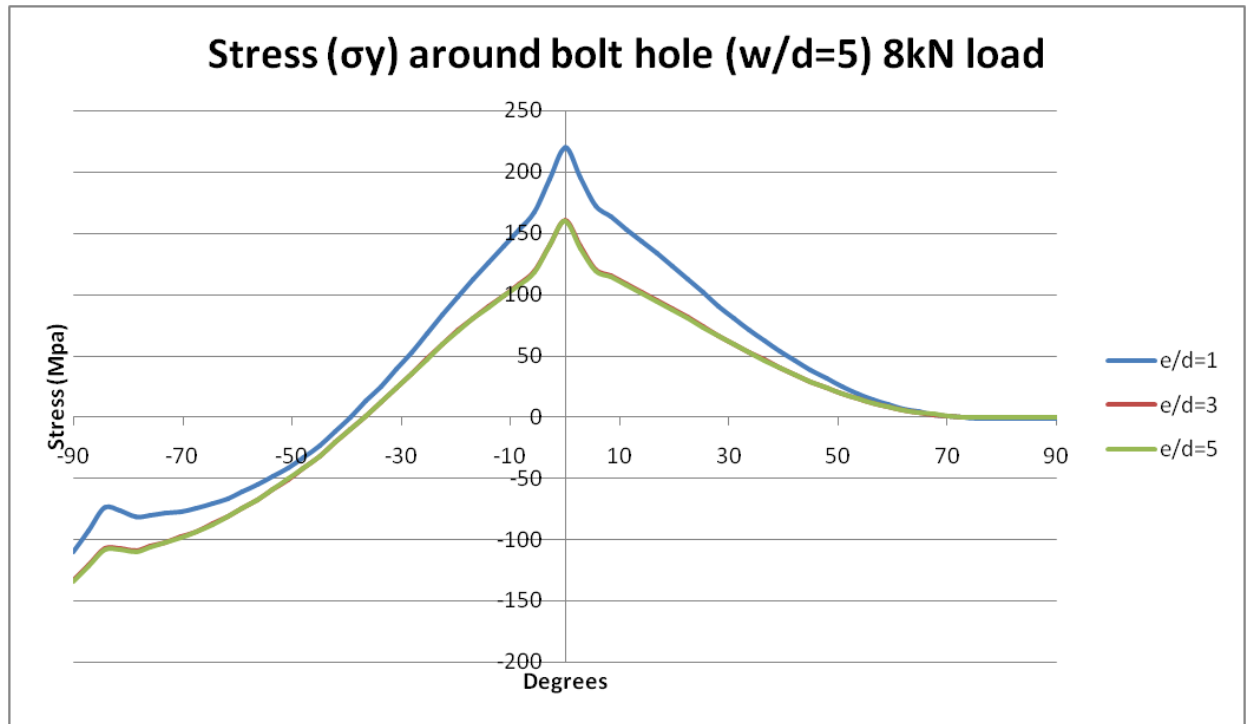


Figure 39 Stress around the bolt hole edge

4.2.2 Shear Stress

The shear stress (τ_{xy}) has been inspected along the shear-out plane which extends from a point on the hole edge at mid-point to the end of the plate parallel to the tension load. This is the failure path the bolt would take as it tears out through the material usually due to low e/d ratios. In figure 40 below it is clear that the shear stress regardless of w/d or e/d ratio will always start and end at zero. The shear stress gradients are all similar initially until the apex is reached at 3-3.5mm along the shear-out plane but what is of greater importance are the gradients from the apex to the plate edge.

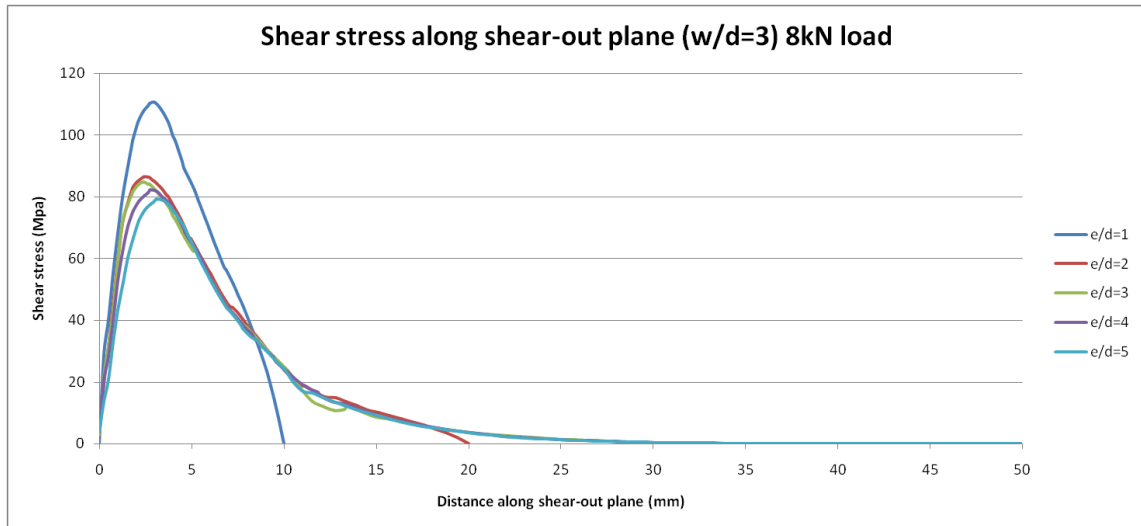


Figure 40 Shear stress profiles for e/d ratios on shear-out plane

When $e/d = 1$ the apex for peak shear stress is at a distance of 33% of the shear-out plane length giving us an indication that failure in shear-out is highly likely. Comparing gradients for other edge distances when $e/d = 2,3,4,5$ the apex is at 15%, 10%, 7.5% and 6% respectively along the shear-out plane lengths. The shear stress profiles were almost identical for all w/d ratios with the exception the e/d ratios of 2-5 when $w/d = 3$. These results shows shear stress levels approximately 10% higher. A tabulated form can be seen below in table 9 indicating percentages of peak stress at mid-point along the shear-out plane.

Table 9 Percentage of peak stress along shear-out plane

% of peak τ_{xy} at distance $0.5 \times$ (shear-out plane length) measured from hole edge					
e/d	1	2	3	4	5
% of peak τ_{xy}	78%	31%	11%	4%	1%

Figure 41 with an $e/d = 1$ and figure 42 with an $e/d = 5$ give a better perspective of the shear stress decay between a changing the e/d ratio.

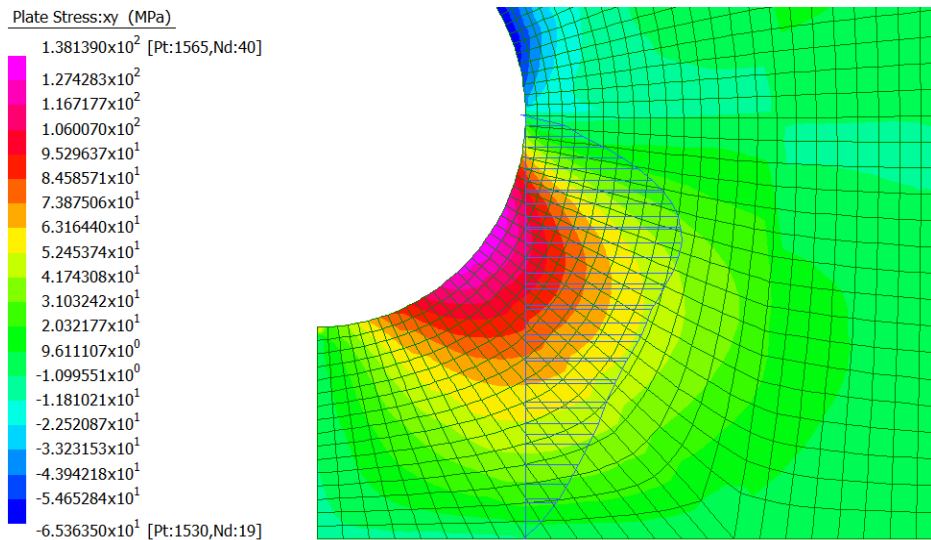


Figure 41 Shear stress along shear-out plane for $e/d = 1$

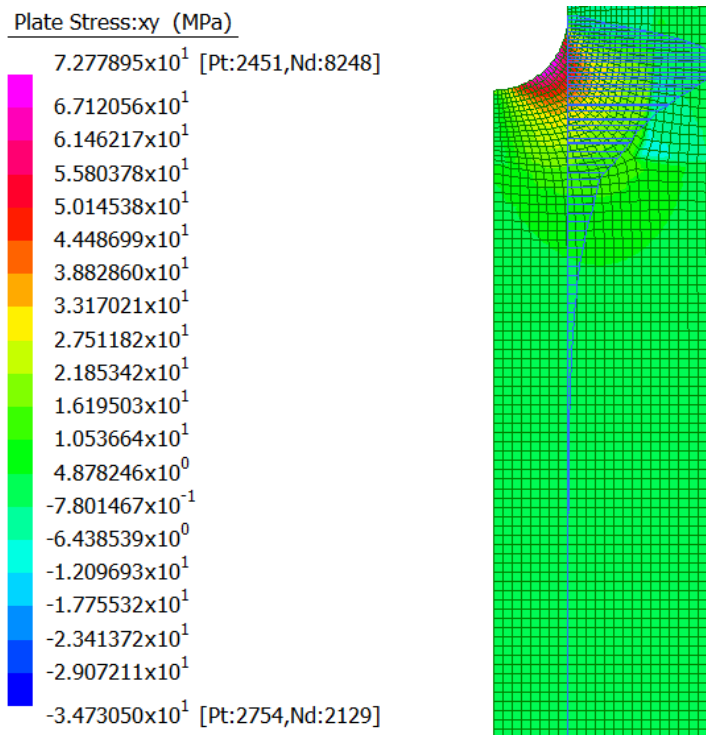


Figure 42 Shear stress along shear-out plane when $e/d = 5$

The shear stress around the bolt hole can be seen in figure 43 below with 0° representing the net-tension plane and -90° the bearing plane. The maximum shear occurs for all widths for $e/d = 1$ at 39° below the net-tension plane and for e/d ratios of 2-5 and $w/d = 3$ the peak stress is located 38° beneath the net-tension plane and progressively moves to 43° as the w/d

ratio is increased to 7 seen in Appendix D figures. The width has only a small effect on the maximum shear stress when $e/d > 2$ and shows an increase of 10% over the range of widths and does move the epicentre of the shear stress concentration between 38 and 43 degrees below the net-tension plane. The end edge distance does tend to effect the stress value being 40% higher for the e/d ratio of 1 compared to higher e/d ratios.

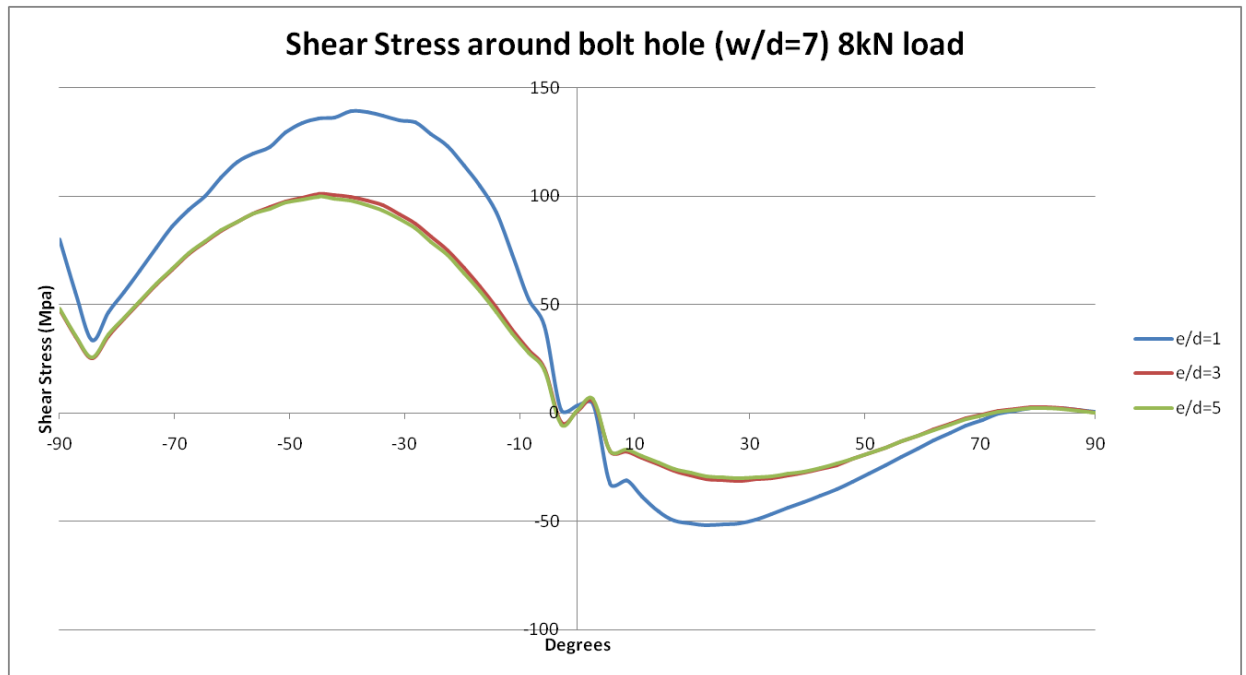


Figure 43 Shear-stress around hole edge

The point of maximum shear stress should also be examined and is not located on the shear-out plane for any of the connections. This was also pointed out by Turvey and Wang (2008) who investigated the validity of EUROCOMP's assumptions for designing tension joints. Figure 44 below is for a connection of $w/d = 3$ and $e/d = 1$ with the maximum peak shear occurring 38° below the net-tension plane and at a distance of 1.5mm from the shear-out plane.

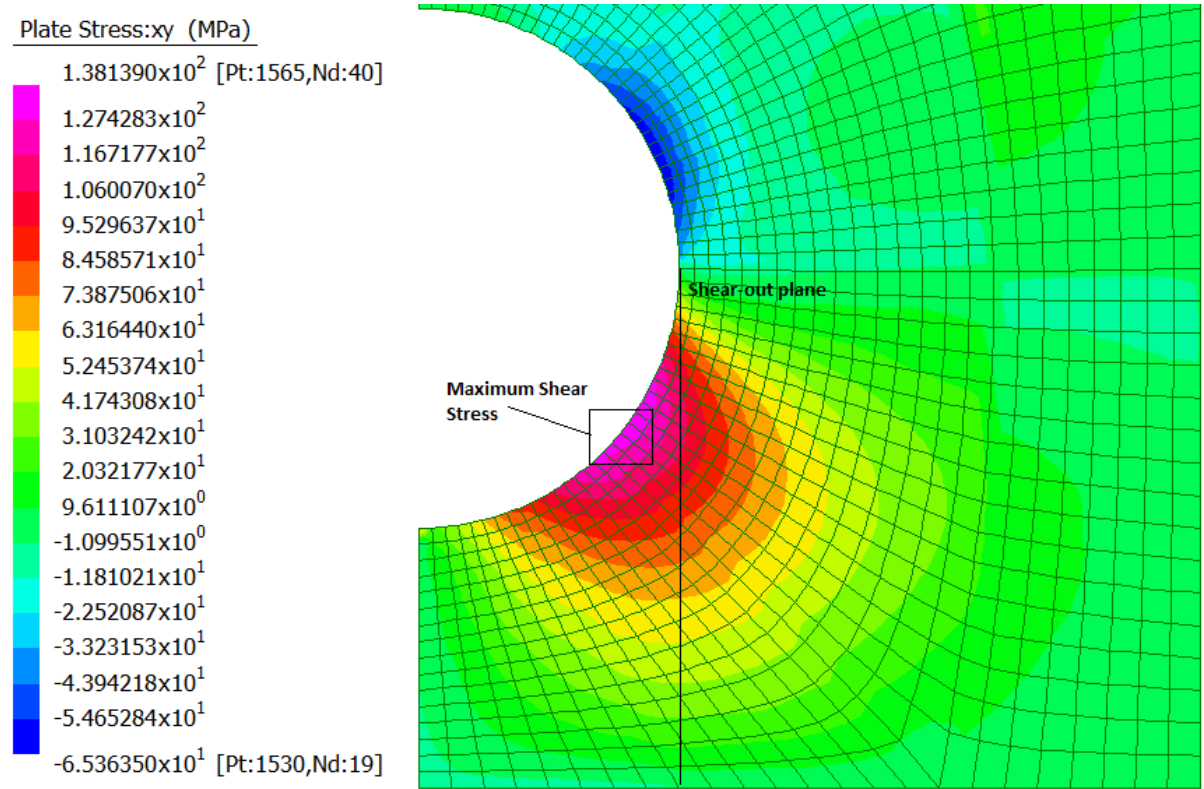


Figure 44 Point of maximum shear stress in relationship to the shear-out plane

4.2.3 Bearing Stress

Examining the bearing stress profiles on the bearing plane for the full range of geometric ratios the shortest end edge connection shows bearing stress of a slightly lower value when compared to all other connections with an $e/d > 2$. Regardless of the width the maximum stress holds constant at approximately 105 MPa at $e/d = 1$ and when the edge distance increases the stress again is constant at approximately 130 MPa. Based on data presented the width does not play a role in bearing stress however the reduction in stress between edge distances of 10 and 20mm is rather significant and may be contributed to the linear FEA modelling of the bolt. Figure 45 below is representative of all w/d ratios.

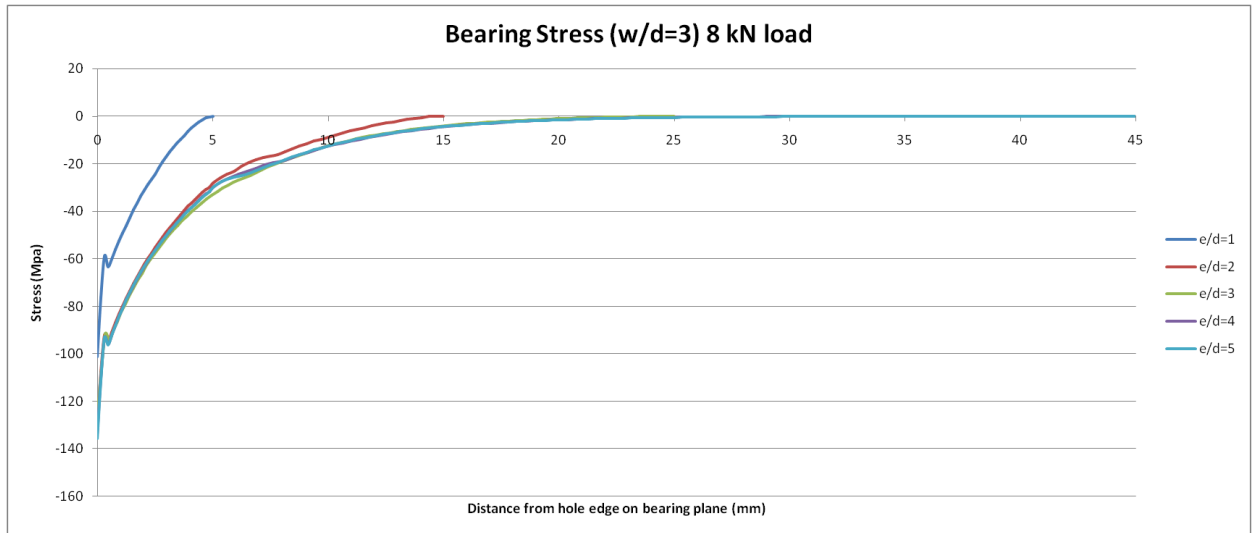


Figure 45 Bearing stress along the bearing plane

At a distance of half the bearing plane or halfway between the hole edge and free edge on the bearing plane the percentage of stress to initial peak stress decays rapidly as the e/d ratio is increased. The table 10 below shows the trend of decay. This provides a good indicator to the decay rate of the compressive stresses along the bearing plane. For $e/d > 3$ the stress has decayed to a value that is not of concern to any failure with at least half the edge distance free of critical stresses.

Table 10 Percentage of stress to peak stress along the bearing plane

% of peak σ_y at distance $0.5 \times$ (bearing plane length) measured from hole edge					
e/d	1	2	3	4	5
% of peak σ_y	24%	13%	6%	2%	<1%

Figure 46a) and b) below shows the decay rates and gradients associated with the bearing stresses for a low and high e/d ratio connection.

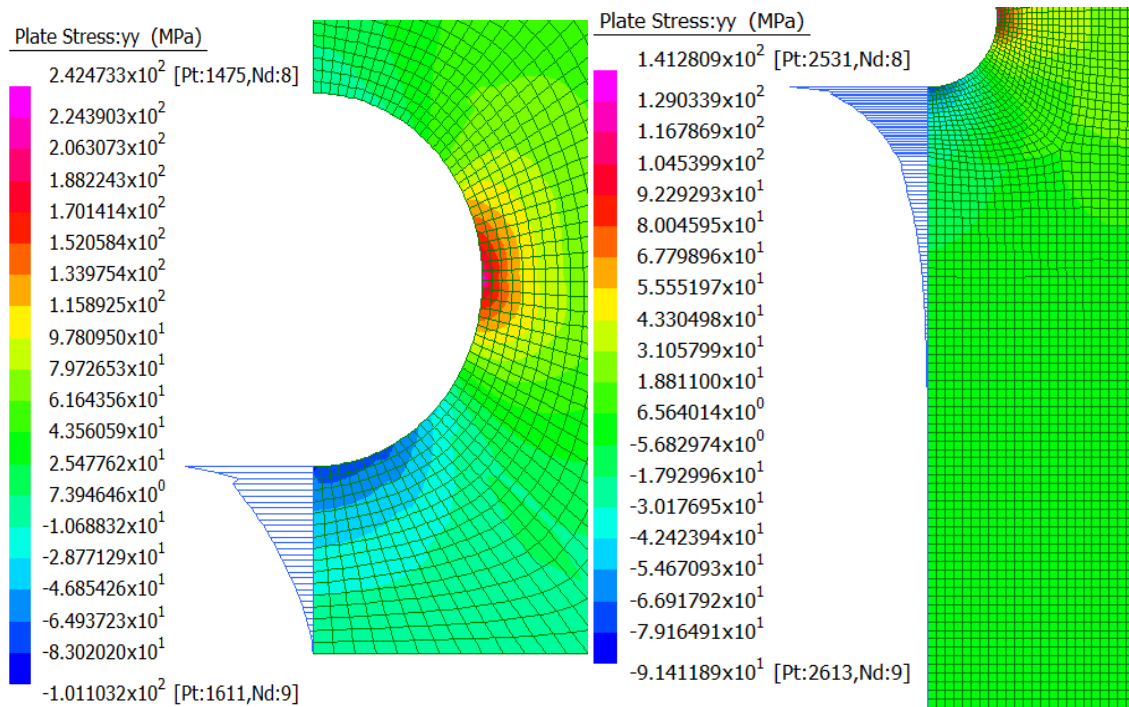


Figure 46 Bearing stress on the bearing plane a) $e/d = 1$ b) $e/d = 5$

4.3 Multi-Bolt Single Row Connection

4.3.1 Net-tension Stress

The stress concentration factors have been calculated using equation 3.5 for multi-bolt connections and results have been plotted in figure 47 below for the connection geometries being tested.

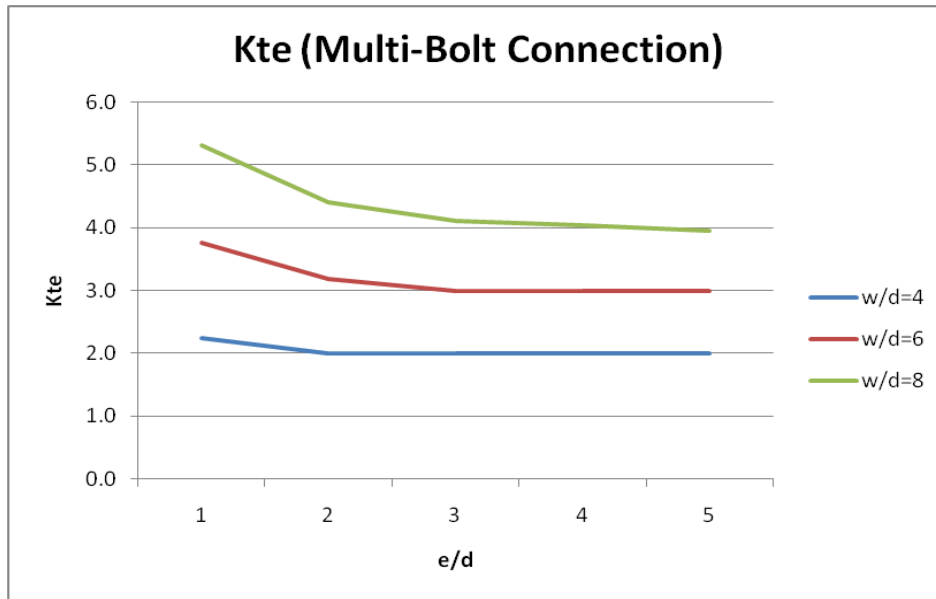


Figure 47 Kte values for multi-bolt connections

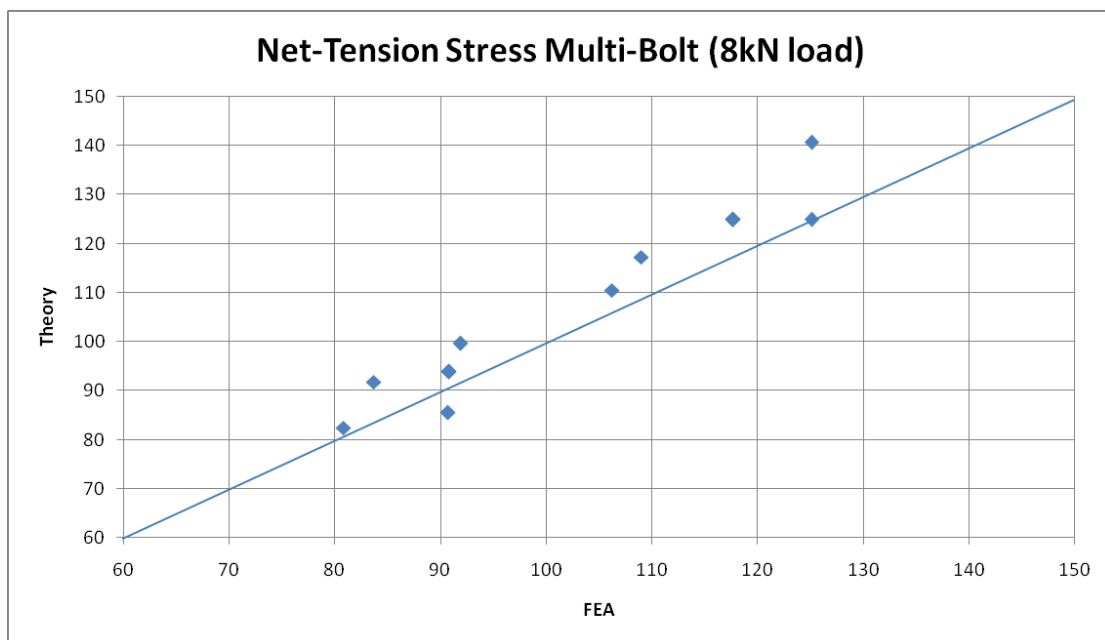


Figure 48 Comparison of FEA and theory results for multi-bolt connections

The theoretical calculations have been plotted against FEA values with the FEA values showing an average of 4.4% higher than the theory. A tabulated form with calculations can be seen in the Appendix B table B2 .

There are differences between single hole and multi-hole connections particularly with the distribution of peak stresses in the net-section seen in figure 49 below. Between bolt holes in a single row multi-bolt connection the stress concentration at the interior hole edge is higher than on the free edge side of the hole and most importantly the stress remains above nominal on the symmetry line as can be seen in the figure 50 below.

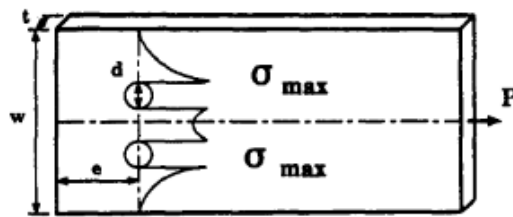


Figure 49 Net-tension stresses in multi-bolt connections (Hassan, 1997)

When viewing the Strand7 analysis for multi-bolt connections it was apparent that the difference between the interior stress at the line of symmetry compared to the free edge stress reduced from approximately 18% difference down to 7% as the w/d was increased from 4 to 8. At all times the free edge stress was less than the interior stress at the symmetry line.

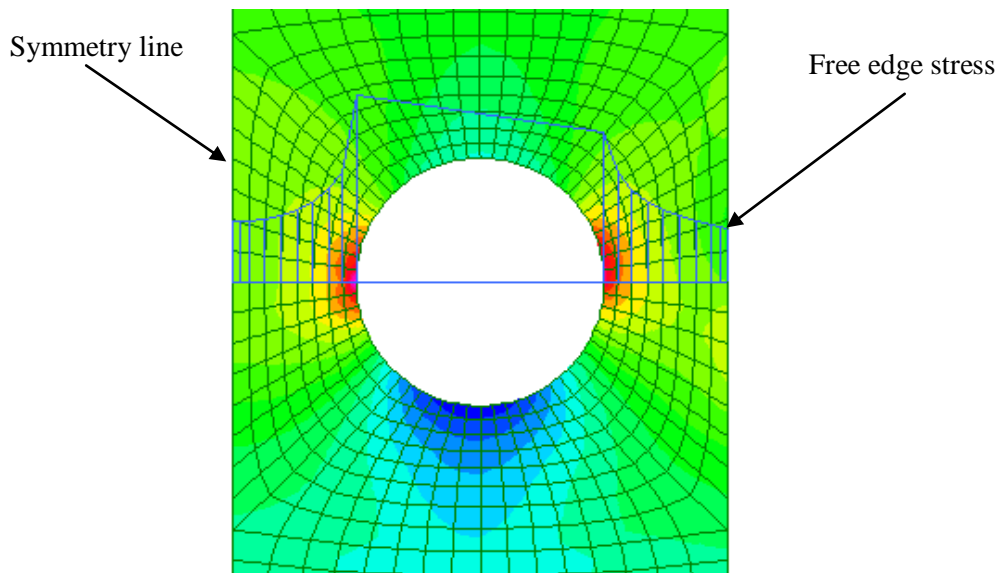


Figure 50 Multi-bolt net-tension stress

Peak net-tension stress always occurred when $e/d = 1$ when compared with other e/d values with the peak stress decreasing as w/d was increased. Peak stress occurred when $w/d = 4$ and $e/d = 1$ with a value of 151 MPa decreasing to 113 MPa when $w/d = 8$ and $e/d = 1$. This can be compared to the other edge distance ratio's of $e/d = 2,3,5$ which showed the same stress levels for each w/d ratio. The variation between stress on the symmetry line and free edge as well as hole edge stress can be seen in figure 51 a) for $w/d = 4$ and b) for $w/d = 6$ with the bolt hole represented in the middle.

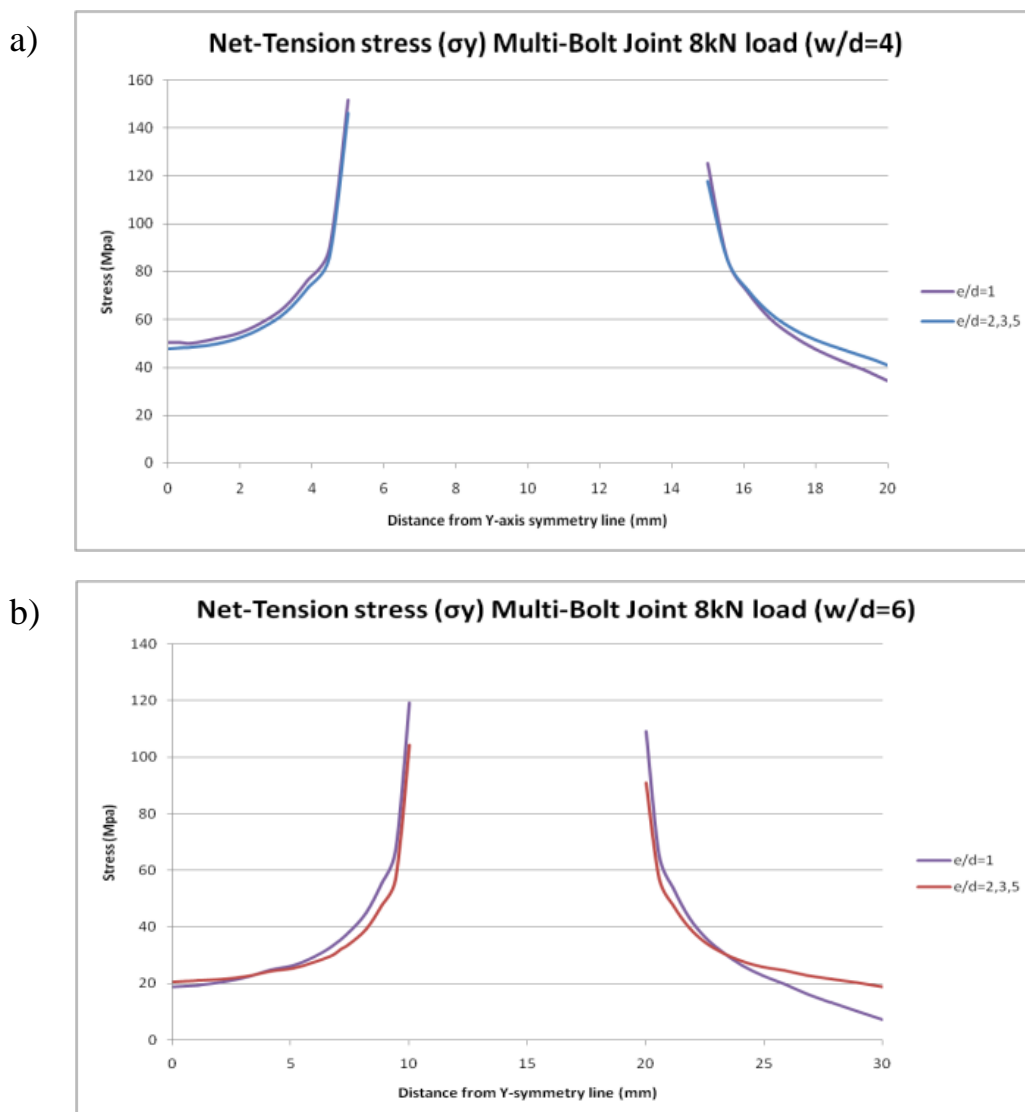


Figure 51 a) Net-tension stress when $w/d=4$ b) Net-tension stress when $w/d=6$

The peak stress concentrations on the hole edge increased significantly as the w/d was increased. As can be seen for the net-tension stress in figure 51 a) $w/d = 4$ b) $w/d = 6$. This variation of approximately 3% progressively increases to 19% variation when $w/d = 8$ as seen in Figure 52 below and can also be seen in a radial plot in figure 53.

At mid-point on the net-tension plane for the exterior side of the hole the percentage of stress compared to peak stress on the hole edge decreased from 42% to 14% as the plate width increased from 40mm to 80mm. Compared to the interior side of the hole the reduction was comparable decreasing from 36% to 12% for the same width increase as seen in table 11 below.

Table 11 Percentage of stress along net-tension plane with a change in w/d

% of peak σ_y at distance $0.5 \times$ (net-tension plane length) measured from hole edge			
w/d	4	6	8
% of peak σ_y (interior n-t plane)	36%	21%	12%
% of peak σ_y (exterior n-t plane)	42%	23%	14%

For narrow connections such as $w/d = 4$ when the σ_y stress was viewed around the bolt hole it was noted that the maximum compressive stress would always occur on the bearing plane (270° in figure 53 below) with zero stress occurring at 40° beneath the net-tension plane for $w/d = 4$ progressively moving to 47° when w/d is increased to 8 (figure 53).

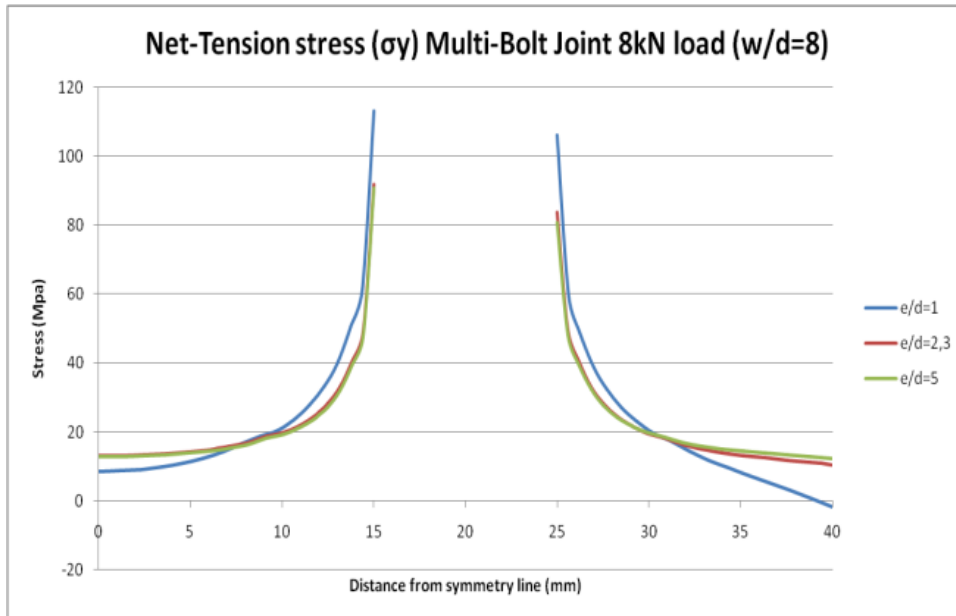


Figure 52 Net-tension stress when $w/d=8$

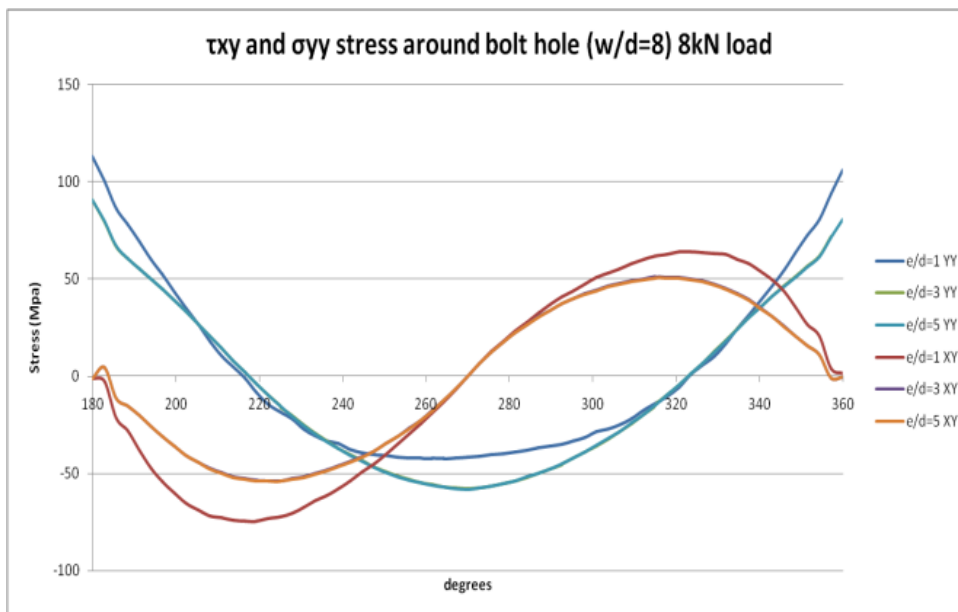


Figure 53 Shear and longitudinal stress around bolt hole edge

The overall trend is that narrow connections such as a 40mm wide plate will show higher stresses at the hole edge when compared to wider connections which can be seen in figure 54 and 55 below. The edge distance also has an effect on the stress level particularly when the e/d ratio is less than 2 showing higher stress levels again.

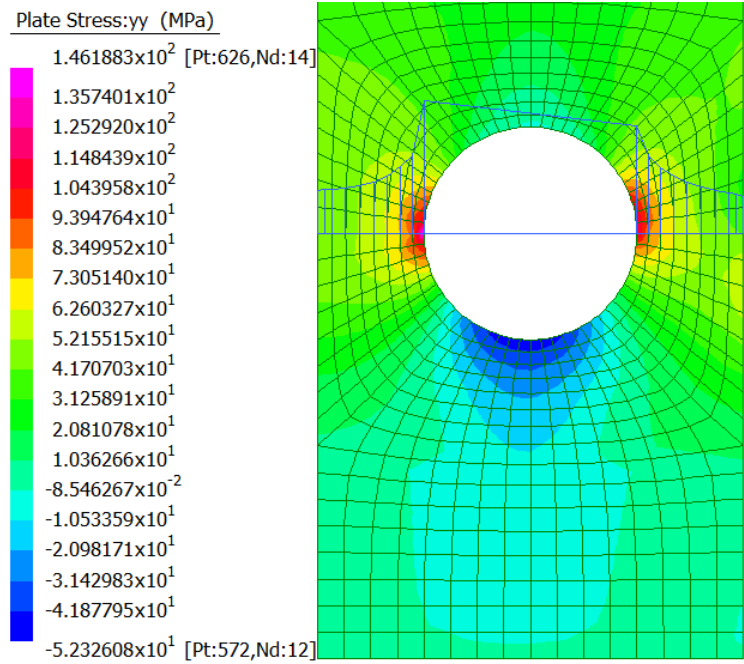


Figure 54 Distribution of net-tension stress on interior and exterior sides of the hole

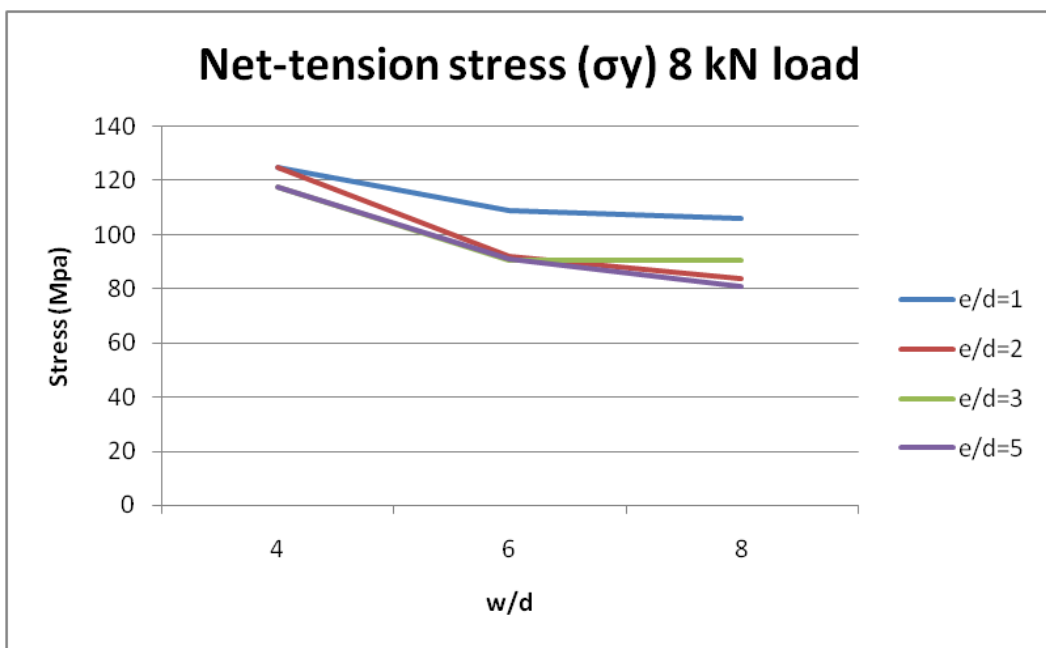


Figure 55 Net-tension stress concentration at hole edge for connection geometry

4.3.2 Shear Stress

Shear stress profiles along the shear-out plane were similar to those of the single bolt connection. For e/d ratios of 3 and 5 the shear stress profile was the same until reaching near zero. The overall value of maximum shear stress (on the shear-out plane) occurred for e/d of 3 and 5 occurred at 3mm along the shear-out plane and is consistent with the single hole value. As the width of the plate is increased from $w/d = 4$ to $w/d = 8$ the shear stress also decreases by about 19%. The gradients on the free edge side are all comparable to the single hole data with one common parameter being critical and that is the e/d ratio.

When inspecting the mid-point of the shear-out plane for the different e/d ratio's (table 12 below) the overall trend is comparable to single-hole connections. When $e/d=1$, at mid-point on the shear-out plane the shear stress is 76% of peak stress and reduces to 13% when $e/d=3$ and is not even a factor when $e/d=5$.

Table 12 Percentage of peak shear stress halfway along shear-out plane

% of peak τ_{xy} at distance $0.5 \times$ (shear-out plane length) measured from hole edge				
e/d	1	2	3	5
% of peak τ_{xy}	76%	26%	13%	2%

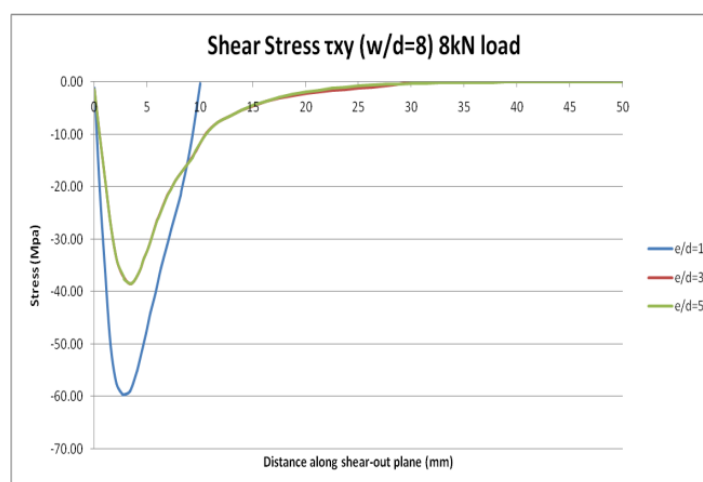


Figure 56 Shear stress on shear-out plane as e/d changes

The stress plot in figure 57 below shows the shear stress values on the hole edge actually vary between sides with the greater shear stress occurring on the interior side of the hole. This value being approximately 10% higher due to the different stress concentrations either side of the hole edge on the net-tension plane. This representation can be seen below in figure 57 (the interior side being the left side) by inspecting the maximum positive and negative shear values on the legend.

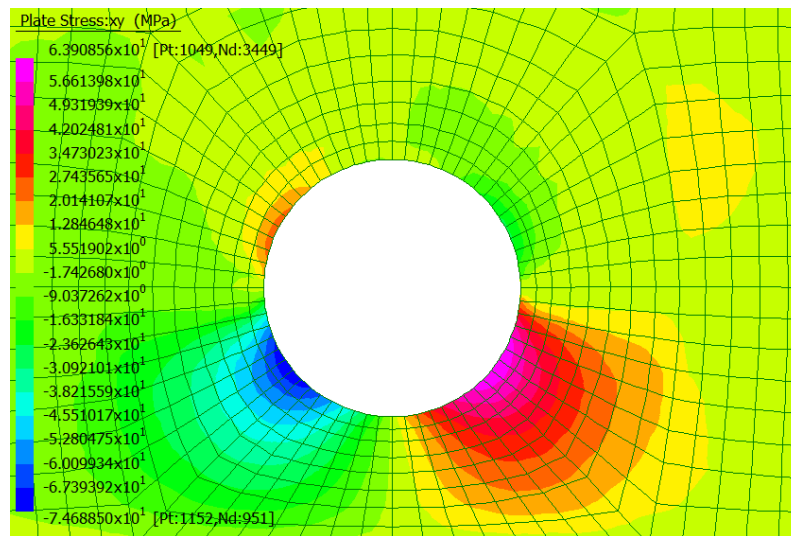


Figure 57 Shear stress on x-y plane for multi-bolt connection

4.3.3 Bearing Stress

The bearing stresses on the multi-bolt connections were significantly less than that of the single bolt connection due to the greater bearing area of 2 bolts rather than 1. The values of bearing stress were higher for the e/d ratios greater than 2 with an average value of 52 MPa while when $e/d = 1$ the value was lower at an average of 42 MPa. The compressive stresses would always dissipate to zero on the free edge at the bottom of the connection plate.

The ratio of bearing stress to net-tension stress varied between single and multi-bolt connections. For single bolt connections the ratio varied from 41% to 60% between $w/d = 3$ and $w/d = 7$ while for multi-bolt connections this was lower in the range of 27% to 37% between $w/d = 4$ and $w/d = 8$.

The bearing area or compressive region on the bolt hole edge does vary considerably depending on the width of the plate. When $w/d = 4$ the compressive region ranges over 95° and increases to 110° when $w/d = 8$ for the multi-bolt connection. While for the single bolt connection the compressive region was approximately 110° regardless of the joint geometry.

At mid-points along the bearing plane as the edge distance is increased the percentage of stress to peak stress reduces at the same rate to that of single-hole connections seen in table 13 below. Keeping in mind the peak bearing stresses on the hole edge are significantly lower for multi-bolt connections.

Table 13 Percentage of stress on bearing plane as e/d changes

% of peak σ_y at distance $0.5 \times$ (bearing plane length) measured from hole edge			
e/d	1	3	5
% of peak σ_y	27%	7%	<1

4.4 Change in thickness

The effects of thickness on stress levels on the connection has been studied using theory and FEA results. The theory uses equation 3.4 to calculate net-tension stress at the hole edge on a 9.5mm thick plate with all results discussed previously are for the 6.4mm thick plate.

The parameter change is based on the Exel Composites© pultruded plate S500 series (6.4mm thickness) and the S650 series (9.5mm thickness).

The results show that by increasing thickness from 6.4mm to 9.5mm the longitudinal stress (σ_y) will decrease by 33%. The longitudinal stress around the bolt hole has been plotted for $w/d = 3$ and $e/d = 1$ showing the decrease in stress with the change in thickness as seen in figure 58 below. All geometries give the same stress reduction with the peaks still occurring on the net-tension plane (0°) and bearing plane (-90°).

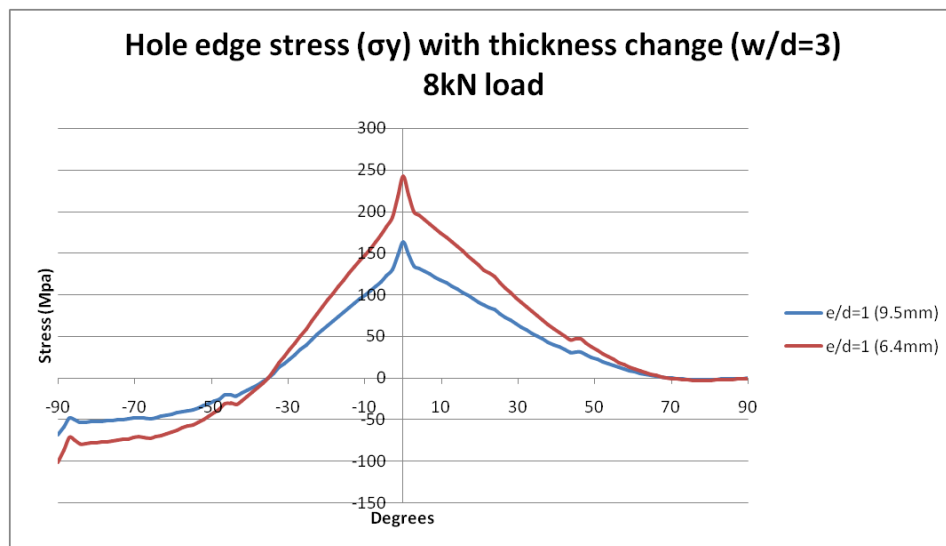


Figure 58 Longitudinal stress around bolt hole edge with a change in thickness

The profile of the net-tension plane shows the same trend giving stress reductions of 33% throughout the x-axis as seen in figure 59 with free edge stress remaining at a value of 8% of the initial stress concentration at the hole edge.

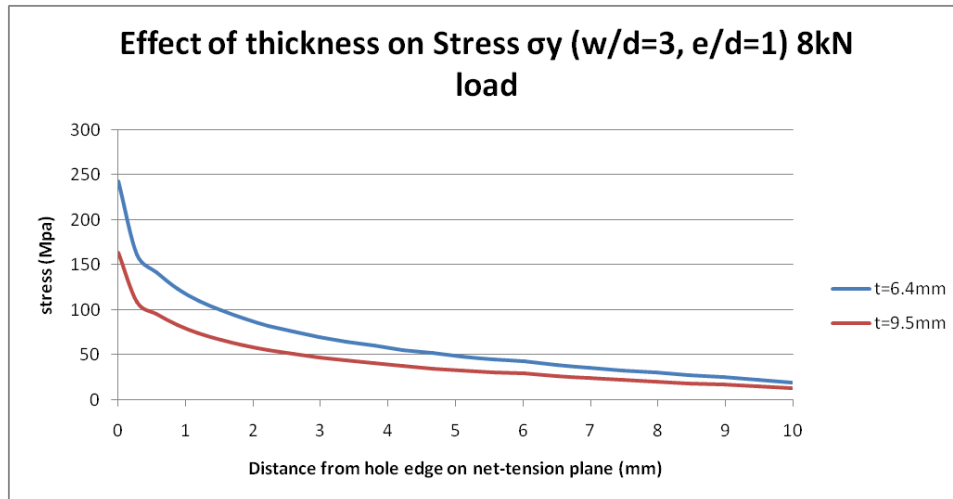


Figure 59 Stress profile for net-tension plane when thickness is changed

All theory and FEA results have been tabulated in Appendix F with the average stress value being 1.8% higher than the theoretical result. This shows good correlation between the FEA and theory for the concentration stress on the net-tension plane.

4.5 Single Bolt Failure mode prediction

The FEA results have been studied using von-Mises criteria to show stress distributions on the connection plate to determine likely failure modes when under a tension load. Although von-Mises is mostly used for ductile material analysis it will still provide data on stressed areas and show areas that are prone to shear-out, net-tension or bearing failure.

Petrovic (2012) has published critical regions that the failure modes will occur in;

$$\begin{array}{ll}
 0 \leq \theta_f \leq 15^\circ & \text{Bearing mode,} \\
 30 \leq \theta_f \leq 60^\circ & \text{Shear-out mode,} \\
 75 \leq \theta_f \leq 90^\circ & \text{Net-tension mode.}
 \end{array}$$

with 0° being the bearing plane and 90° the net-tension plane measure anti-clockwise from the hole centre.

A graphical presentation of a shear out failure can be seen in figure 60 ($e/d = 1$) below starting with $e/d = 1$ and progressing to $e/d = 5$. An approximate prediction can be made by analysing the geometry and the stress areas in Figure 60. Shear-out failure can be predicted and is obvious with lower $e/d < 2$ and as the e/d is increased to 4 the failure area changes to the net-section. Although width plays an important part in net-tension failure the width shown is 30mm making it clearer that failure in net-tension is likely when the e/d ratio is above 3.

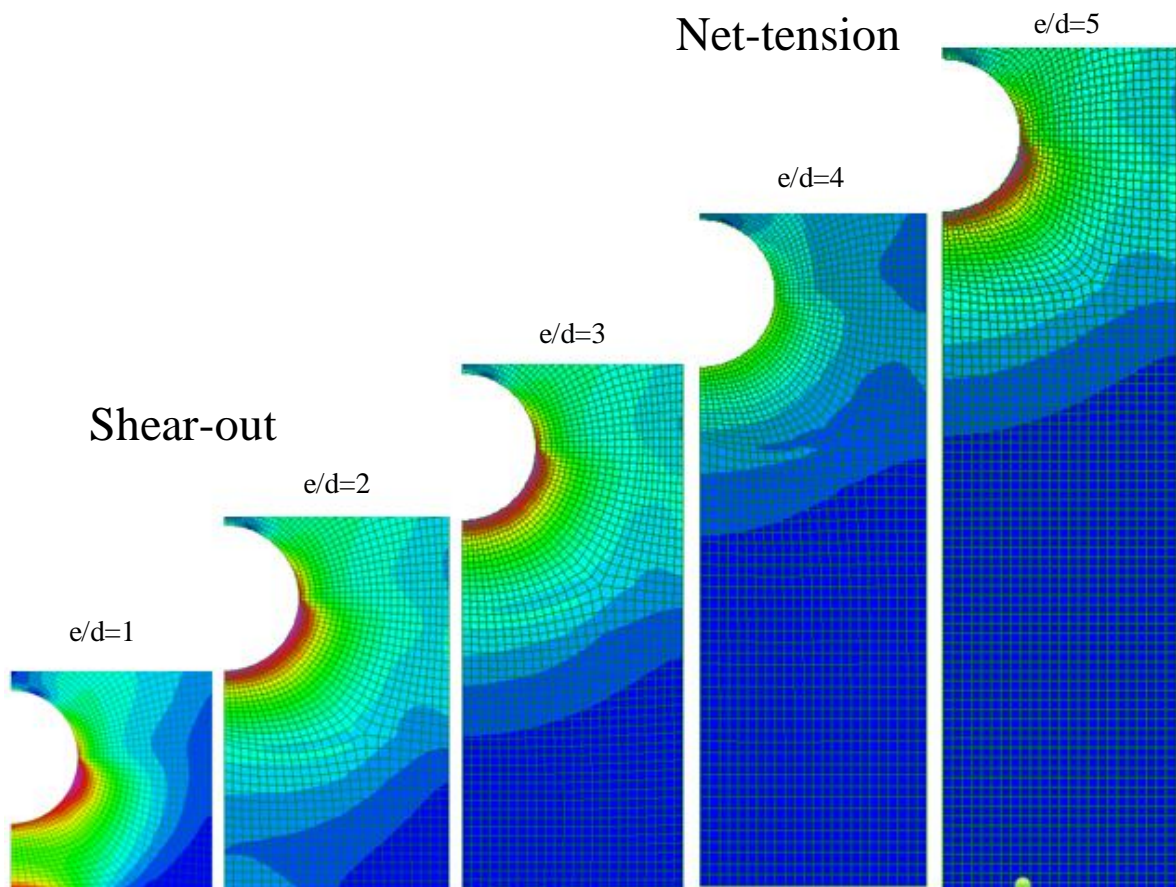


Figure 60 Von Mises stress distribution showing shear-out failure to net-tension failure

The effect of width is important to avoid net-tension failure. As can be seen above the stress contours favour a net-tension failure mode when the w/d is low. By eliminating shear-out failure by keeping the e/d high a progression can be seen from a net-tension failure to bearing failure simply by increasing the width of the connection as seen in figure 61 below.

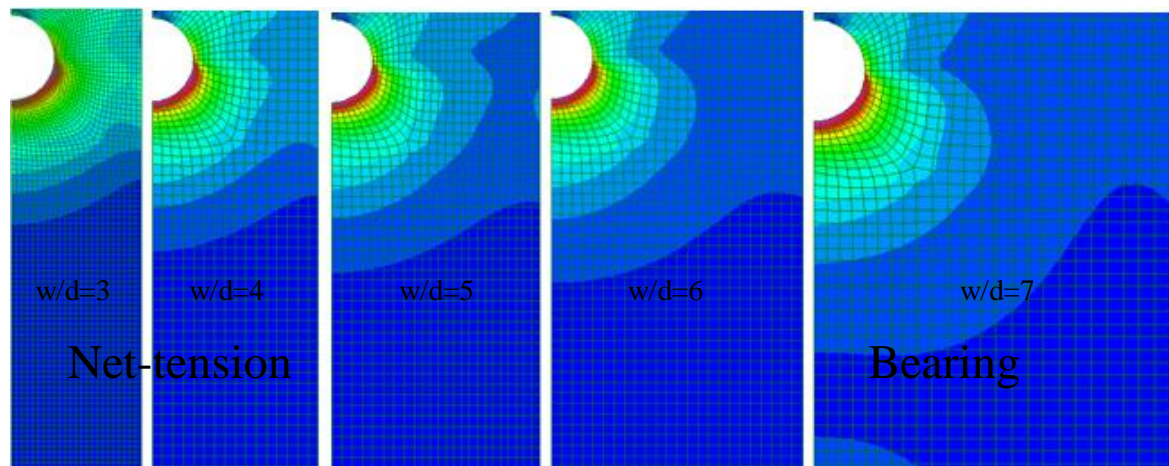


Figure 61 Progression from net-tension to bearing failure modes

The shear-out failures in figure 60 are a result of the shear stress on the x-y plane being greater than the shear strength of the material. The stress gradients on the shear-out plane as seen in figure 40, 41 and 42 show $e/d < 2$ as critical which correlates to the von-Mises distribution.

The net-tension failures as seen in von-Mises distributions above in figure 61 also correlate to the plots shown for the net-tension plane stress profiles. When the end edge distance is not a factor in failure the width is critical. When $w/d < 4$ the net-tension stress is highest indicating likely failure would be in the net-section. This can be seen in the von-Mises presentation above showing favourable contours along the net-section to initiate the failure.

When neither net-tension or shear-out failure occur the most likely failure mode will be bearing failure which results in crushing of the material in the bearing area. This is considered the safest failure mode as it often occurs gradually rather than catastrophically. For higher e/d and w/d ratio's bearing failure is predominantly likely as can be seen in figure 61 where there is a progression from net-tension failure to bearing failure as the width of the connection is increased.

Using both von-Mises stress distributions and the stress plots from the failure planes an estimate as to the likely failure mode can be made. Values of $e/d < 2$ should be avoided with a preferred value of $e/d > 3$ for an added safety margin should be used to avoid shear-out failures. To eliminate net-tension failure $w/d < 4$ should be avoided and with an added safety margin $w/d > 5$. By using both these guidelines a bearing failure would likely be induced rather than a catastrophic failure.

4.6 Multi-Bolt Failure Mode Prediction

Failure modes for multi-bolt (single row) connections show similar behaviour to that of single bolt joints with one major difference being that the middle section between the two bolts may tear out due to both shear and tension.

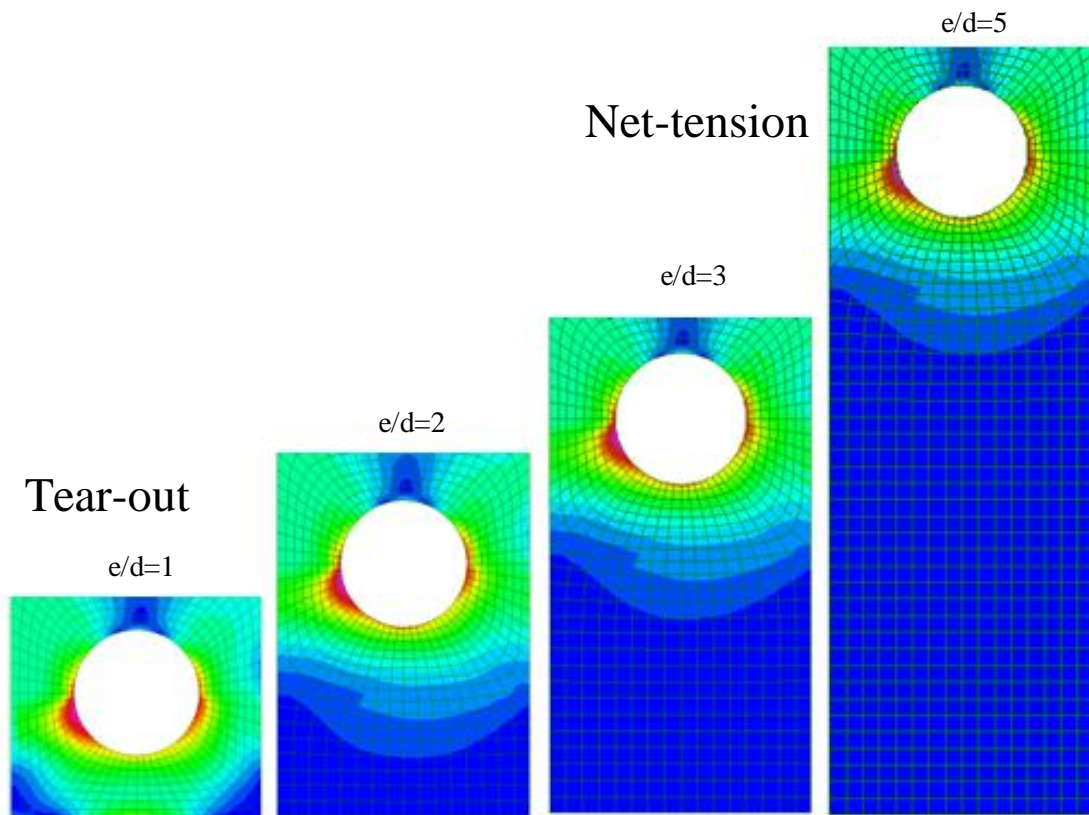


Figure 62 Progression from tear-out failure to net-tension failure mode

In figure 62 above, $e/d = 1$ shows susceptibility to the tear-out of the entire middle section with higher stress area seen left of the bolt (interior) and beneath the bearing area of the bolt creating potential for tear-out. As the e/d ratio is increased the progression is from a tear-out to net-tension failure as the e/d increases to 5. The tear-out example can be seen in figure 63 below with a) being the failure planes associated with the connection and b) showing the end result of the middle section being torn out.

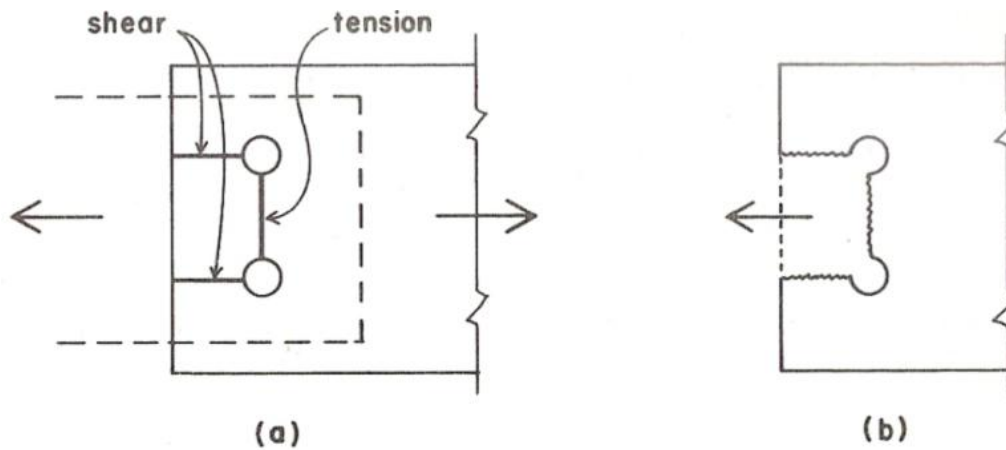


Figure 63 Tear-out failure a result of shear and tension stress (PADA, 2011)

Progression from a net-tension failure when $w/d = 4$ to a more localized bearing failure as the width of the plate is increased can be seen in figure 64. Provided there is no possibility of shear-out or tear-out than the behaviour is the same as single bolt connections.

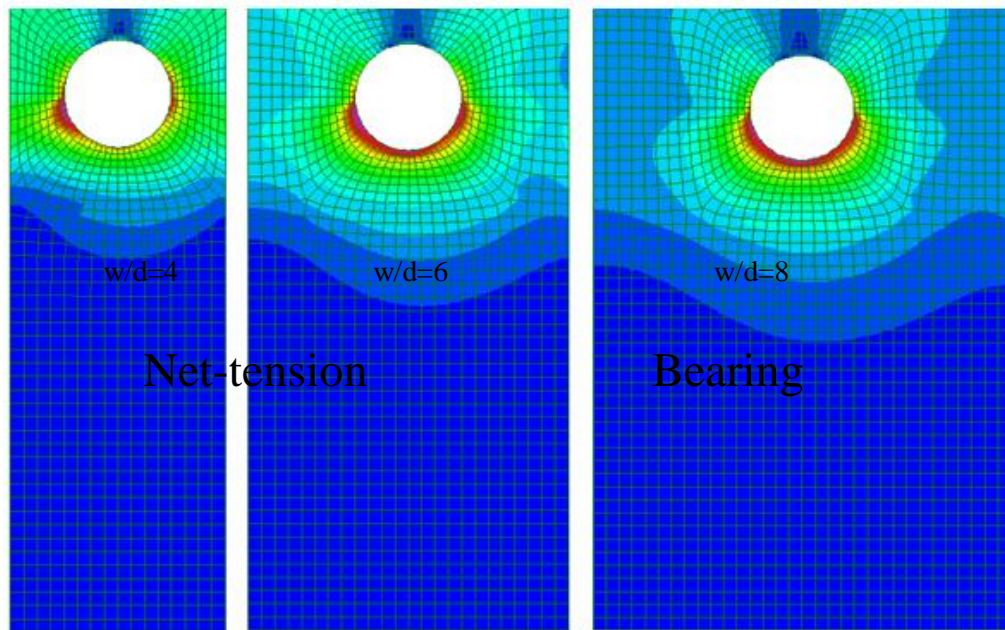


Figure 64 Progression from net-tension failure to bearing failure mode

4.7 Summary of Results

Net-tension stresses are at a maximum at the hole edge on the net-tension plane with a dramatic reduction in stress to the free edge where stress remains at a nominal level. When the width of the plate increases the stress at the hole edge decreases and when the e/d is increased the stress decreases until $e/d = 2$ then the stress remains fairly constant.

The shear stress peak always remains in approximately the same location regardless of the e/d and w/d ratio's. The peak shear stress is highly effected by the e/d ratio being at maximum when e/d is low and decreasing to a fairly constant level when $e/d > 2$. The location of the maximum peak value of shear on the x-y plane is not on the shear-out plane but lies 1.5mm inwards from the shear-out plane. When $e/d > 3$ the shear stress falls to zero at a distance of $3d$ from the hole centre.

Bearing stress changes very little with any width change and only showed an increase when the e/d was changed from 1 to 2 with the stress increasing. The compressive region in

the bearing area of the material did change between 95° and 110° for multi-bolt connection and remained constant at 110° for single bolt connections.

The overall stress reduction when the thickness was increased was 33% for σ_y and τ_{xy} stress. The likely failure mode such as net-tension, bearing or shear-out does not change when altering the thickness.

Chapter 5

Conclusion

5.1 Summary

This research has revealed further knowledge and reinforced previous knowledge in both single and multi-bolt FRP connections. The use of FEA has allowed a detailed stress analysis to take place which would not be possible with experimental testing. By studying the failure planes with a parametric study of joint geometry the stress behaviour has been investigated and abnormalities recorded which should be part of future research.

5.2 Conclusions

Based on the findings from chapter 4 some conclusions can be made with some aspects similar to both single and multi-bolt connections.

When the net-tension plane for single bolt joints was studied it was found in order to avoid high stresses on the hole edge $e/d < 2$, and $w/d < 4$ should be the minimum. Compared to multi-bolt connections the ratios to avoid the peak stress concentrations were $e/d < 2$ and $w/d < 6$ as a minimum. If the design used these ratio's as a minimum the stress reduction from peak stress would be 29% for single hole connections and 27% for multi-bolt connections.

In both connection types on the net-tension plane the stress contours were higher beneath the net-tension plane which may indicate that if failure was to occur in the net-section it may be directed slightly beneath the net-tension plane initially. What also is common between the connections types is that peak concentration of net-tension stress on the hole edge always occurred when $e/d = 1$. This was rather surprising as the e/d ratio should not adversely affect the net-tension stress. In both single and multi-bolt connections the same occurred with a 23% drop in peak stress for single bolt and 17% drop in multi-bolt connections when the e/d changed from 1 to 2.

When investigating the shear stress for both configurations of connections the point of maximum shear is always approximately 1.5mm inside of the shear-out plane on the hole edge. EUROCOMP's requirement for analysis of the shear-out plane for joint design doesn't consider the point of maximum shear is not on the line of failure. Commonly, the decay rates of maximum shear stress are the same between single and multi-bolt connections with the apex of shear on the shear-out plane in the same location as well. Minimum e/d ratio to avoid shear-out based on the finding should be $e/d = 2$.

The single bolt connection shear stress on the hole edge does in fact move from 38° below the net-tension plane to 43° as the w/d increases from 3 to 7 and does not occur in multi-bolt connections. However, in multi-bolt connections there is unequal shear stress distribution between the interior and exterior sides of the hole with the interior side having 10% greater shear stress than the exterior side due to the higher tension concentration on the interior net-tension plane.

After evaluating the bearing plane for stress one common occurrence is that when $e/d = 1$ the bearing stress is about 20% lower than all other e/d ratio's and when $e/d \geq 2$ it is basically constant. Overall as expected the bearing stresses are significantly lower for the multi-bolt

connections as compared to single bolt connections for the same load due to the increased bearing area. Further investigation needs to be done in evaluating the bearing stress as the FEA may not reflect accurate data due to the differences encountered between modelling of the bolt and the interaction involved with the non-linear contact method and linear "radial restraint" method.

When the thickness of the material is changed from 6.4mm to 9.5mm there is a 33% reduction for all stress values with no changes in behaviour which would affect failure modes.

Prediction of the failure modes is a difficult procedure but with a combination of FEA and stress plots used in conjunction with each other high stress concentrations can be avoided which may initiate failure. The following table summarises suggested and minimum connection ratio's based on this research.

Table 14 Suggested connection geometry from research

Suggested Joint Geometry based on this Research		
Geometric ratio	Recommended	Minimum
edge distance/bolt diameter e/d	≥ 3	2
width/bolt diameter w/d (Single-bolt connection)	≥ 5	4
width/bolt diameter w/d (Multi-bolt connection)*	≥ 7	6

*Assumes $s/d = 0.5g/d$ for all cases

The e/d ratio's and single bolt w/d ratio's are consistent with previous research and EUROCOMP (1996) however the multi-bolt w/d ratio is higher. Although the research altered the s/d and g/d ratio's based on width changes ($s/d = 0.5g/d$), the bolt hole centre was always mid-point between the line of symmetry and the free edge. The reduced scope and limited data on varying s/d and g/d ratio's may be attributed variation between this research and others.

The results of the research can be directly compared to the already established steel design codes for connections such as the AS4100 9.6, design details for bolts and pins. AS4100 has published minimum geometry for edge distances as $1.5d$ for all edges from the hole centre and the gauge (pitch) as $2.5d$. For the single bolt and multi-bolt (single row) connections the equivalent e/d and w/d ratio's are shown below in table 15 from AS4100.

Table 15 Steel and FRP minimum geometry

Comparison of steel and FRP minimum geometry		
Geometric ratio	minimum	
	steel*	FRP^
e/d	1.5	2
w/d (single bolt)	3	4
w/d (multi bolt, single row)	5.5	6

*AS4100 9.6 AS steel structures (rolled, flat bar, sections)

^based on this research

5.3 Achievement of Objectives

1. Conduct a literature review and research into mechanical connections of composites.

This has been fulfilled in Chapter 2 where literature on FEA, experimental and theoretical research had been accomplished with gaps and discrepancies in previous research identified.

2. Theoretical analysis of composite connections, single and multiple bolts under tension loads.

The methodology has been set out in Chapter 3 and results presented in Chapter 4 for theory on the validation process of the FEA and calculation of net-tension stress concentrations for tension joints.

3. Develop models of connections in Strand7 and analyse their behaviour.

A thorough analysis schedule was prepared for single and multi-bolt joints with results presented in Chapter 4.

4. Comparisons of theoretical results and computer model outputs and explaining the causes of variation, if any.

Theoretical results for the net-tension were compared to FEA and results proved to be accurate as seen in Chapter 4. Initial validation using theory showed minor discrepancy in initial peak stress on the hole edge but was further validated using other models in chapter 3.

5. Conclusions on current research and recommendations for future research.

This is presented in Chapter 5 and includes suggested joint geometry based on findings.

6. Produce and submit an academic dissertation on the research.

Completed.

5.4 Recommended Future Research

Below are some future research that should take place that was outside the scope of this project or should be investigated further;

- Based on findings in this research and the lack of previous research data further investigation should be made into appropriate and representative ways to model bolt and connection material interactions. The difference in results between the cosine distribution, radial restraint method and contact need further study to detail differences particularly with bearing stresses.
- FEA modelling of a composite with variation in ply angle should be attempted and can be compared to experimental data with particular attention paid to the failure modes as joint geometry changes.

List of References

Ascione, F, 2010, '*A preliminary numerical and experimental investigation on the shear stress distribution on multi row bolted FRP joints*', *Mechanics Research Communications*, Vol.34, pp164-168.

Bank, Lawrence C 2006, *Composites for Construction: Structural Design with FRP Materials*, Wiley, Hoboken, NJ.

Broughton, W.R, Crocker, L.E, Gower, M.R.L, 2002, '*Design requirements for bonded and bolted composite structures*', NPL Materials Centre, National Physical Laboratory, Middlesex, UK.

Callus, P, 2007, "*The effect of hole size and environment on the mechanical behaviour of Quasi-isotropic AS4/3501-6 laminate in tension, compression and bending*", Defence Science and Technology Centre, VIC , Australia

Creative Pultrusions, "*Products and Solutions*", viewed 18th July, 2015,
<http://www.creativepultrusions.com/>

Clarke, J, 1996, "*Structural Design of Polymer Composites*", *EUROCOMP design code and handbook*, The European structural polymeric composites group, Chapman and Hall, UK.

Dura Composites, "*GRP Products for the rail industry*", viewed July 5, 2015,
<http://www.duracomposites.com/rail-industry-products/grp-frp-structures>

Clarke, J, 1996, "*Structural Design of Polymer Composites*", *EUROCOMP design code and handbook*, The European structural polymeric composites group, Chapman and Hall, UK.

Feo, L, Marra, G, Mossallam A.S, 2012, '*Stress analysis of multi-bolted joints for FRP pultruded composite structures*', *Composite structures*, vol. 94, pp 3769-3780.

Hart-Smith, L,J, 1979, "*Mechanically fastened joints for advanced composites*", Conference on fibrous composites design, New York

Hebei Shangqi Environmental Protection Sci-tech, "*FRP Products*", viewed August 10, 2015, http://www.sunkeyfrp.com/watertanks/other_frp_products.html

Jones, Robert M 1999, *Mechanics of Composite Materials*, 2nd edn, Taylor and Francis Inc, Philadelphia, PA.

Lee, Y, Choi, E, Yoon, S, 2015, '*Effect of geometric parameters on the mechanical behaviour of PFRP single bolted connection*', *Composites Part B*, vol. 75, pp 1-10.

Marra, G, 2011, '*A numerical and experimental analysis on the mechanical behaviour of bolted joints between pultruded profiles and T-stubs of glass fibre reinforced polymer*', PhD thesis, University Degli Studi di Salerno.

McClendon, J, 2011, '*Determine bearing stress distribution in Composite*', thesis, University of NSW, ADFA.

Mottram, J.T, 2002, "*Why is the design of primary structural connections an issue?*", 6th CoSACNet workshop, Warwick, UK.

Mottram, J.T, 2009, '*Design guidance for bolted connections in structures of pultruded shapes: gaps in knowledge*', University of Warwick, UK.

Mottram, J.T, Zafari, B, 2010, '*Pin bearing strengths for bolted connections in fibre-reinforced polymer structures*', *Structures and Buildings*, vol. 164, pp 291-305.

NPTEL 2007, National Programme on Technology Enhanced Learning, Ministry of HRD Government of India "*Strength and Failure theories*"

Vipel, 2012, "*Vinyl-ester resin guide*", AOC world headquarters, TN, 38017

Park, J.S, Lee, S, Joo, H.J, Yoon, S.J, 2009, '*Experimental and analytical investigations on the bolted joints in pultruded FRP structural members*', *International Institute for FRP in Construction for the Asia-Pacific Region*, pp 395-400

Rossner, C, 1992, '*Single bolted connections for orthotropic fibre-reinforced composite structural members*', Masters of Science Thesis, University of Manitoba.

Sommer, R, 2011, '*Fiber reinforced polymer (FRP) pultruded shape structural connections*', Masters of Science Thesis, Kansas State University.

Standards Australia International, 1998, "*Australian Standards, Steel Structures*", AS4100, Sydney, NSW, 2001, Australia.

Strand7, 2010, "*Reference Manual*" Release 2.4.6, edition 3, Sydney, NSW

Turvey, G.J, Wang, P, 2007, '*An FE analysis of the stresses in pultruded GRP single-bolt tension joints and their implications for joint designs*', *Computers and structures*, vol. 86, pp 1014-1021.

Turvey, G.J, 2011, '*Failure of single-lap single bolt tension joints in pultruded glass fibre reinforced plate*', Lancaster University, pp 1-8.

Okutan, B, 2001, "*Stress and failure analysis of laminated composite pin joints*", Doctor of philosophy in Mechanical Engineering, Docuz Eylul University.

PADA Structure, 2012, "Engineering from an Architect's perspective", <http://pada-structure.blogspot.com.au/2011/07/section-12-bolted-connections.html>, viewed August 8, 2015

Whitney, J, 1990, "*Delaware Composites Design Encyclopedia*", Technomic publishing company Inc, Lancaster, Pennsylvania, USA

Wheeler Construction, "*Past Projects*", viewed July 15th, 2015, <http://www.wheeler-con.com/recreation-bridges/covered-recreation-bridges/>

Appendix A Project Specification

University of Southern Queensland

FACULTY OF ENGINEERING AND SURVEYING

ENG4111/4112 Research Project

PROJECT SPECIFICATION

FOR: Adam ROBINSON

TOPIC: A STUDY INTO THE BEHAVIOUR OF FRP BOLTED CONNECTIONS

SUPERVISOR: Dr Sourish Banerjee

PROJECT AIM: Analysis of the mechanical behaviour of bolted connections

PROGRAMME: (rev 1, 11th March 2015)

1. Literature review and research into mechanical connections of composites
2. Theoretical analysis of composite connections, single and multiple bolts under tension loads
3. Develop models of connections in Strand7 and analyse their behaviour
4. Comparisons of theoretical results and computer model outputs and explaining the causes of variation, if any
5. Conclusions on current research and recommendations for future research
6. Produce and submit academic dissertation on research

As time permits:

7. Theoretical and computer modelling of composite connections in a truss

AGREED: _____(student) _____(supervisor)

Date: / /2015

Date: / /2015

Appendix B Theoretical Calculations

Table B1 Single bolt theoretical calculations with FEA comparison

geometry		geometric ratio		concentration data				oy results		% error
w	e	w/d	e/d	α	β	Θ	Kte/Ktc	theory	FEA	
30	10	3	1	3	0.33	0.00	4.0	246.2	242.6	1.4
	20		2		0.67	0.75	3.4	214.8	203.1	5.5
	30		3		1.00	1.00	3.3	203.1	204.5	-0.7
	40		4		1.33	1.00	3.3	203.1	209.2	-3.0
	50		5		1.67	1.00	3.3	203.1	209.2	-3.0
40	10	4	1	4	0.25	-0.50	5.5	227.1	221.8	2.3
	20		2		0.50	0.50	4.6	189.6	173.0	8.7
	30		3		0.75	0.83	4.3	177.1	169.9	4.1
	40		4		1.00	1.00	4.1	170.8	169.8	0.6
	50		5		1.25	1.00	4.1	170.8	169.8	0.6
50	10	5	1	5	0.20	-1.00	7.0	218.8	219.8	-0.5
	20		2		0.40	0.25	5.8	179.7	166.5	7.3
	30		3		0.60	0.67	5.3	166.7	160.5	3.7
	40		4		0.80	0.88	5.1	160.2	159.9	0.2
	50		5		1.00	1.00	5.0	156.3	159.8	-2.3
60	10	6	1	6	0.17	-1.50	8.6	215.2	225.3	-4.7
	20		2		0.33	0.00	7.0	175.0	161.3	7.8
	30		3		0.50	0.50	6.5	161.6	152.4	5.7
	40		4		0.67	0.75	6.2	154.9	151.3	2.3
	50		5		0.83	0.90	6.0	150.9	150.9	0.0
70	10	7	1	7	0.14	-2.00	10.3	213.5	221.3	-3.6
	20		2		0.29	-0.25	8.3	172.5	159.1	7.8
	30		3		0.43	0.33	7.6	158.9	148.0	6.8
	40		4		0.57	0.63	7.3	152.0	145.7	4.2
	50		5		0.71	0.80	7.1	147.9	145.3	1.8
average error %									2.1	

Table B2 Multi-Bolt theoretical calculations with FEA comparison

geometry		geometric ratio		concentration data				oy results		% error	
w	e	w/d	e/d	α	β	δ	Θ	Kte/Ktc	theory		FEA
40	10	4	1	2	0.50	0.50	0.50	2.2	94.7	125.1	-32.1
	20		2		1.00	0.50	1.00	2.0	125.0	125.1	-0.1
	30		3		1.50	0.50	1.00	2.0	125.0	117.7	5.8
	50		5		2.50	0.50	1.00	2.0	125.0	117.7	5.8
60	10	6	1	3	0.33	0.33	0.00	3.8	117.3	109	7.1
	20		2		0.67	0.33	0.75	3.2	99.7	91.9	7.8
	30		3		1.00	0.33	1.00	3.0	93.8	90.8	3.2
	50		5		1.67	0.33	1.00	3.0	93.8	90.8	3.2
80	10	8	1	4	0.25	0.25	-0.50	5.3	110.5	106.2	3.9
	20		2		0.50	0.25	0.50	4.4	91.8	83.7	8.8
	30		3		0.75	0.25	0.83	4.1	85.5	90.7	-6.0
	50		5		1.25	0.25	1.00	4.0	82.4	80.8	2.0
average error									0.8		

Appendix C Net-tension plots

Single Bolt Connections

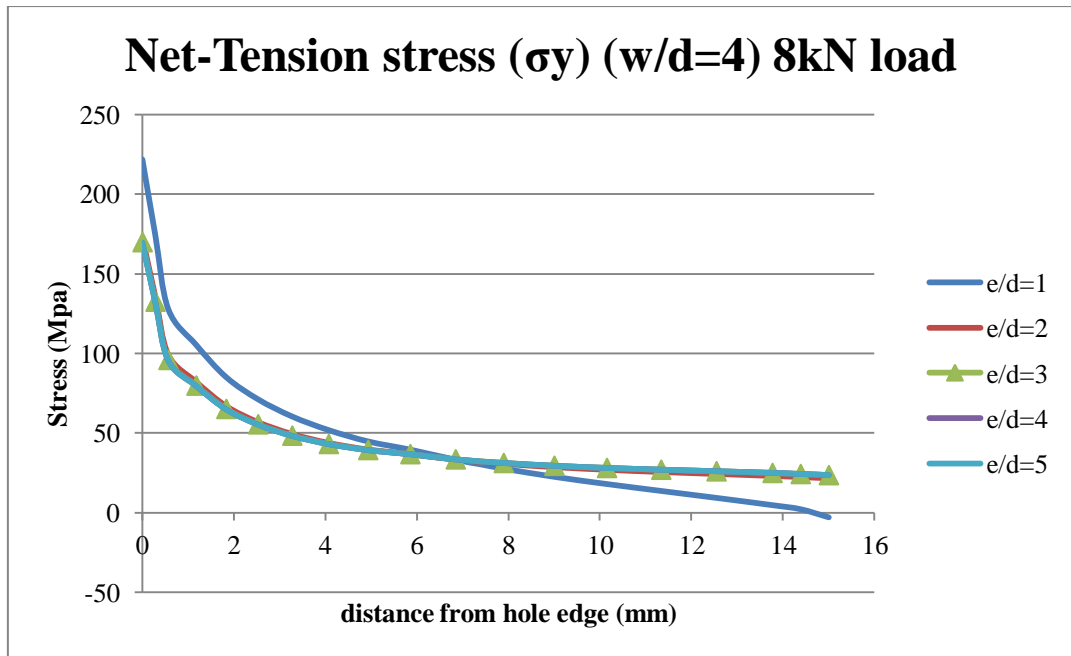


Figure C1 Net-tension stress $w/d=4$

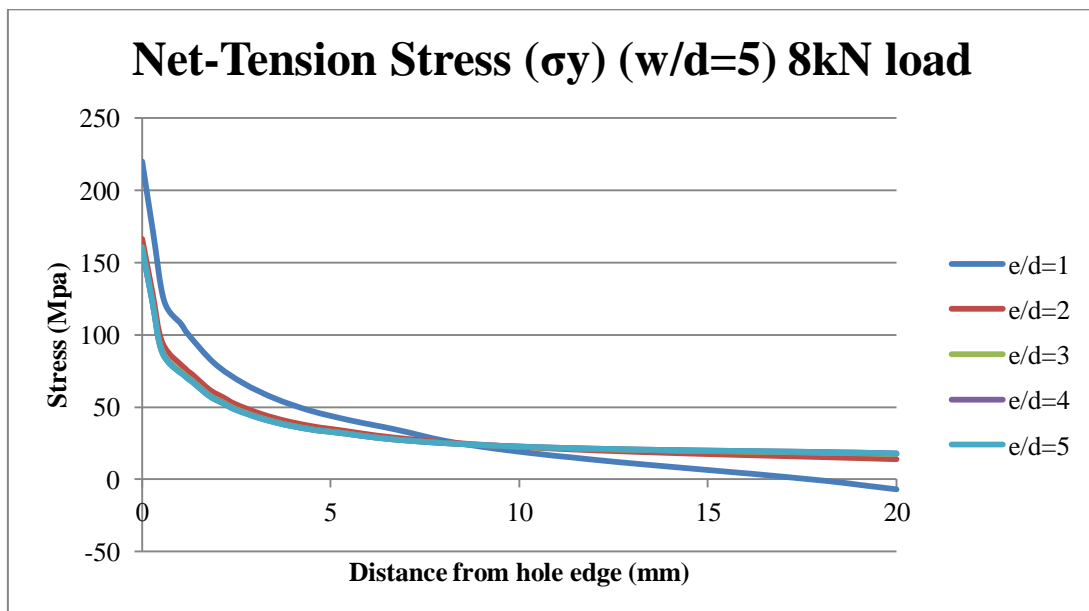


Figure C2 Net-tension stress $w/d=5$

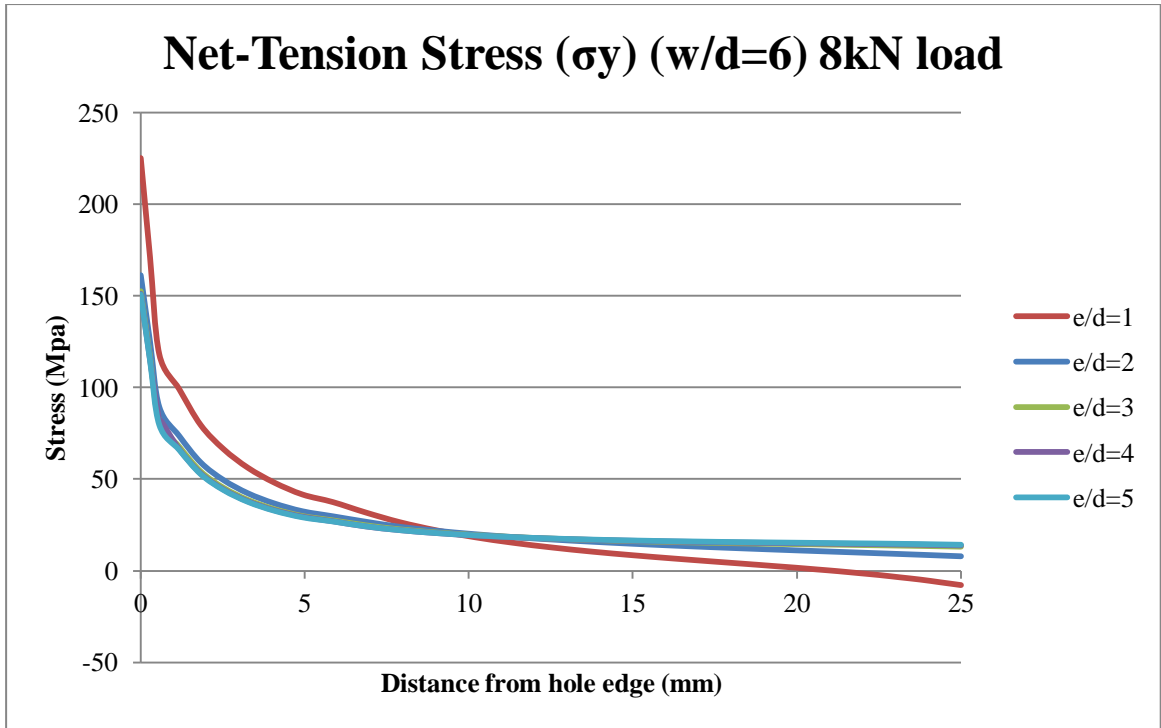


Figure C3 Net-tension stress w/d=6

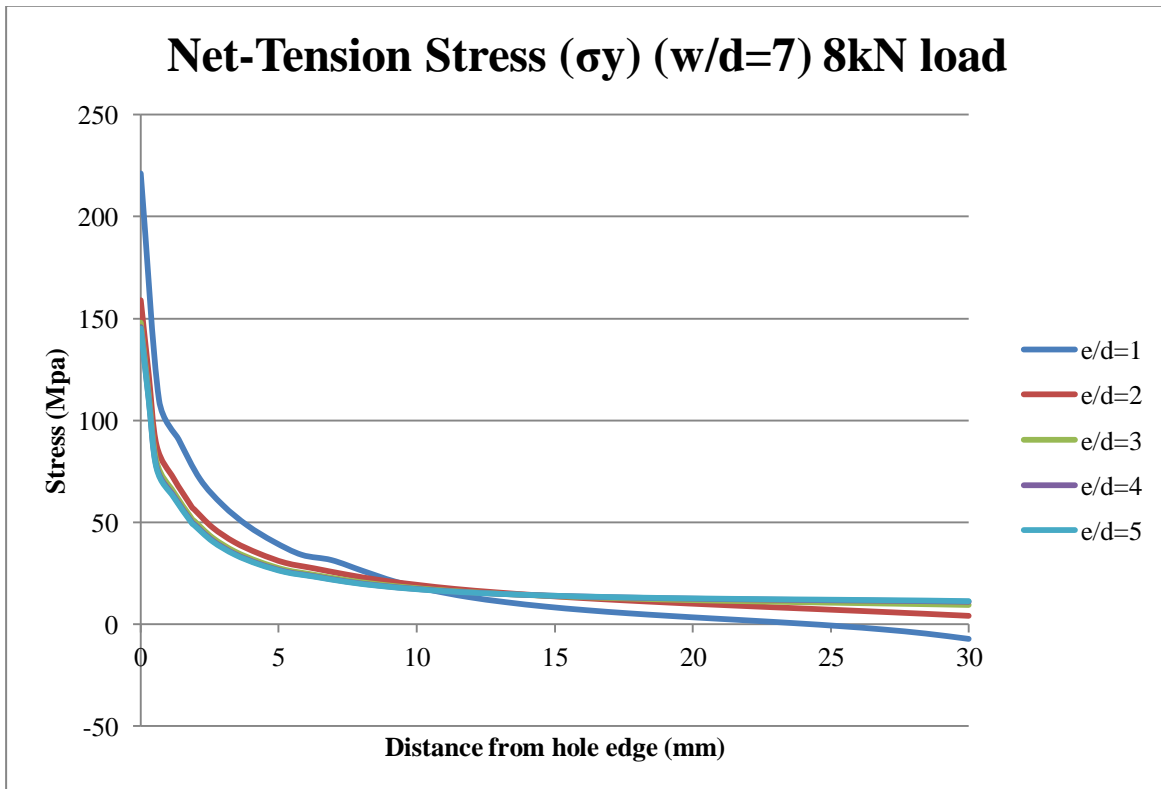


Figure C4 Net-tension stress w/d=7

Multi-bolt connections

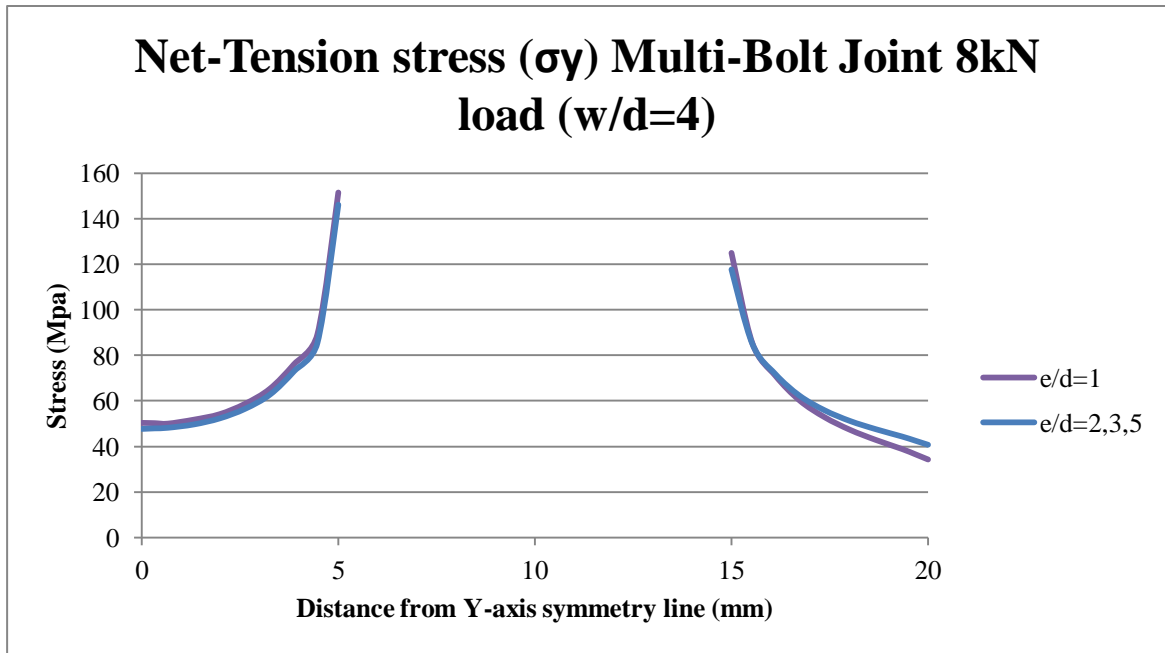


Figure C5 Net-tension stress w/d=4

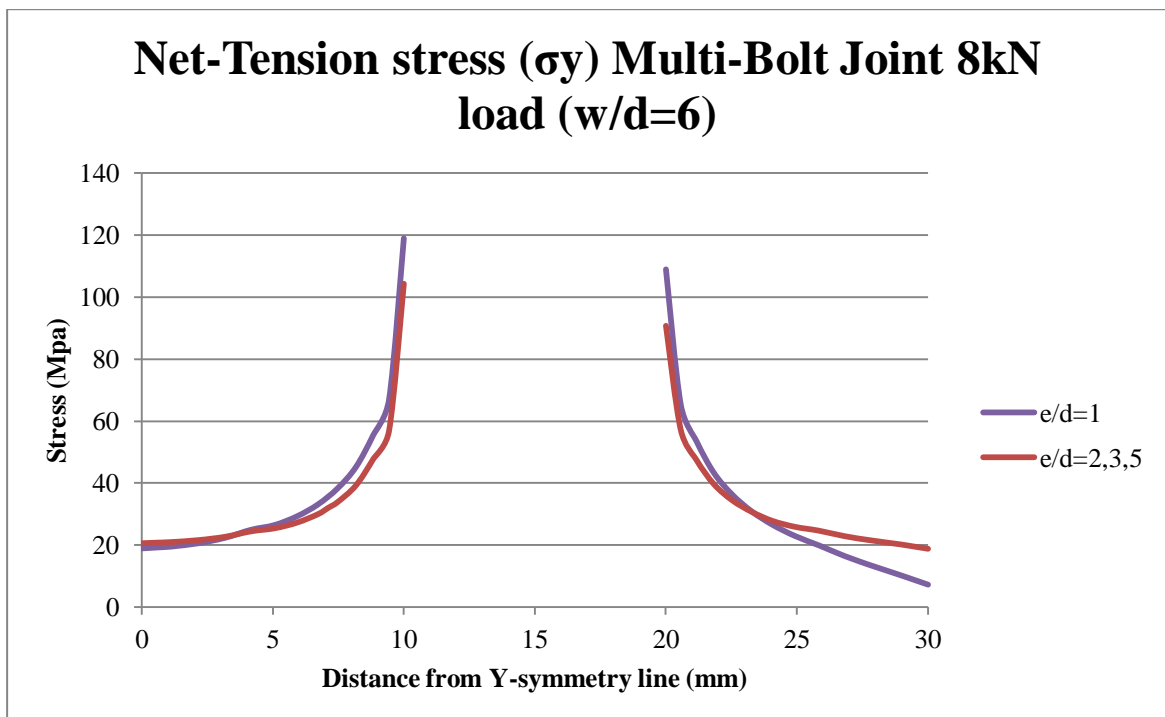


Figure C6 Net-tension stress w/d=6

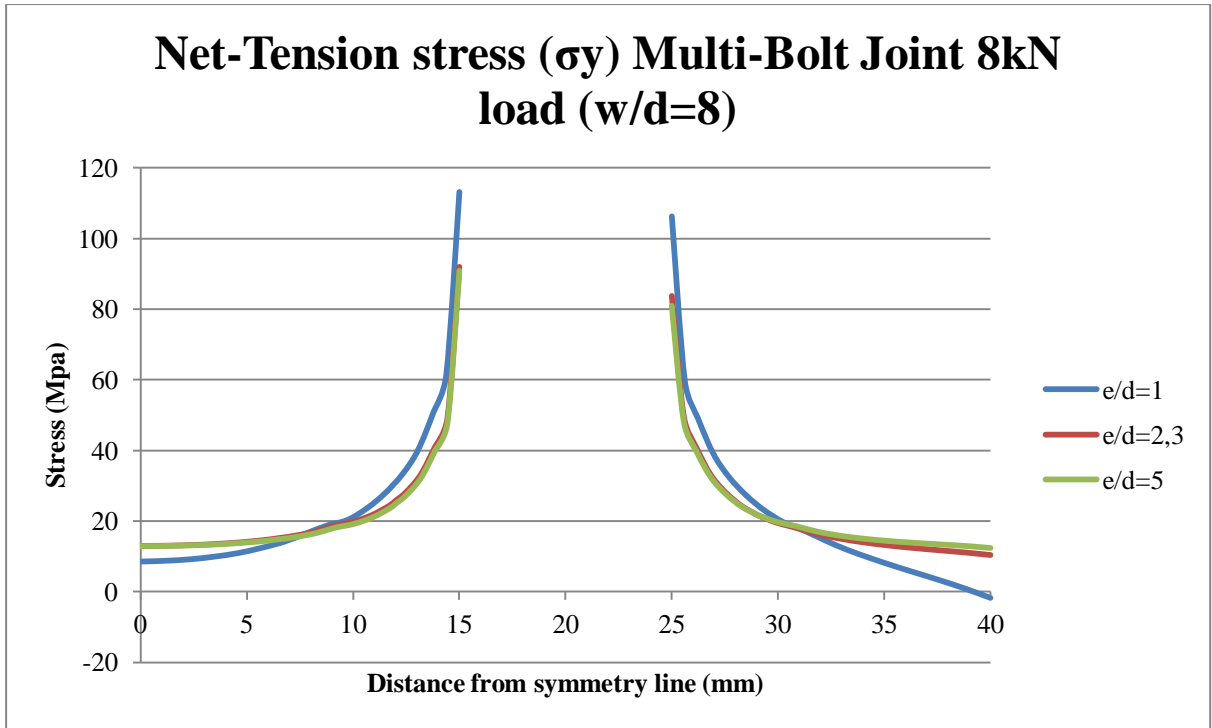


Figure C7 Net-tension stress w/d=8

Appendix D Shear stress plots

Single bolt connections

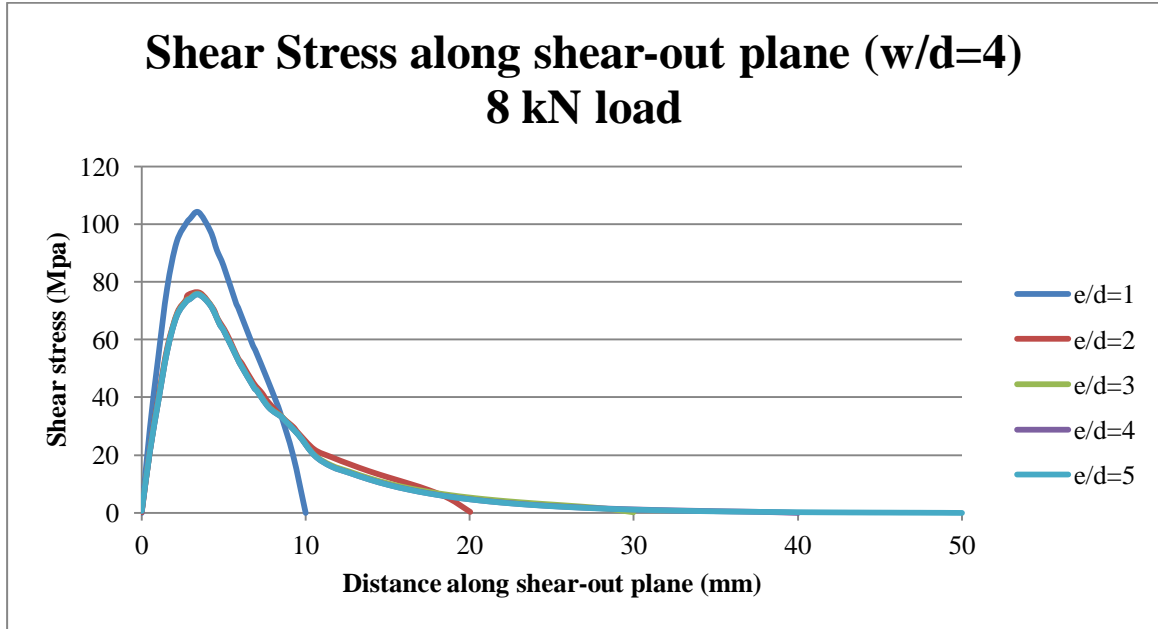


Figure D1 Shear stress w/d=4

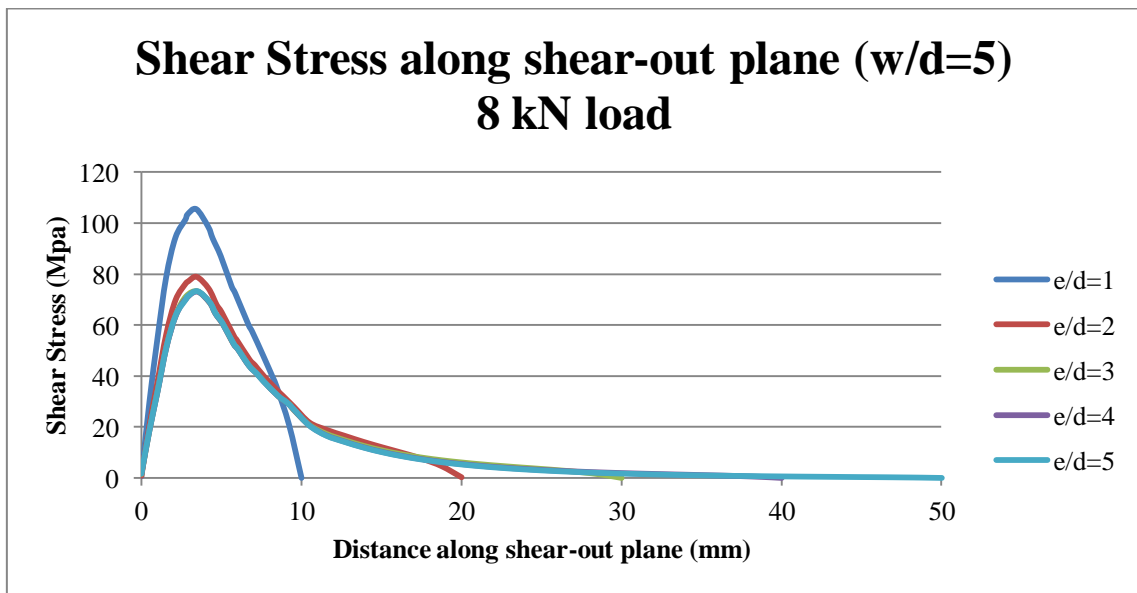


Figure D2 Shear stress w/d=5

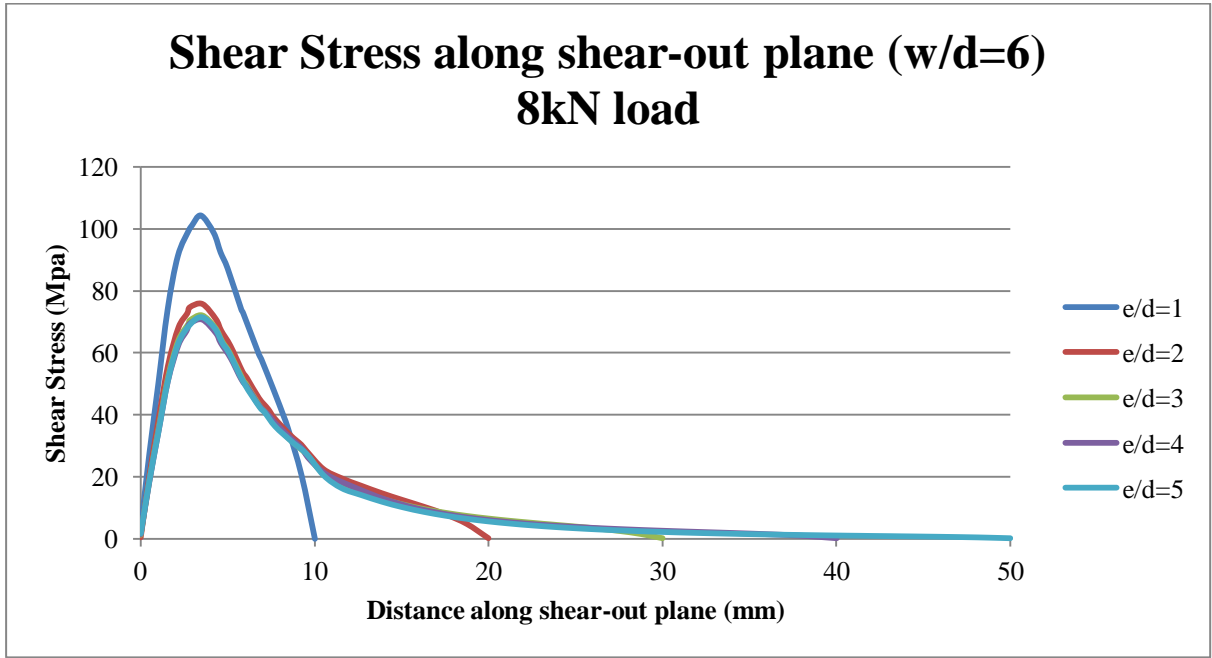


Figure D3 Shear stress w/d=6

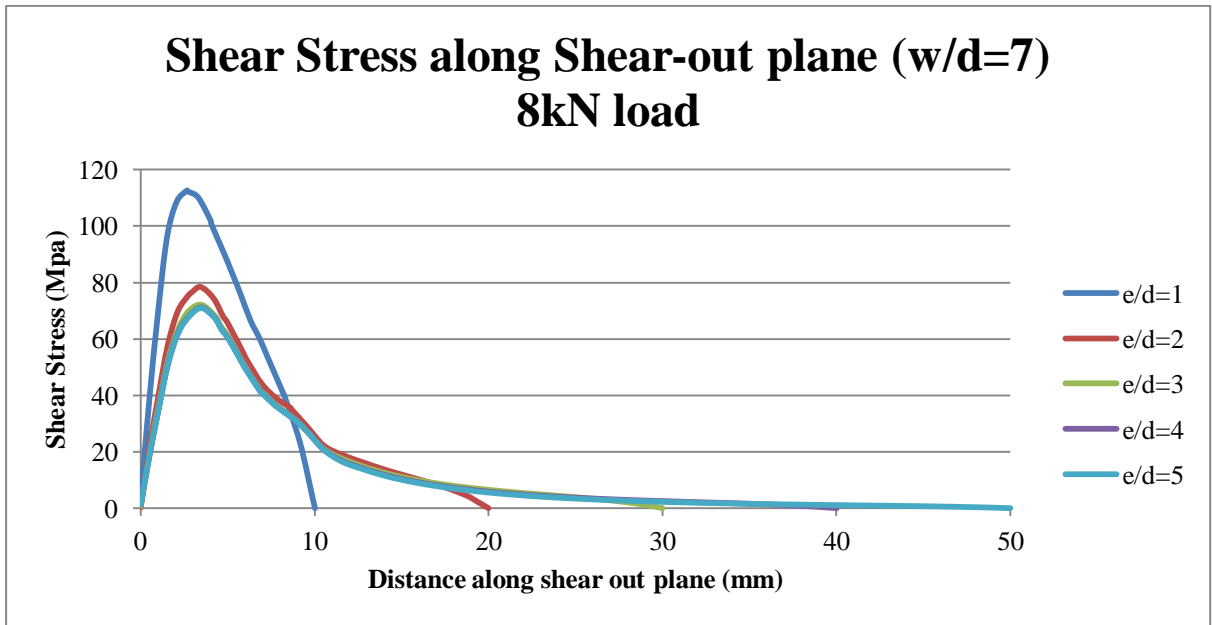


Figure D4 Shear stress w/d=7

Multi-bolt connections

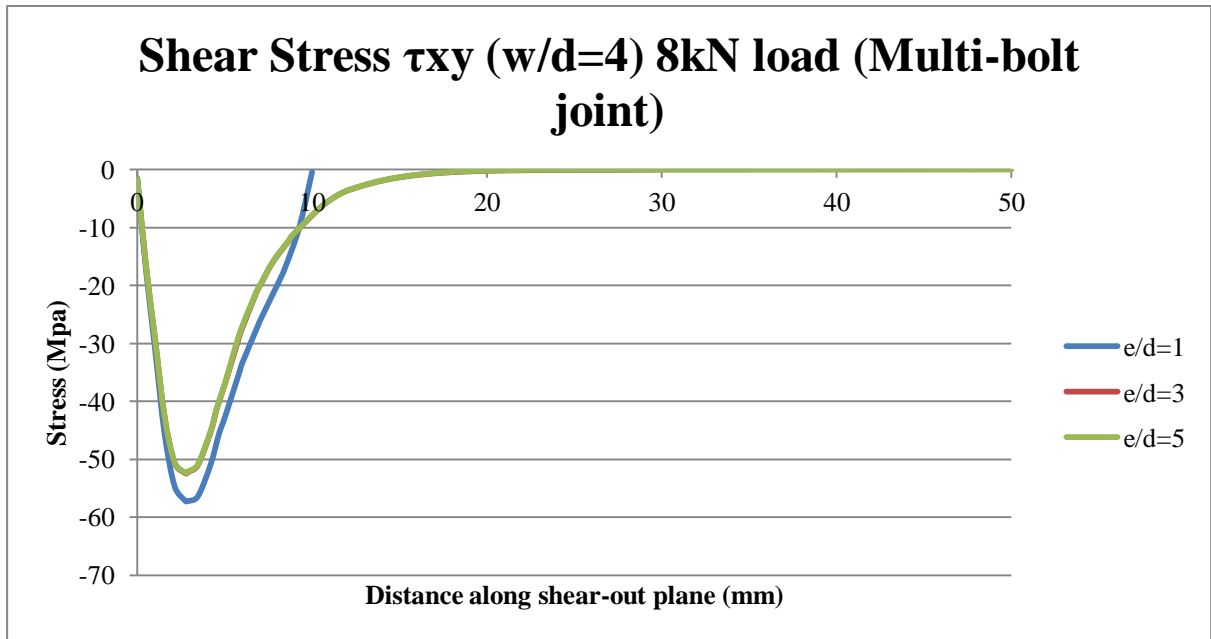


Figure D5 Shear stress w/d=4

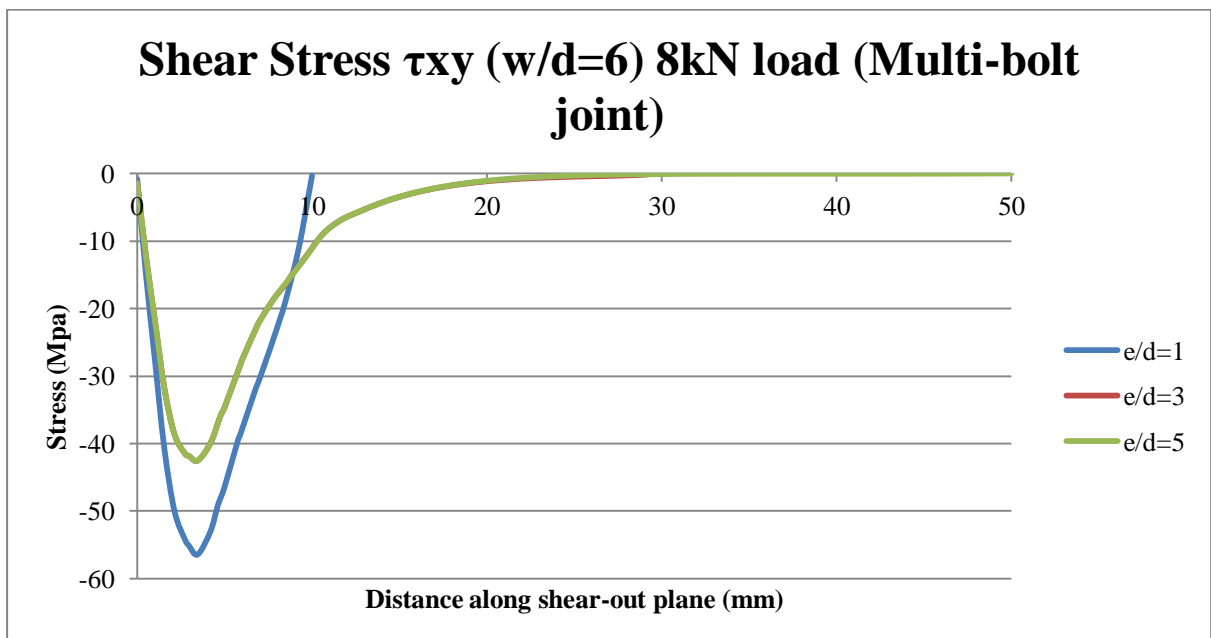


Figure D6 Shear stress w/d=6

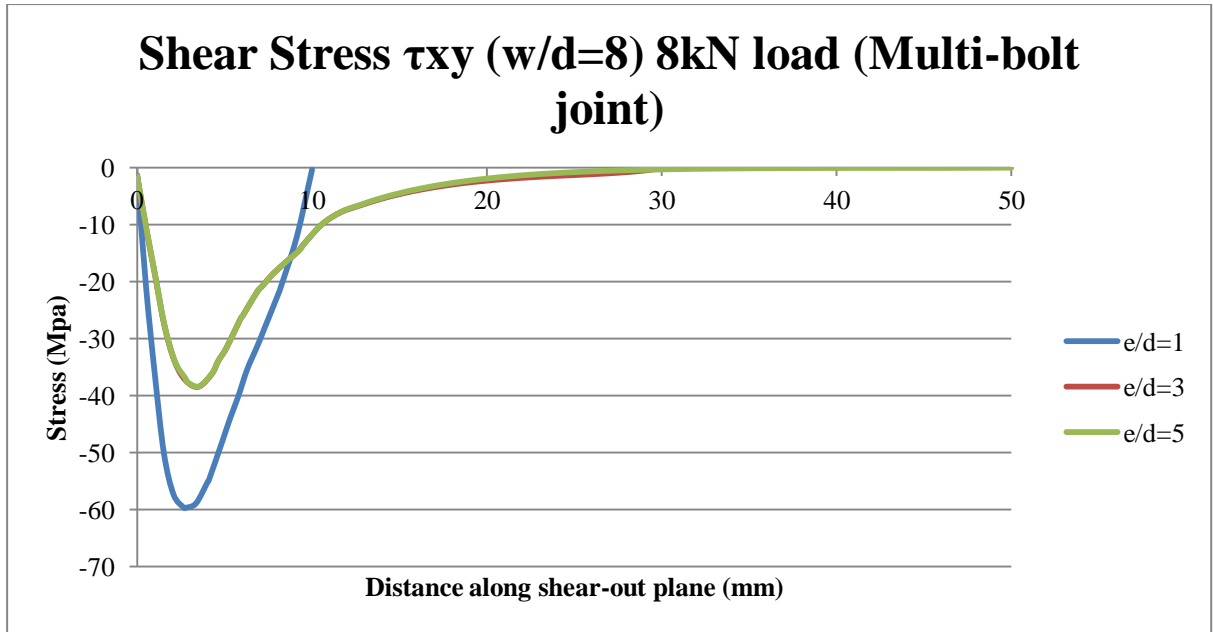


Figure D7 Shear stress $w/d=8$

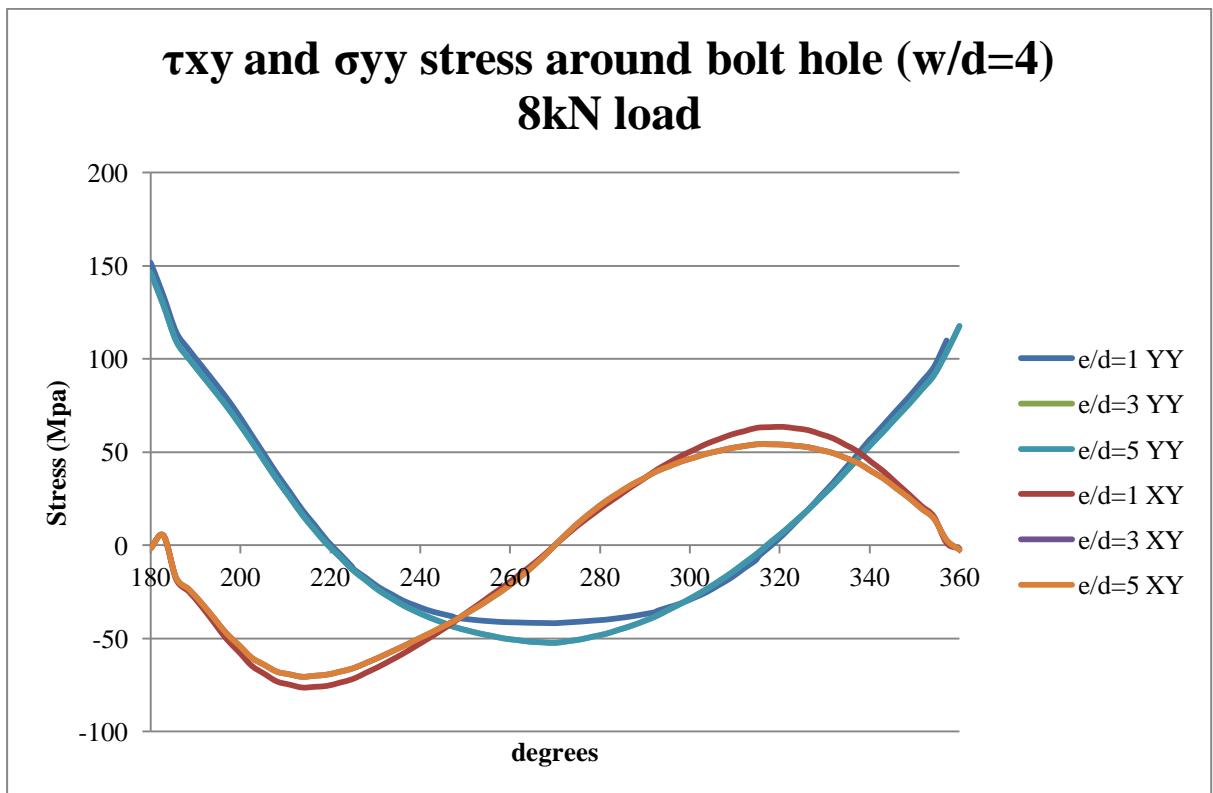


Figure D8 Bolt Hole Edge stress $w/d=4$

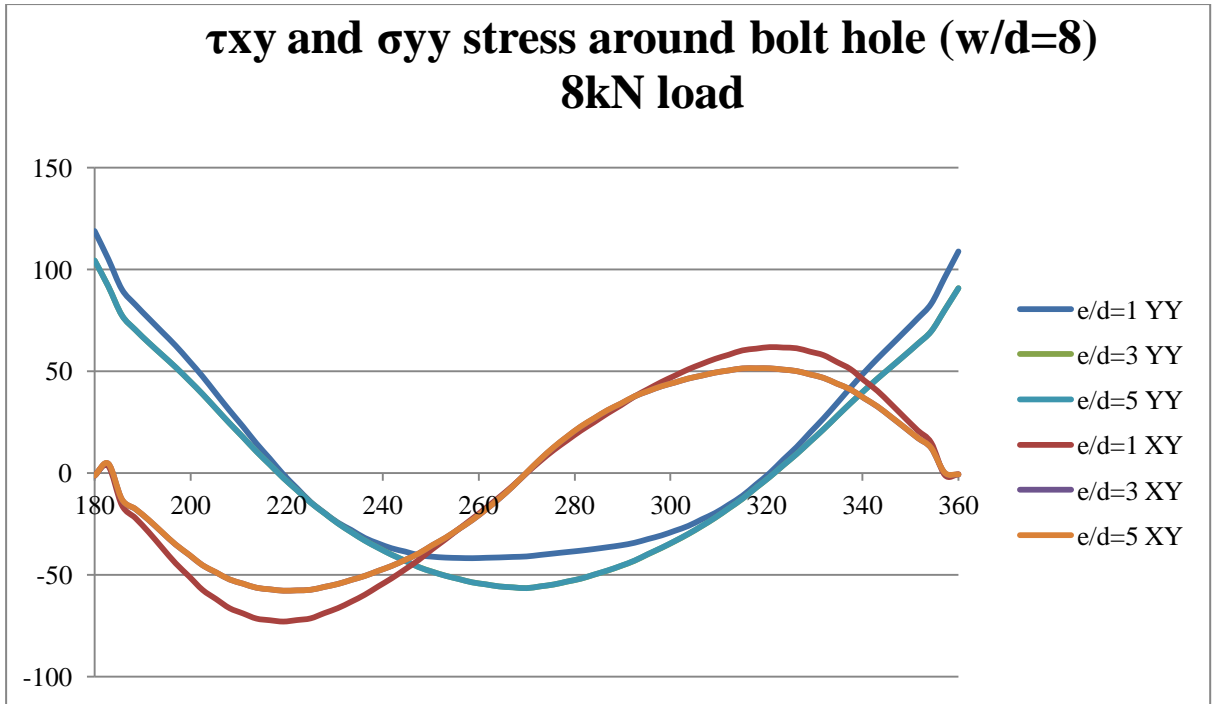


Figure D9 Bolt Hole Edge stress w/d=6

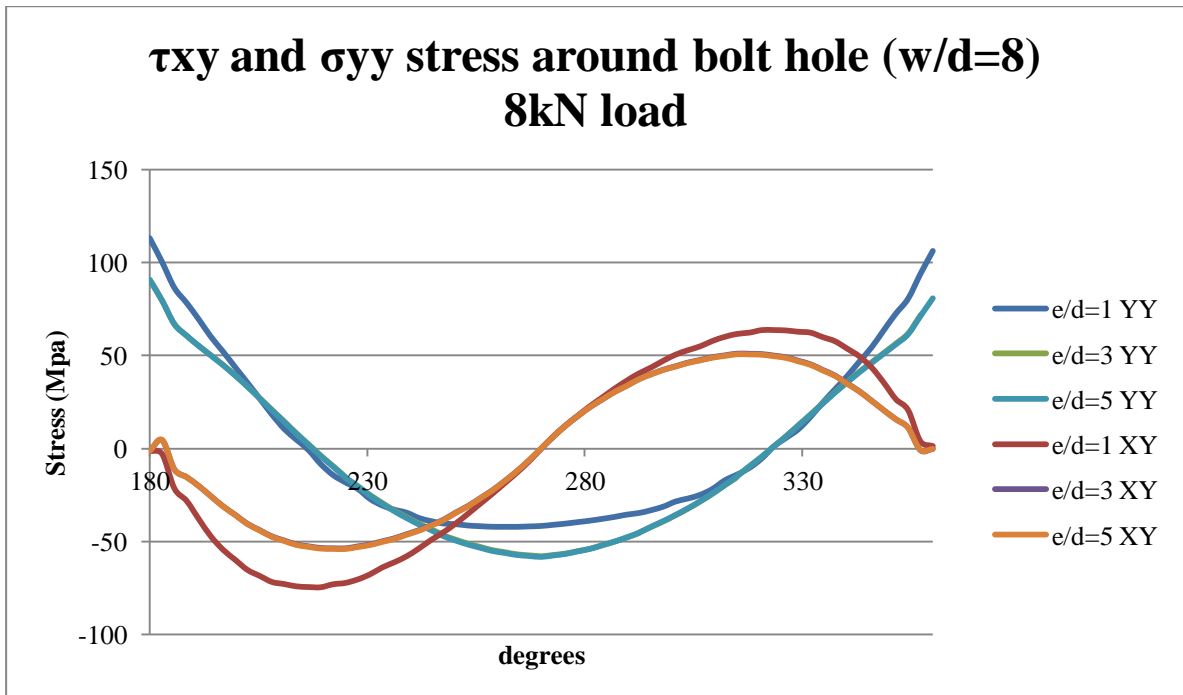


Figure D10 Bolt Hole Edge stress w/d=8

Appendix E Bearing stress plots
Single bolt connections

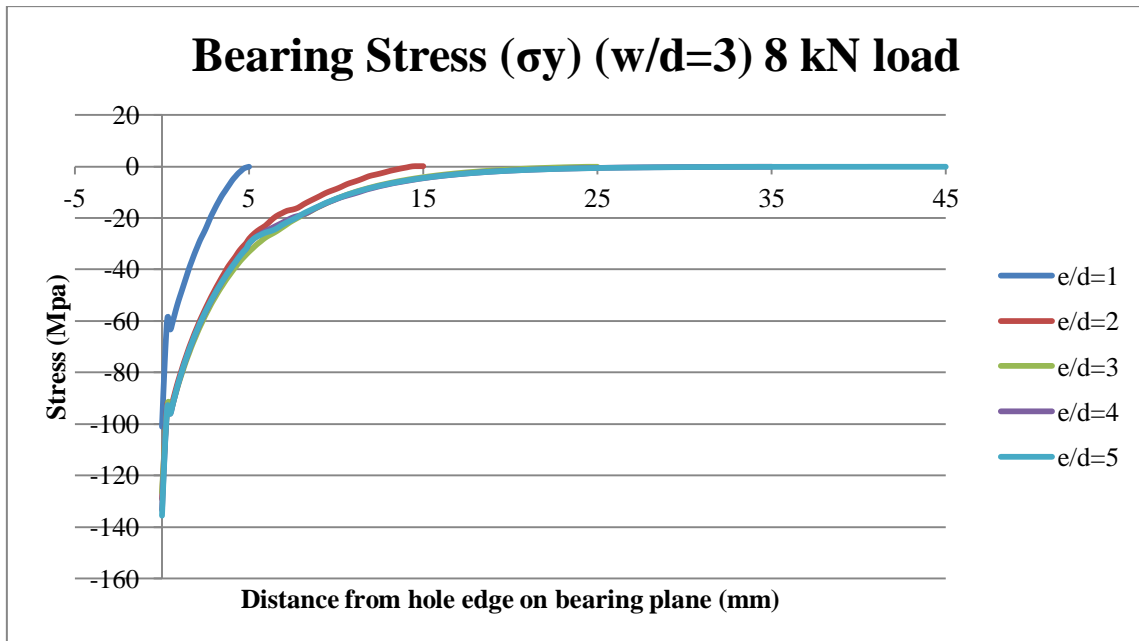


Figure E1 Bearing Stress $w/d=3$

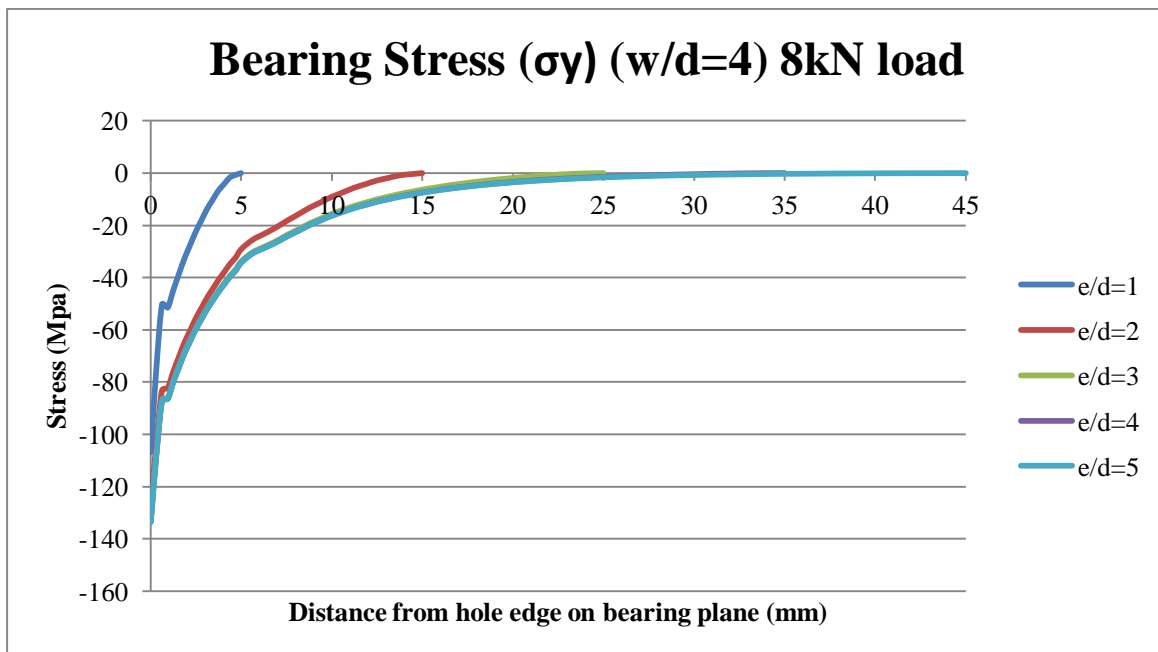


Figure E2 Bearing Stress $w/d=4$

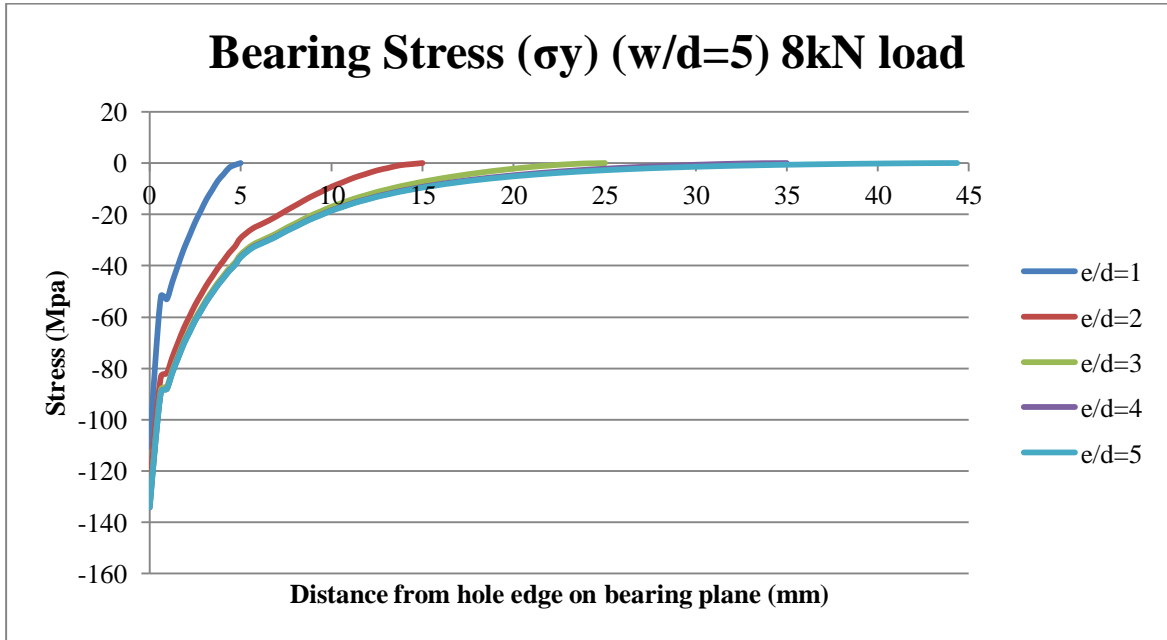


Figure E3 Bearing Stress w/d=5

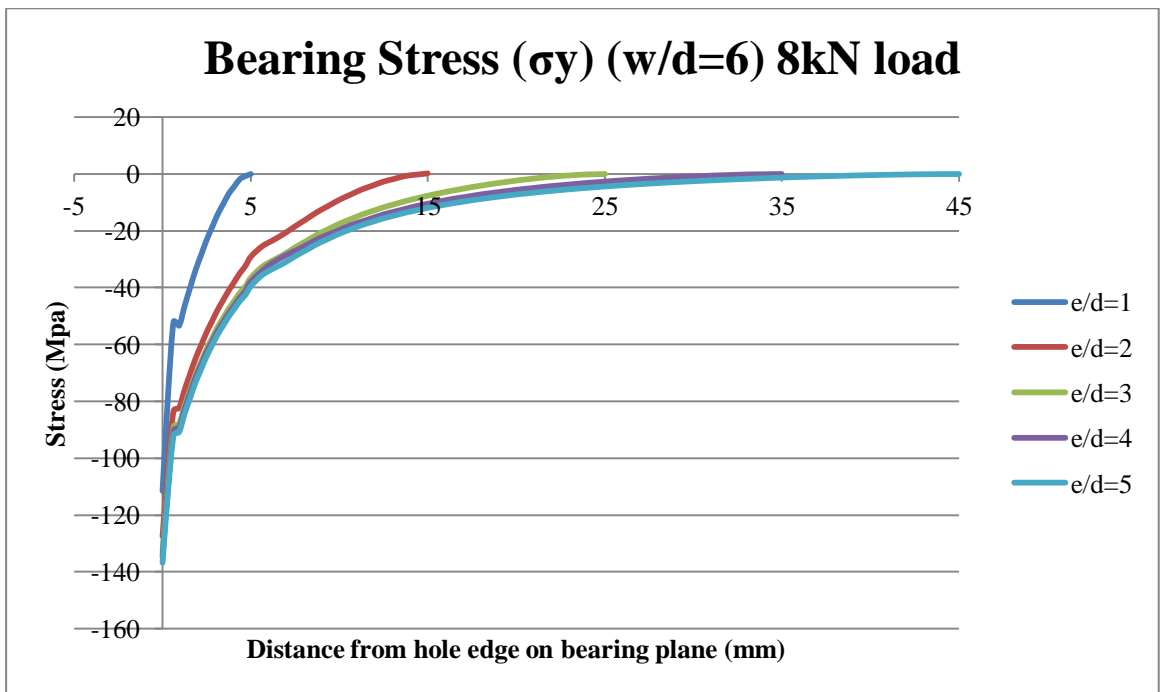


Figure E5 Bearing Stress w/d=6

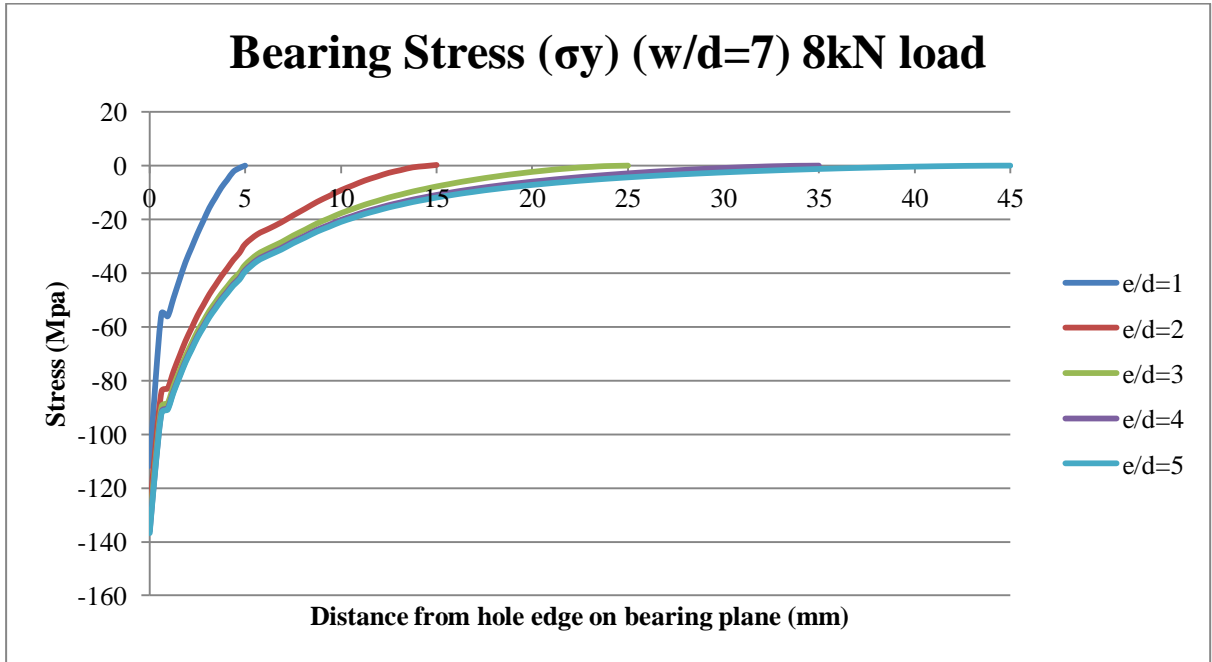


Figure E6 Bearing Stress w/d=7

Multi-bolt connections

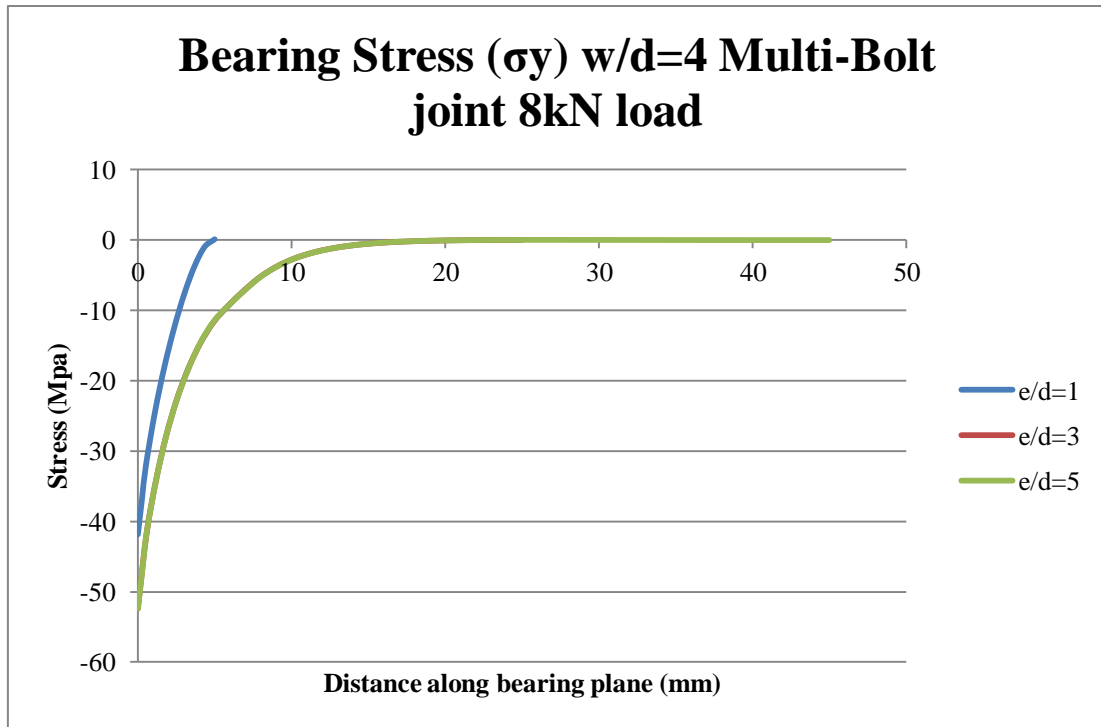


Figure E7 Bearing Stress w/d=4

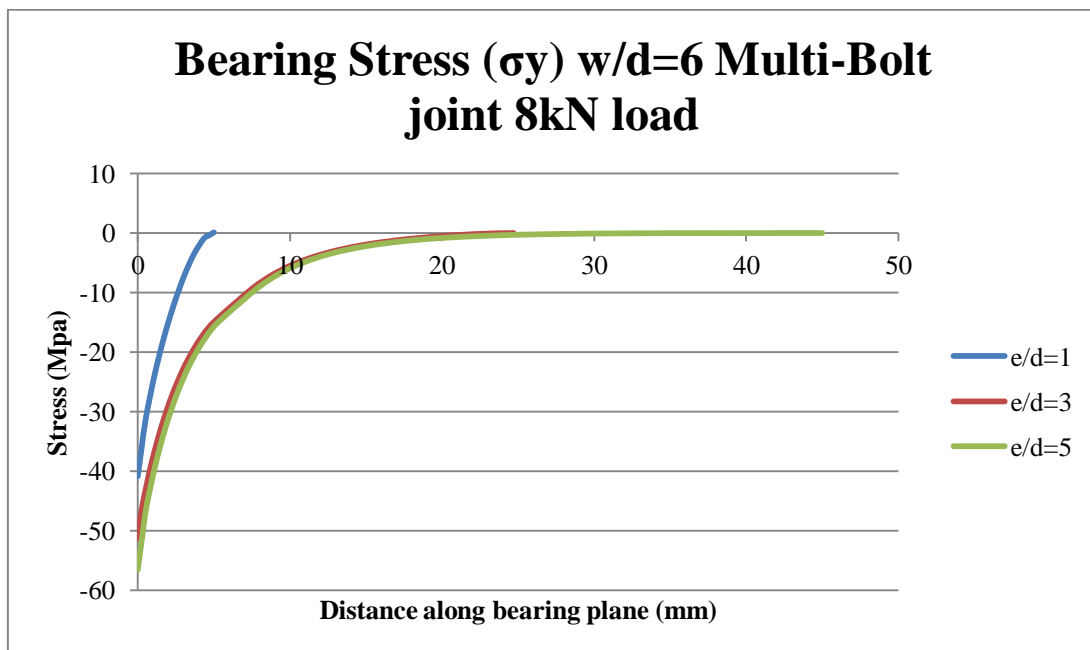


Figure E8 Bearing Stress w/d=6

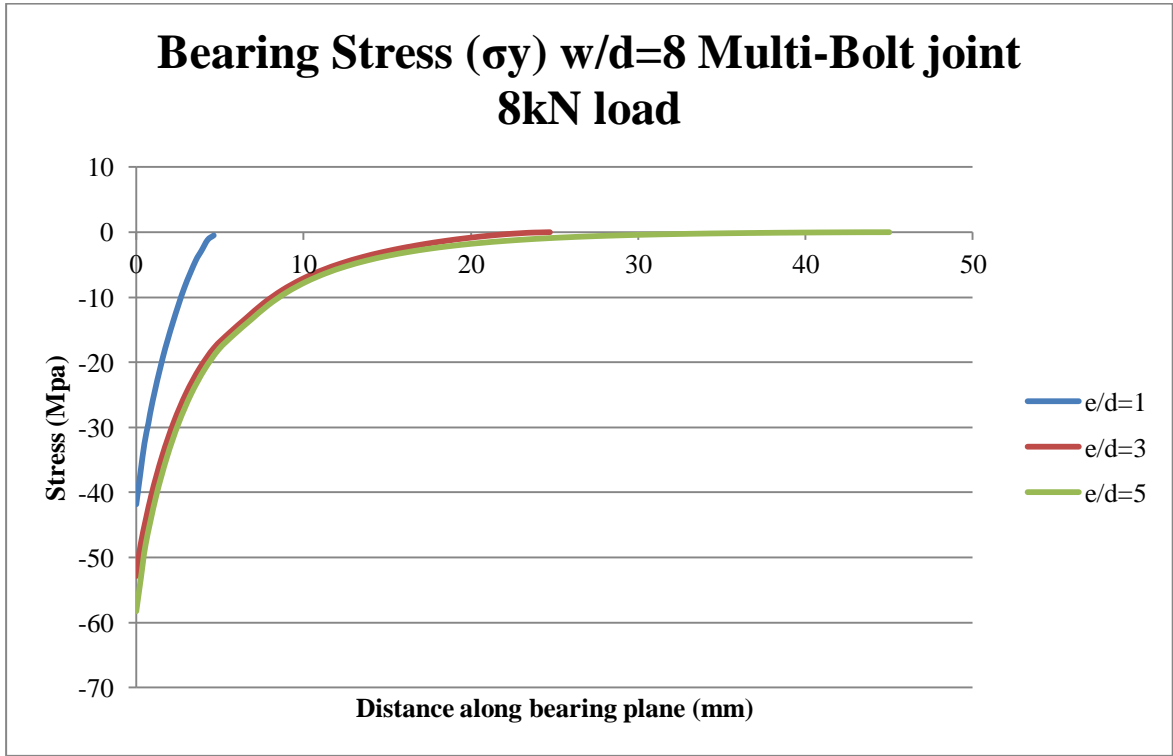


Figure E9 Bearing Stress w/d=8

Appendix F Theoretical data for thickness effects

Table F1 Effects of thickness change

Single bolt connection S650 (t=9.5mm) Stress data										
geometry		geometric ratio		concentration data				oy results		% error
w	e	w/d	e/d	α	β	Θ	Kte	theory	FEA	
30	10	3	1	3	0.33	0.00	4.0	168.4	163.4	3.0
	20		2		0.67	0.75	3.4	144.7	136.8	5.5
	30		3		1.00	1.00	3.3	136.8	137.6	-0.6
	40		4		1.33	1.00	3.3	136.8	140.9	-3.0
	50		5		1.67	1.00	3.3	136.8	141.3	-3.3
40	10	4	1	4	0.25	-0.50	5.5	153.0	149.4	2.3
	20		2		0.50	0.50	4.6	127.7	116.5	8.8
	30		3		0.75	0.83	4.3	119.3	114.5	4.0
	40		4		1.00	1.00	4.1	115.1	114.4	0.6
	50		5		1.25	1.00	4.1	115.1	114.4	0.6
50	10	5	1	5	0.20	-1.00	7.0	147.4	148.1	-0.5
	20		2		0.40	0.25	5.8	121.1	112.2	7.3
	30		3		0.60	0.67	5.3	112.3	108.0	3.8
	40		4		0.80	0.88	5.1	107.9	107.0	0.8
	50		5		1.00	1.00	5.0	105.3	107.5	-2.1
60	10	6	1	6	0.17	-1.50	8.6	145.0	142.0	2.0
	20		2		0.33	0.00	7.0	117.9	106.6	9.6
	30		3		0.50	0.50	6.5	108.9	104.0	4.5
	40		4		0.67	0.75	6.2	104.4	104.3	0.1
	50		5		0.83	0.90	6.0	101.7	102.3	-0.6
70	10	7	1	7	0.14	-2.00	10.3	143.9	144.4	-0.4
	20		2		0.29	-0.25	8.3	116.2	110.2	5.2
	30		3		0.43	0.33	7.6	107.0	102.4	4.3
	40		4		0.57	0.63	7.3	102.4	105.2	-2.7
	50		5		0.71	0.80	7.1	99.6	105.2	-5.6
									average error %	1.8

Appendix G FEA plots - minimum and recommended joint ratio's

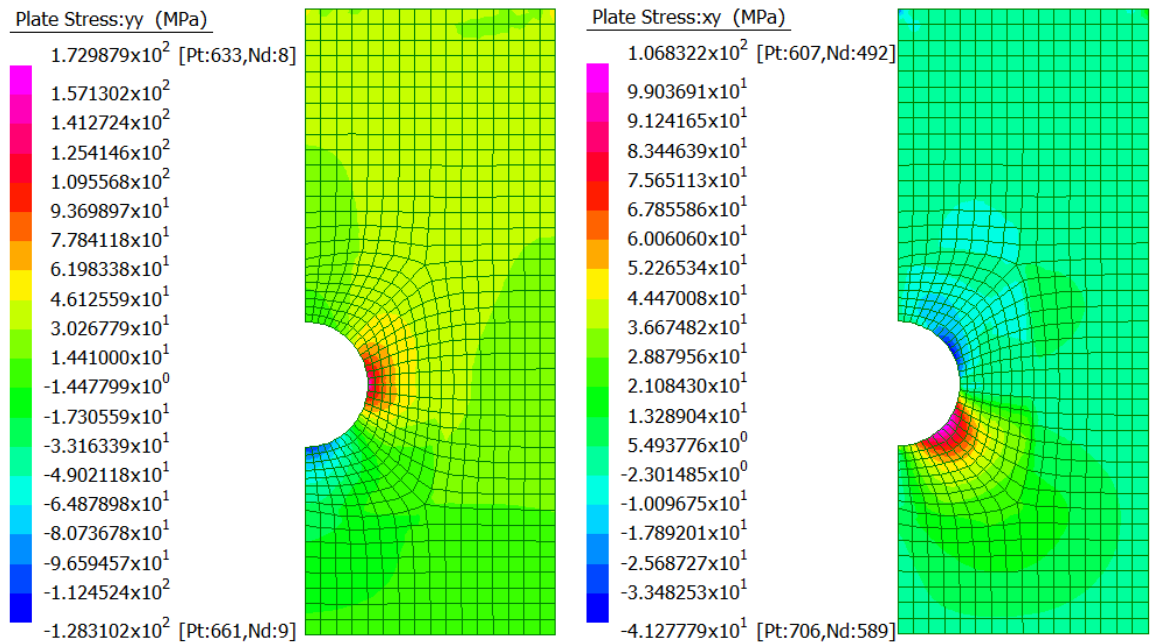


Figure G1 Minimum joint ratio's w/d=4,e/d=2 a) σ_{yy} stress b) shear stress

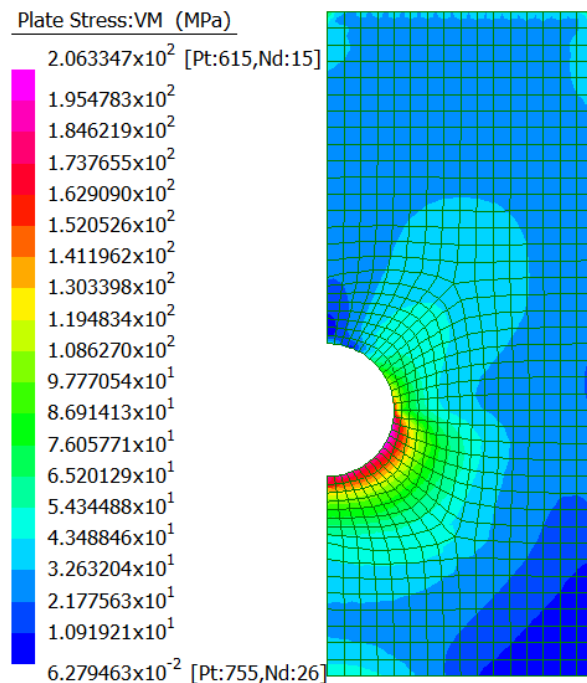


Figure G2 Minimum joint ratio's w/d=4,e/d=2 VM stress

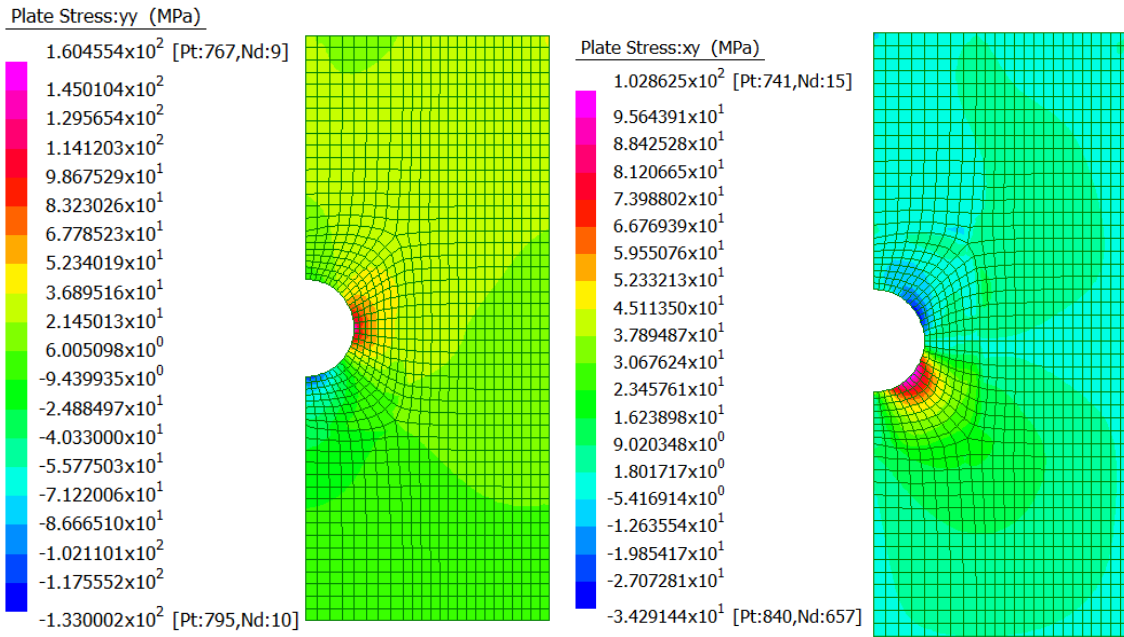


Figure G4 Recommended joint ratio's w/d=5,e/d=3 a) σ_y stress b) shear stress

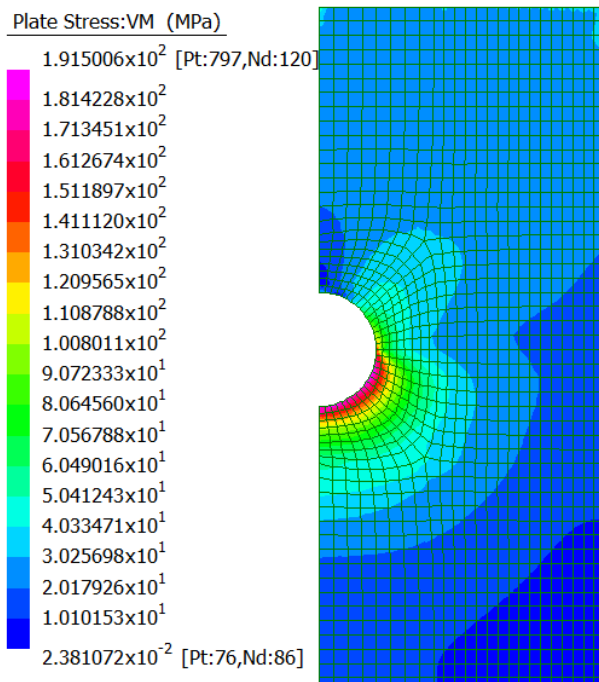


Figure G5 Recommended joint ratio's w/d=5,e/d=3 VM stress

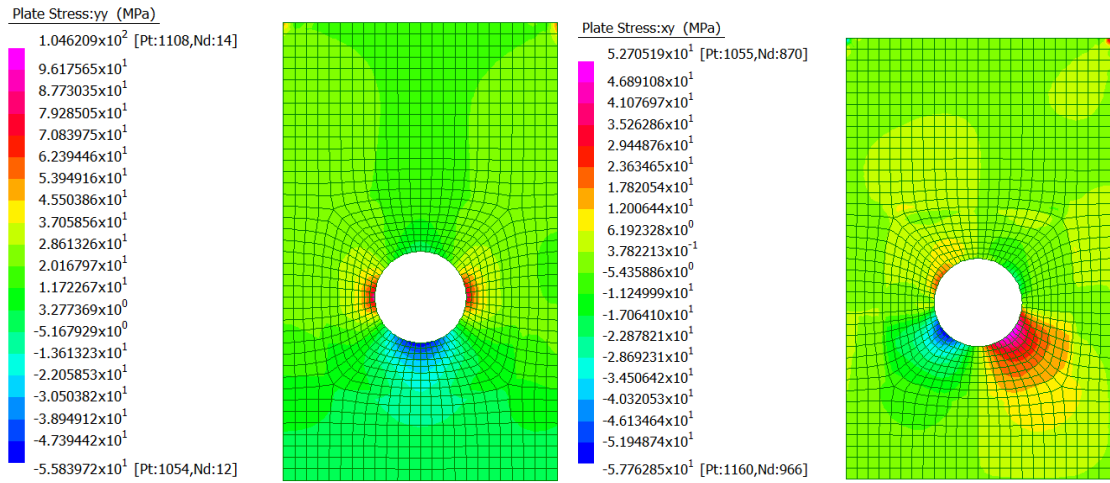


Figure G6 Minimum joint ratio's $w/d=6$, $e/d=2$ a) σ_y stress b) shear stress

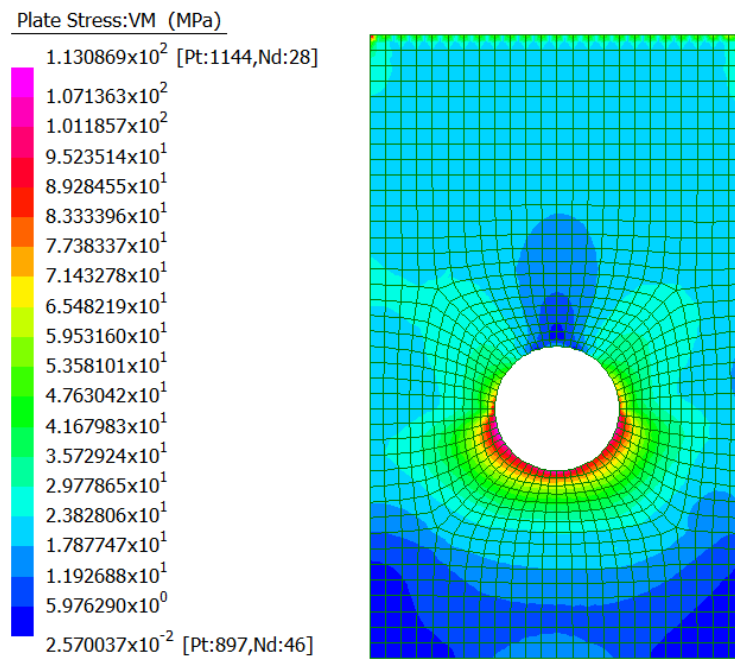


Figure G7 Minimum joint ratio's $w/d=6$, $e/d=2$ VM stress

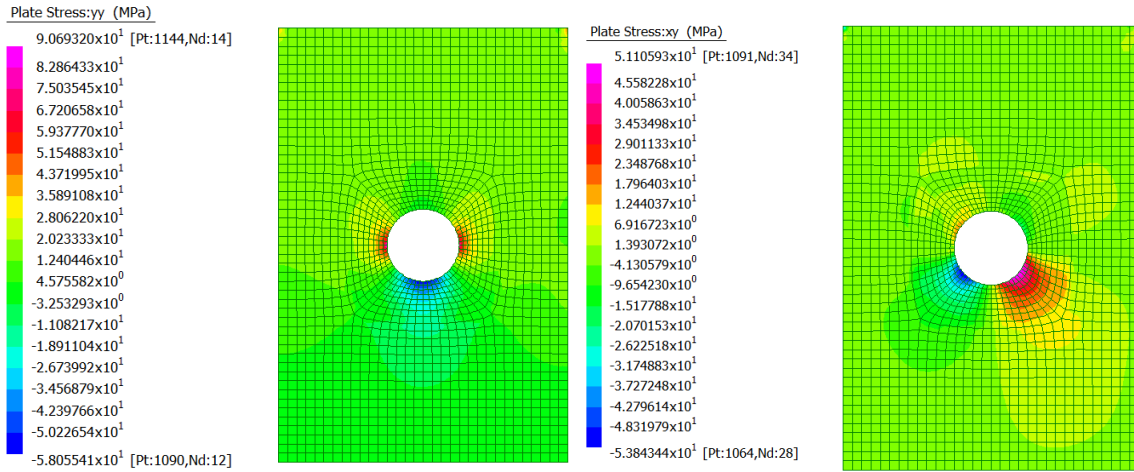


Figure G8 Recommended joint ratio's $w/d=8$, $e/d=3$ a) σ_y stress b) shear stress

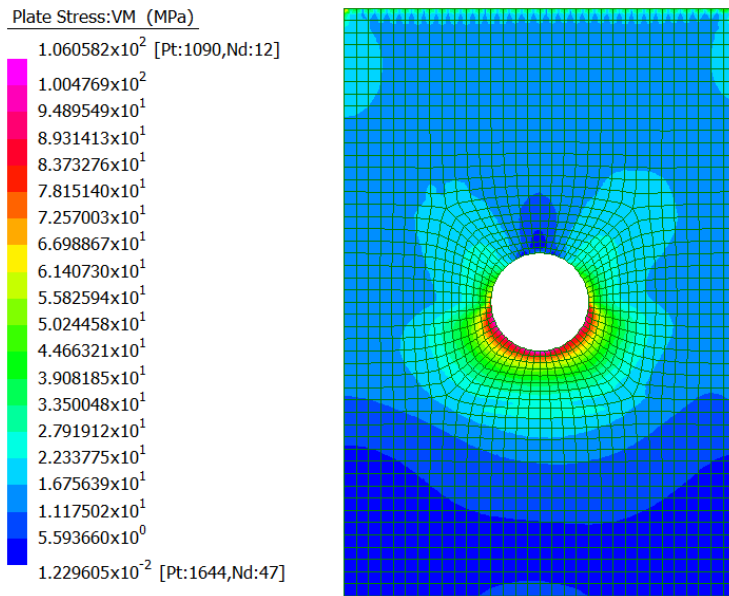


Figure G9 Recommended joint ratio's $w/d=6$, $e/d=2$ VM stress